2019

Air void clustering in retempering concrete and its contribution to compressive strength

Wen Sun
Iowa State University

Air void clustering in retempering concrete and its contribution to compressive strength

by

Wen Sun

A thesis submitted to the graduate faculty

in partial fulfillment of the requirements for the degree of

MASTER OF SCIENCE

Major: Civil Engineering (Civil Engineering Materials)

Program of Study Committee:

Kejin Wang, Major Professor
Peter C. Taylor, Co-major Professor
Charles T. Jahren
Ashley F. Buss

The student author, whose presentation of the scholarship herein was approved by the program of study committee, is solely responsible for the content of this thesis. The Graduate College will ensure this thesis is globally accessible and will not permit alterations after a degree is conferred.

Iowa State University

Ames, Iowa

2019

TABLE OF CONTENTS

Page

LIST OF FIGURES

Page

LIST OF TABLES

Page

ACKNOWLEDGMENTS

First and foremost, I would like to thank my major professor, Kejin Wang for her teaching, assistance and continuous encouragement during my graduate life and I also would like to express my greatest gratitude to Dr. Peter C. Taylor for his generous funding support, academic assistance and gentle guidance throughout my MS study. Because of them, I have this opportunity to join the NCHRP project to explore the world of concrete.

I sincerely thank my committee members, Dr. Charles T. Jahren, and Dr. Ashley Buss for their valuable advice and comments throughout my research work.

Also, I appreciate Dr. Xin Wang, Dr. Yifeng Lin, and Dr. Seyedhamed Sadati for their kind help and discussions, which allowed my experiments to go smoothly. I also particularly thank Paul J. McIntyre, who always provided me with sufficient materials on time. Meanwhile, I want to offer my appreciation to lab assistants, Fan Zhou, and Qinwei Meng. Without their work, I would not have completed experimental work and tests on time. I very much appreciate Dr. Duo Zhang in the ECE department, who answered a lot of questions about statistical analysis in this study. I would also like to thank my friends, colleagues, the department faculty, and staff for making my time at Iowa State University a wonderful experience.

Particularly, I would like to thank singer Jay Zhou for his music and spirit of not giving up, which gave me power and bravery when facing difficulties. Finally, I would like to thank my parents, sister and girlfriend for their love, unconditional support, and encouragement throughout my life.

ABSTRACT

Air void clustering is a phenomenon in concrete in which air bubbles accumulate around the coarse aggregate. It is considered as a major cause of reduction of concrete strength.

This thesis focuses on the effect of different variables on air void clustering and its contribution to the performance of concrete. Six variables were considered in the study, including cement type (low alkali cement and TIL cement), fly ash (fly ash A and B), coarse aggregate type (lime stone and river gravel), chemical admixture type (admixture 1 and 2) , mixing water temperature (70°F and 90°F), and retempering (with and without). A total of 64 mixtures were prepared. The slump, unit weight and air content were tested on the fresh concrete. For hardened concrete, compressive strength at 7 and 28 days was determined. Air void structure including spacing factor and specific surface, and air void clustering were evaluated using rapid air and imagine analysis respectively. To study the temperature influence on air void clustering in more details, additional mixtures with all concrete materials heated to 90°F before mixing were made. Statistical method including stepwise linear regression and neural network were utilized for data analysis to investigate relationships among variables, fresh and hardened properties of concrete.

This study found that air void clustering was observed in mixtures with and without retempering; thus retempering might not be the single cause for air void clustering, though it does exacerbate the severity of air void clustering. Fly ash type and coarse aggregate type had significant effects on air content and air void clustering. However, cement type and admixture type only had significant effects on air void clustering. The higher temperature increased air content, air void clustering, and strength loss of concrete due to air void clustering. Although

retempering and more air content could increase air void clustering around the aggregate, they still had a limited function on growth of air void clustering.

Clustering sensitive index (CSI) was first proposed to describe the sensitivity of concrete to clustering. The smaller value of CIS indicated higher sensitivity of concrete to air void clustering with retempering. Air void clustering causing strength loss was observed and it was possibly happened more easily in an air void system with low spacing factor and high specific surface. The model established by the neural network had a good fit with experimental data, and it reveals clearly the negative effect of air content and air void clustering on compressive strength.

CHAPTER 1. INTRODUCTION

1.1 Research Background

Air void clustering is a phenomenon in which air bubbles collect around coarse aggregate particles. It commonly occurs in air-entrained concrete containing synthetic air entraining agents and reportedly reduces the interface bonding between aggregates and cement paste. Thus, it has been cited as a major cause of concrete strength loss in numerous cases (Gutmann 1987; Mehta and Hover 2010; Cross et al. 2000; Kozikowski and Zemajtis 2006). However, later studies found that the loss of compressive strength of concrete was controlled by air content rather than air clustering (Naranjo, 2007; Riding, Esmaeily, and Vosahlik 2015). Whether air void clustering affects concrete strength loss has been debated for a long time. Further, the air void clustering first observed on job sites was placed in the summer season along with retempering. Thus, both the temperature and the retempering process should be reviewed.

1.2 Research Objective

The aim of this study is to:

(1) Evaluate the effect of retempering on performance of concrete including fresh properties (slump, unit weight, fresh air content) and hardened properties (compressive strength, air void clustering and air void system),

(2) Investigate effect of materials (cement type, fly ash type, aggregate type and chemical admixture type) on air content and air void clustering,

(3) Explore temperature effects on air content and air void clustering,

(4) Determine whether the loss of compressive strength is associated with air void clustering

(5) Assess the correlation between air void clustering and air void systems.

(6) Discuss air void clustering evaluation methods.

To achieve the goal of this study, the following steps were conducted:

(1) A full factorial design was used to identify the significance of factors and combination of interactions that affects fresh properties of concrete

(2) The severity of air void clustering of each mixture was evaluated by a clustering rating method

(3) The relationships between air void clustering and fresh properties of concrete were assessed by statistical analysis.

(4) The relationship between compressive strength of concrete and air void clustering was investigated

(5) The effect of hardened air void system on air void clustering was analyzed.

(6) The effect of temperature on air void clustering and its relationship with compressive strength were investigated

1.3 Thesis Organization

This thesis consists of 5 chapters as described below:

Chapter 1: Introduction-This chapter introduces the topic of air void clustering, including air void entraining mechanisms, the definition of air void clustering, factors affecting air void clustering and the effect of air void clustering in concrete. The research significance and objectives are also presented.

Chapter 2: Literature Review- This chapter includes 5 sections discussing the literature covering the mechanism of air entrainment, observation of air void clustering, factors affecting void clustering and the relationship between air void clustering and compressive strength.

Chapter 3: Experimental work- This chapter provides an overview of the experimental program including materials, mix design and proportions, and sample preparation, curing and testing. The preparation and evaluation of hardened air void analysis and air void clustering are presented. The statistical method is also introduced.

Chapter 4: Results and Discussion- This chapter presents and discusses the data. The results of fresh properties with the statistical analysis are presented and factors affecting clustering and whether the compressive strength reduction related to the air void clustering are discussed in detail. A neural network analysis was conducted to establish a model for the prediction of compressive strength. The relationship between air content, clustering, and compressive strength is presented by the surface model in three-dimensions. Based on hardened air void analysis, the correlation between air void systems and air void clustering was identified. Finally, the limitations and deviations of the visual rating method are discussed.

Chapter 5: Conclusions and recommendations- This chapter provides the key findings of this thesis, limitation, and future research recommendations.

CHAPTER 2. LITERATURE REVIEW

2.1 Air Entraining Admixtures

In 1930, people accidentally observed that concrete with added "crushed oil" would resist surface scaling. Then, concrete with cement grinding aids, such as beef fat, calcium stearate, and fish oil showed an excellent resistance to freezing environment (Jackson 1944).

During the freezing and thawing cycles, concrete is susceptible to deterioration, which affects the performance of pavement, dams, and other structures. Due to this problem, air-entraining admixtures have become widely used to increase resistance to freezing and thawing, as shown in Figure 2-1 (Sidney Mindess et al. 2003).

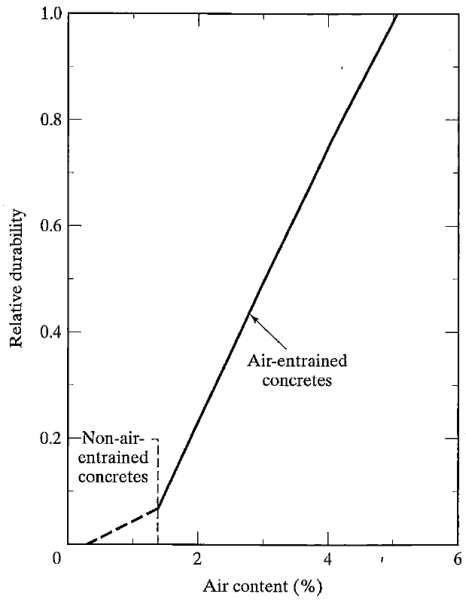

Figure 2-1 Effect of air entrainment on the frost resistance of concrete (Sidney Mindess et. al., 2003)

Air entraining admixtures are types of soluble surface active agents. Their primary function is to reduce the surface tension of water to decrease the energy of air void formation. Thus, small bubbles can be stabilized (Pigeon and Pleau 1995). There are several chemicals used

in air-entraining admixtures, which have been classified by Kosmatka et al. Table 2-1 shows four different air-entrained agents and their performance characteristics. (Kosmatka et al. 2003; adapted from Naranjo, 2007 and Riding, Esmaeily, and Vosahlik 2015).

Table 2-1 Air-entraining admixture classification and characteristics (Kosmatka et al. 2003; Adapted from Naranjo 2007, page 7 and from Riding, Esmaeily, and Vosahlik 2015, page 6)

Classification	Performance Characteristics
Wood resin and rosin	Quick air generation. Minor air gain with initial mixing. Air loss with prolonged mixing. Mid-size air bubbles formed. Compatible with most other admixtures.
Tall oil	Slower air generation. Air may increase with prolonged mixing. Smallest air bubbles of all agents. Compatible with most other admixtures
Synthetic detergents	Quick air generation. Minor air loss with mixing. Coarser bubbles. May be incompatible with some HRWR. Also applicable to cellular concretes.
Vegetable oil acids	Slower air generation than wood rosins. Moderate air loss with mixing. Coarser air bubbles relative to wood rosin. Compatible with most other admixtures.

A surface-active agent is a kind of molecule with both a hydrophilic group and a hydrophobic group to form and stabilize bubbles (Figure 2-2) (Sidney Mindess et al. 2003). The hydrophilic head can be, anionic, cationic nonionic or amphoteric. In modern AEAs, the commonly used agents are anionic (Du and Folliard 2005).

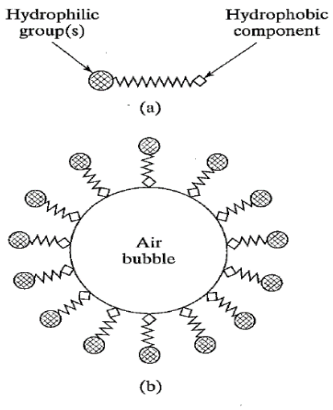

Figure 2-2 a) characteristics of a surface-active molecule; b) stabilized air bubbles (Sidney Mindess et al, 2003)

2.2 Air Void Categories

Air entrained concrete comprises a large number of small bubbles dispersed randomly throughout the paste. The size of bubbles is around 0.05mm to 1.25mm diameter with an approximately spherical shape. Figure 2-3 illustrates a sample of air entrained concrete under a microscope (Sidney Mindes et al. 2003).

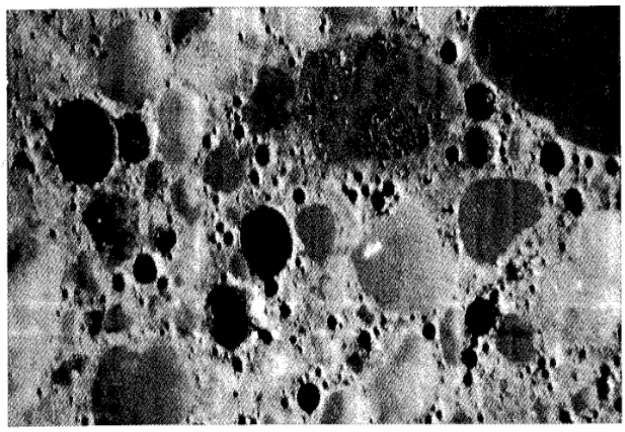

Figure 2-3 Micrograph of air-entrained concrete (Photograph courtesy of Portland Cement Association)

An important parameter used to estimate the performance of an air void system is the spacing factor determined according to ASTM C457. The relationship between spacing factor and durability is indicated in Figure 2-4. It shows that durability has a sharp decrease after the spacing factor exceeds 0.2mm. Another two parameters, specific surface area, and bubble frequency, are other considerations for a protective air void system (Sidney Mindess et al.).

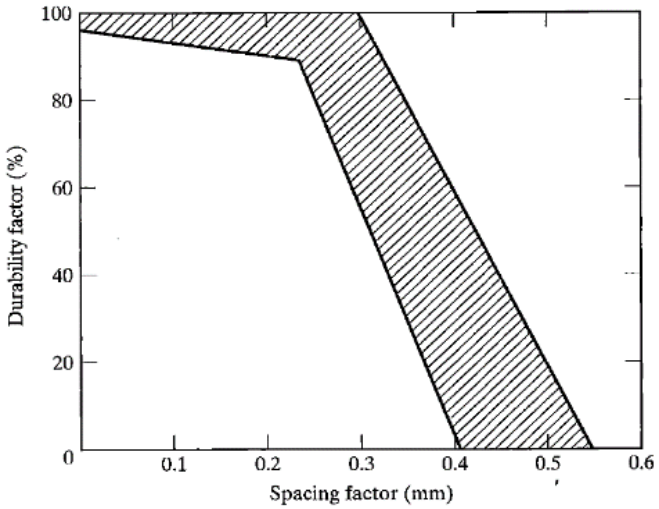

Figure 2-4 Relationship between spacing factor and durability factor (Sidney Mindess et. Al.)

Voids in concrete are not all "entrained". Entrained voids are produced by the mixer, and the surface tension of AEA's keeps a certain percentage of these small voids stable. The presence of entrained air voids in the concrete not only increases the fluidity of the paste but also improves resistance to freezing and thawing. Entrapped air voids are defined as voids with a dimension of more than 1mm and generally are non-spherical. This kind of air void has negative effects on the appearance, strength and durability of concrete and is normally a consequence of inadequate consolidation (Walker, Lane, & Stutzman, 2006).

Other types of voids include capillary voids, Table 2-2. Capillary voids are those left behind in the hydrated cement paste after un-hydrated water leaves the system. The distribution and number of capillary voids are related to the water-cement ratio and hydration degree. Their size varies from 50 nm to 10 microns (Pigeon & Pleau, 1995; Walker, Lane, & Stutzman, 2006).

Table 2-2 Types of void and characteristics (Walker, Lane, & Stutzman, 2006)

Types of void	Characteristics
Capillary voids	Capillary voids are irregularly shaped and are very small (less than 5 μm on the lapped surface of the slice examined). They represent space originally filled by mixing water, remain after the hydration of the cement gels, and are an integral part of the paste. Although they contain air at the time of examination, they are not considered part of the air-void system.
Entrained air voids	Entrained air voids are defined by VTRC as spherical voids larger than the capillaries, but less than 1 mm on the lapped surface of the slice examined. They are formed by the folding action of the concrete mixer, and their shape, size, and abundance are influenced by the addition of surface-active, air-entraining admixtures to the mixture.
Entrapped air voids	Entrapped air voids are voids that are larger than entrained voids, but have internal surfaces that indicate that they were formed by air bubbles or pockets. They may be spherical or irregularly shaped.
Water voids	Water voids are irregularly shaped voids whose shape, location, or internal surface indicates that they were formed by water. Usually they are larger than entrained air voids.

2.3 Air-Entrainment Mechanism

In order to entrain air to concrete, two important processes are in play: formation and stabilization of the air void. For formation, two basic processes were described by Powers, one is folding of air by vortex action (stirring a liquid), and the other is a *three-dimensional screen* formed by the fine aggregate when the concrete mass cascades onto itself during mixing. As for the stabilization process, small bubbles will naturally tend to coalesce into large bubbles unless prevented from doing so by the air-entraining admixtures.

The hydrophilic, negatively charged, heads of surfactants are attracted and adsorbed onto the charged surfaces of cement particles. The surfactants also reduce the surface tension of water. The surfactant molecules also accumulate around a water-air interface shown in Figure 2-5. The

electrostatic and steric repulsions between surfactants promote stabilization of the small air bubbles which are then dispersed through the cement paste with mixing. (Du & Folliard, 2005).

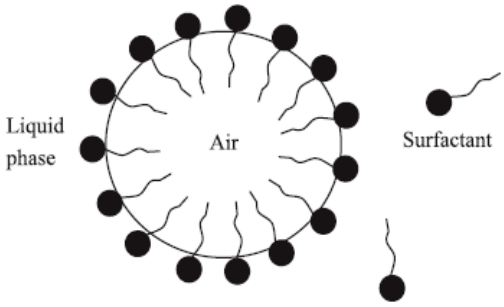

Figure 2-5 Stable air bubble with surfactant (Du & Folliard, 2005).

2.4 Air Void Clustering in Concrete

Air void clustering: the collection of air bubbles around coarse aggregate particles, occurred in some air-entrained concrete. Some Departments of Transportation (DOTs) including those in Minnesota, Virginia, New York, Delaware and Kansas have reported the observation of air void clustering in low strength concrete (Cross et al. 2000, Riding et al. 2015). This has occurred not only in the field, but also in laboratory settings. (Kozikowski et al. 2005, Riding, Esmaeily, and Vosahlik 2015). Several factors behind air void clustering have been discussed, including types of AEAs, mixing temperature, aggregate characteristics and air content. Meanwhile, strength loss has been blamed on air void clustering (Gutmann 1988, Hover 1989, Cross et al. 2000, Kozikowski et al. 2005).

2.5 Factors Affecting Air Void Clustering

2.5.1 Cement Type

Kozikowski et al. (2005) evaluated the effect of cement alkalinity on clustering and reported that alkali content in cement does not have a significant effect on air void clustering.

However, in research by Kansas State University and the University of Texas, clustering was observed around the aggregate as a function of cement alkali content (Naranjo, A. 2007; Riding, Esmaeily, and Vosahlik 2015).

Hansen et al. (2010) reported that concrete using slag cement exhibited no air void clustering. Figure 2-6 shows the difference in the interface zone with or without slag-cement.

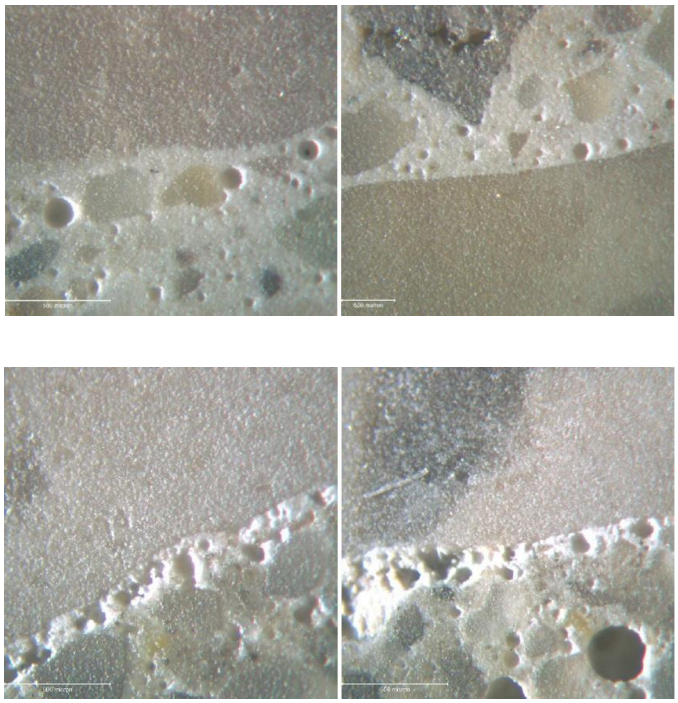

Figure 2-6 Top left and right: Interface Zone in slag cement concrete; Bottom left and right: Interface Zone in slag cement concrete (Hansen et al., 2010)

2.5.2 Aggregate Type

Gutmann (1988) stated that the reduction of compressive strength was due to attraction between the coarse aggregate and the bubbles. Coalesced air voids adjacent to coarse aggregate were observed in concrete with vinsol resin AEA, shown in Figure 2-7.

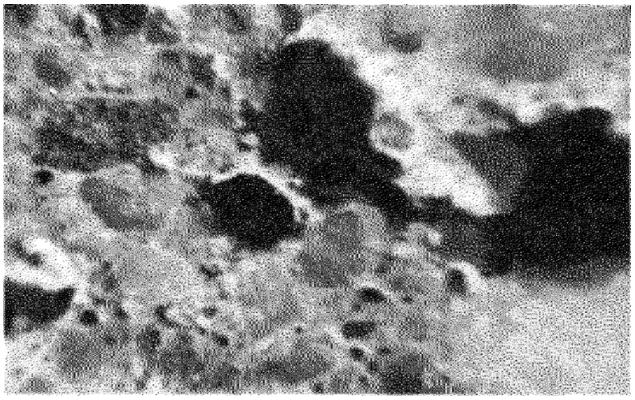

Figure 2-7 Air voids associated with coarse aggregate (Gutmann, 1988)

Marx (1987) proposed that air bubbles were produced first around the aggregate surface rather than air voids migrating from paste to aggregate surface. The irregular surface of coarse aggregate promoted the formation of air bubbles at the surface.

Cross et al. (2000) showed that more aggregates in a mixture meant that, more surfaces were available to attract bubbles. When the amount of aggregate in the concrete increased from 40%-50% to 75%, the 28-days compressive strength decreased from~ 4500 psi to 3500 psi. In their mixtures, two types of aggregate were used: those containing limestone and those containing quartzite. Air void clustering was observed in specimens with both types of aggregate in SEM micrographs shown in Figure 2-8.

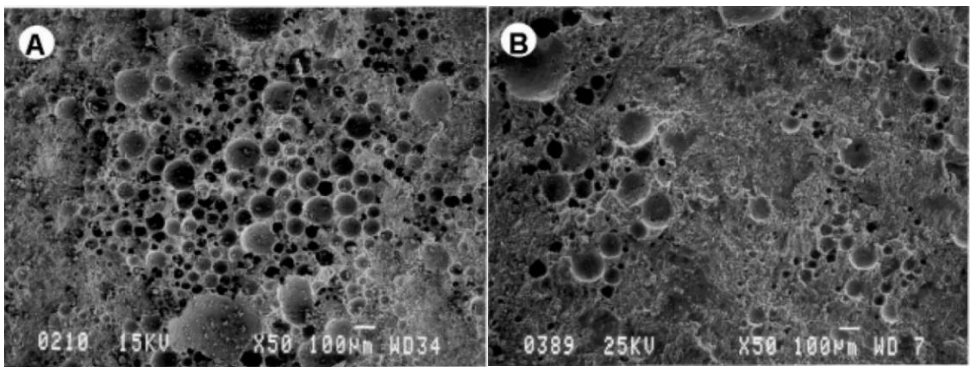

Figure 2-8 SEM micrographs of low strength specimens with limestone aggregate (A, 3520 psi) and quartzite aggregate (B, 3272 psi) (Cross et al., 2000)

Kozikowski et al. (2005) used two types of aggregate, crushed limestone and rounded siliceous to investigate the influence of aggregate shape and mineralogy on air void clustering. The results suggested that aggregate shape/mineralogy affected the severity of air void clustering and then led to strength loss. But further studies were needed to establish the relationship between aggregate shape/mineralogy and clustering. In addition, the moisture conditions of aggregate did not contribute to the clustering.

Riding, Esmaeily, and Vosahlik (2015) indicated that the dirty aggregate might increase the potential of air void clustering. However, the types of aggregate had a little effect on air void clustering around the aggregate.

2.5.3 Air Entraining Admixture

Different types of air entrained admixture have effects on air void performance in concrete, including speed of bubbles formation, air content, air void shape and size, and distribution of air voids (Gutmann, 1988).

Gutmann (1988) investigated effects of several air-entrained agents in concrete using a foam test. The result between Cocamide DEA, Vinsol resin, and a multicomponent agent showed that Cocamide DEA bubble had thicker bubble walls than wood resin bubbles. The shape of the Cocamide DEA bubble was closest to a sphere. However, wood resin bubbles had some irregular shapes. Clustering was observed in both the vinsol resin sample and the multicomponent sample. In an SEM image, air void clustering around the aggregate is clearly seen in Figure 2-9. However, this phenomenon was not found in the Cocamide DEA sample, shown in 2-10.

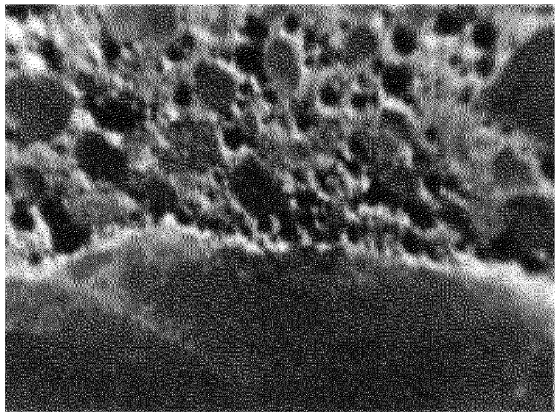

Figure 2-9 Multicomponent agent with clustering of air void at interface of aggregate (Gutmann, 1988)

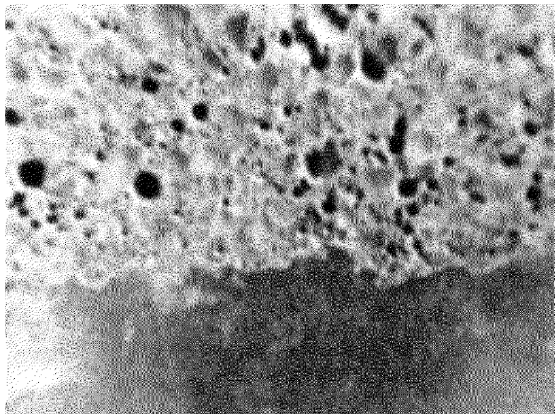

Figure 2-10 Cocamide DEA with no air bubbles around coarse aggregate surface (Gutmann, 1988)

Cross et al. (2000) compared foam tests between synthetic AEAs and vinsol resin agents, and showed that synthetic air entraining admixtures were more hydrophobic, drained faster and formed thin-walled air bubbles, and air void clustering was observed in mixtures with synthetic AEA.

A similar conclusion was reached by Kozikowski et al. (2005). The concrete mix with vinsol resin AEAs showed no air void clustering. However, a relative high clustering rating was gained from the non-vinsol resin admixture. In Table 2-3 and Figure 2-11, MIX A with vinsol

resin AEAs showed no problematic air void clustering. Meanwhile, there was an interesting finding that different AEA formulations with concrete mixture showed similar clustering ratings but different degree of strength loss.

In addition, air void clustering appears to have nothing to do with AEAs addition time. Whatever with or without retempering, air void clustering could occur with all types of AEAs. Further, with high dosages of AEAs, additional air would not be entrained above a certain amount (Naranjo, A., 2007).

Table 2-3 Petrographic Air-Void Clustering Rating and Concrete Properties for vinsol resin AEAs (Kozikowski et al, 2005)

Mix ID	Cycle no.	Clustering rating*	Fresh air content, %	Slump, mm (in.)	Actual compressive strength, MPa (psi)	Strength loss from cycle 1, %	Adjusted compressive strength, MPa (psi)	Strength loss due to clustering %
A	1	0.26	4.7	89 (3 ½)	39.1 (5670)	---	39.1 (5670)	---
	2	0.09	5.0	64 (2 ½)	37.9 (5500)	-3	38.6 (5600)	-2
	3	0.21	6.0	127 (5)	37.4 (5430)	-4	37.1 (5375)	+1
	4	0.17	6.2	114 (4 ½)	35.9 (5210)	-8	36.7 5330	-2

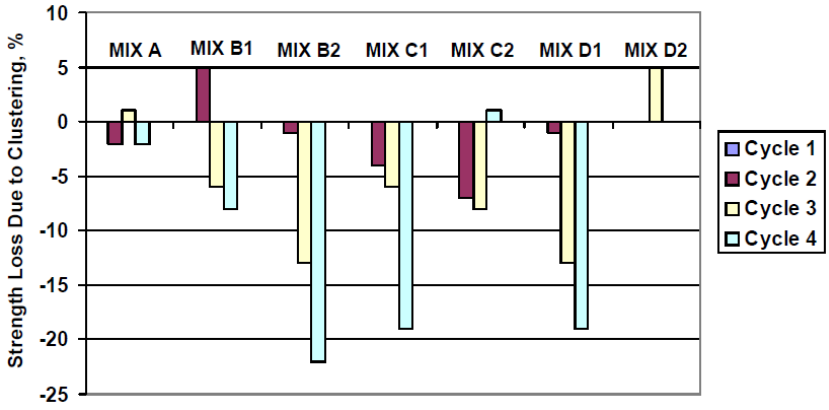

Figure 2-11 Percent strength loss attributable to air-void clustering for various mixes (Kozikowski et al, 2005)

Contrary to previous studies that found that non-vinsol resin AEA was responsible for air void clustering. Riding, Esmaeily, and Vosahlik (2015) reported that, in retempering mixes, types of AEAs had an effect on air void system generation, but no significant effect on clustering rating.

2.5.4 Temperature

28-day compressive strength decreases with increasing temperature, while air content in concrete increases (Hover, 1989). A case study has showed that air content tested using a roll-a-meter was around 6% in a cold environment and around 10%-12% at warmer temperatures. In this process, air void clustering was identified around the coarse aggregate. It seemed that the smallest air voids around the aggregate could not be detected in fresh concrete with cold weather (Hover, 1989). Another report on air void clustering by the South Dakota Department of Transportation (SDDOT) was based on work in the summer season. High temperature can increase the surfactant adsorption to the aggregate surface, so producing more stable air bubbles (Cross et al., 2000). Kozikowski et al (2005) indicated that the air-void clustering could increase at high temperature.

Taylor et al. (2006) reported two of three mixtures with air void clustering were made at 90°F.

2.5.5 Retempering

Even though retempering is not recommended, it is a common practice to control workability in the field (Kozikowski et al., 2005, Naranjo, A., 2007).

Kozikowski et al. (2005) designed a mixing procedure with a water addition to investigate the influence of retempering on air void clustering. The results showed that there is no sign of clustering in non-retempered concrete. However, retempering contributed to clustering formation.

Naranjo, A. (2007) reported that when retempering the concrete, there were more air voids formed around the aggregate. In most case, the clustering rating would increase with retempering, as shown in Figure 2-12. The mixtures with vinsol resin (14-17) performed differently, which might result from types of AEAs, but not retempering. In the plot of clustering rating versus air content, retempering mixtures with 0.48 w/c had higher clustering ratings than that of 0.48 w/c control mixtures without retempering.

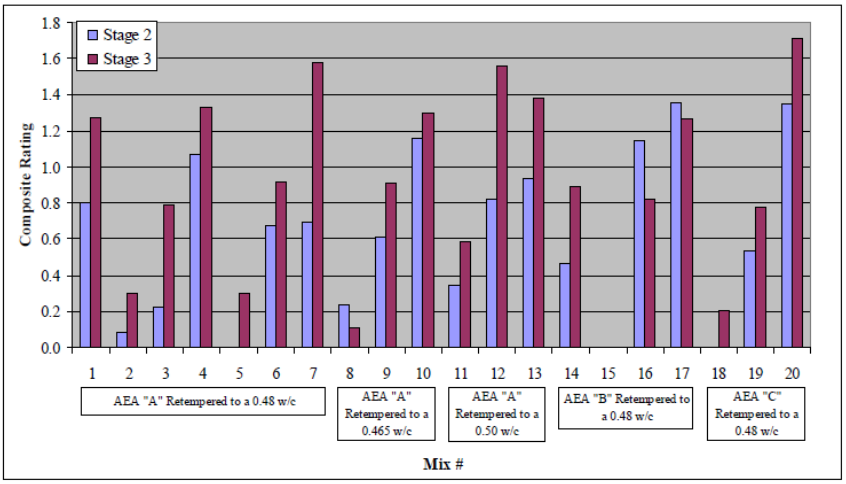

Figure 2-12 Change in composite rating after retempering (Naranjo, A. 2007)

Riding, Esmaeily, and Vosahlik (2015) conducted tests on mixtures with initial w/c ratios of 0.40 and 0.42. The corresponding initial w/c ratio after retempering was 0.43 and 0.45. The procedure was divided into two phases. Phase 1 had no retempering with initial w/c ratio, and Phase 2 had retempering with a w/c ratio of 0.03 increase. In addition, control mixtures with the

higher w/c ratio were also made without retempering. The data of clustering index and clustering rate from all concrete specimens are reported in Figure 2-13. In comparing clustering index before and after retempering, many mixes with retempering showed a smaller clustering index. They concluded that retempering had no significant effect on air void clustering.

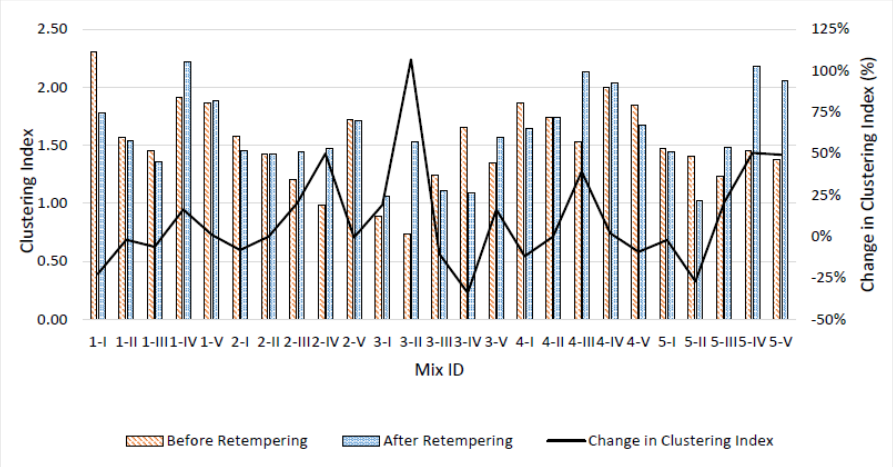

Figure 2-13 Clustering Index - Before and After Retempering（Riding et al., 2015)

Erdoğdu (2005) discussed a phenomenon called micelle formation in concrete, which is an aggregation of surfactant molecules in a liquid colloid, which could explain the increase of air content after retempering. If excessive surfactant is used in concrete, micelles are formed at the air-water surface, but do not contribute to reducing the surface tension of water. The retempering process disperses these micelles, and more available surfactant helps to form more entrained air voids. A good correlation between air content and clustering rating was found. So, an increase of air content promoted clustering growth.

2.5.6 Mixing Time and Vibration

More air bubbles are produced and absorbed on the aggregate surface with increasd mixing time. In retempered concrete, a prolonged mixing time increases the potential occurrence of air void clustering (Cross et al., 2000, Kozikowski et al., 2005).

Riding, Esmaeily, and Vosahlik (2015) suggested that concrete experiences an internal vibration during consolidation, thus, leading to clustering around the coarse aggregate.

2.5.7 Air Content

Air void clustering has a positive correlation with air content. With the retempering process, mixtures with air content more than 6% had a large increase of clustering ratings, even through the air content change was small (Naranjo, A. 2007).

2.6 Test Methods of Air Void Clustering

An air void clustering rating system method was established by Kozikowski et al. (2005). The rating system has four levels (0-4). Each number represents a different level of severity of air void clustering. For example, ‘0’ indicates that the concrete has no air void clustering, and ‘4’ shows that the concrete has severe clustering. The photos in their project are used as a visual reference to determine the clustering situation in concrete, shown in Figure 2-14.

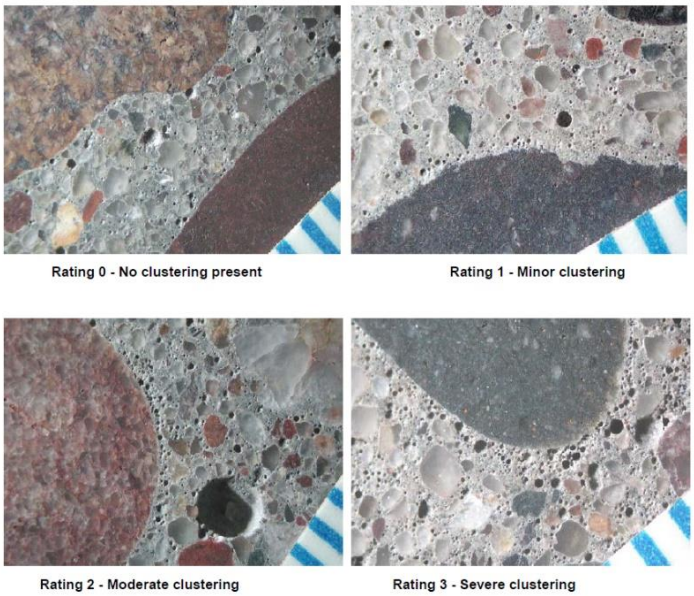

Figure 2-14 Clustering Categories (Kozikowski et al 2005)

The clustering analysis sample is made by cutting a concrete cylinder, shown in Figure 2-15(a). The completed sample is shown in Figure 2-15(b). All samples are polished using a procedure developed by Ley (2007). Then all the polished samples are scanned in a photo scanner. (Kozikowski et al 2005).

Figure 2-15 Cutting setup and cut sample (Riding et al. (2015)

Only coarse aggregate particles greater than 0.25 inches are rated. Each particle is assigned one of the clustering categories. The average clustering rating is defined as the sum of the rating values divided by the number of aggregate particles.

Figure 2-16 and Table 2-3 gave an example for how to calculate the average clustering rating (Taylor et al. 2006).

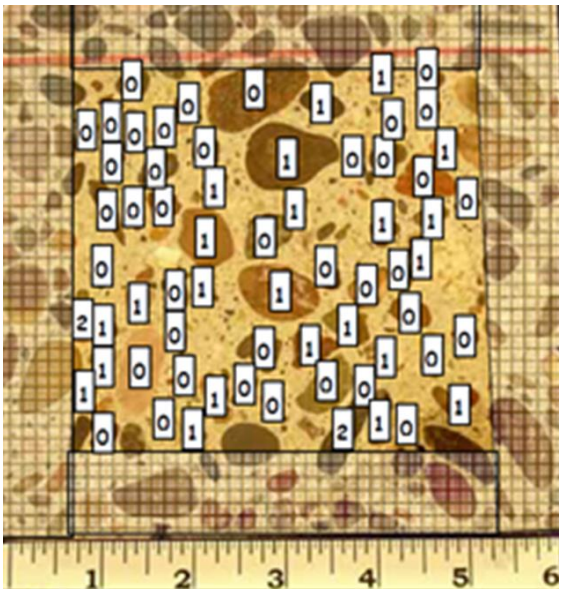

Figure 2-16 Clustering rating for a cylinder (Taylor et al, 2006).

Table 2-4 Calculations for average clustering rate (Taylor et al, 2006).

Clustering Rating	Aggregates Affected	Calculation
0–None	39	0 × 39 = 0
1–Minor	24	1 × 24 = 24
2–Moderate	2	2 × 2 = 4
3–Severe	0	3 × 0 = 0
Sum	65	28
Clustering rate = 28/65 = 0.43		

This rating system brings convenience to the study of different factors affecting air void clustering. However, there are still some errors and imprecisions. For example, only one sample is used for determination, and the clustering rating is the average value representing the whole sample. In order to get a more accurate conclusion, the rating technique still needs further refinement.

Riding, Esmaeily, and Vosahlik (2015) utilized particular software, the KSU Void Analyzer, to quantify air clustering severity. In this analysis, the software provides two important parameters: area of particles and the location of air void centroid. The area of a particle should be more than 20,000,000 pixels (0.86 inch2). Before testing, a boundary line is drawn around particles. The distance between the particle and the boundary line is the thickness of the clustering layer, which corresponded to the resolution of 100 pixels. 0.26 mm is selected as the thickness of the clustering layer. Only an air void with a diameter less than 0.52 mm is included in the analysis (Figure 2-17). The total percentage of air void within the clustering layer is recorded. The local values are determined through the software and are compared to the total air content of the sample. The clustering index is defined as air void content of the clustering layer over the total air void content of the whole sample.

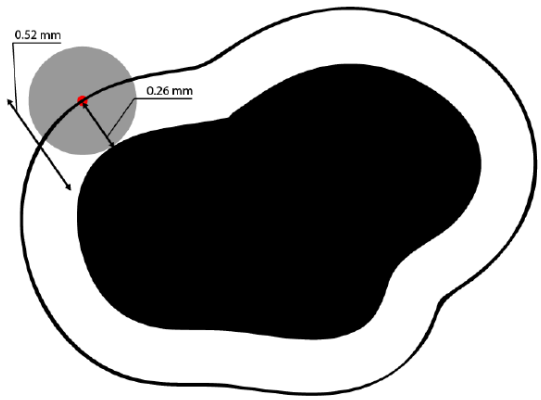

Figure 2-17 Clustering zone Riding et al. (2015)

Comparing, the above two methods, clustering rating was gained by visual evaluation and manual calculation, and the clustering index was obtained through image processing techniques. The clustering evaluation result from the two methods was not 100% matched. It was found that the manual analysis had a lack of objectivity and that visual judgment by a human tend to overrate the level of clustering severity (Riding, Esmaeily, and Vosahlik, 2015)

However, Esmaeily et al. (2016) discussed the clustering idex developed by Riding et al. (2005) and found the parameters used in their study could not result in air void clustering formation. Thus, the clustering index was invalid to measure the severity of air void clustering.

2.7 Effects of Air Void Clustering on Concrete Properties

Strength reduction related to air void clustering was reported by Paul in 1988. Under the microscope, reduction of interface bonding between cement paste and the aggregate could have been caused by air bubbles collected around coarse aggregate particles (Hover, 1989). These accumulated air voids at the paste/aggregate interface form a zone of weakness. When load is applied to the concrete, cracks propagate through the air voids around aggregates causing premature failure (Kozikowski et al. 2005).

In the summer of 1997, the South Dakota Department of Transportation (SDDOT) reported an unexpected series of compressive strength tests, which had a low compressive strength at 28days. Air void clustering was observed through scanning electron microscopy (SEM) examination and was regarded as a possible cause of the low compressive strengths. Figure 2-18 (A), illustrates a high strength sample with rare low concentration of air void clustering and (B) shows a low strength sample with a high concentration of clustering. There was no other evidence to explain how the concrete cylinders exhibited low compressive strength.

In further research conducted by SDDOT, SDM&T, and Campbell, low-strength specimens exhibited a low bonding between the cement paste and aggregate. A high concentration of air voids at the aggregate interface was clearly seen, which was absent in normal strength specimens (Cross et al., 2000).

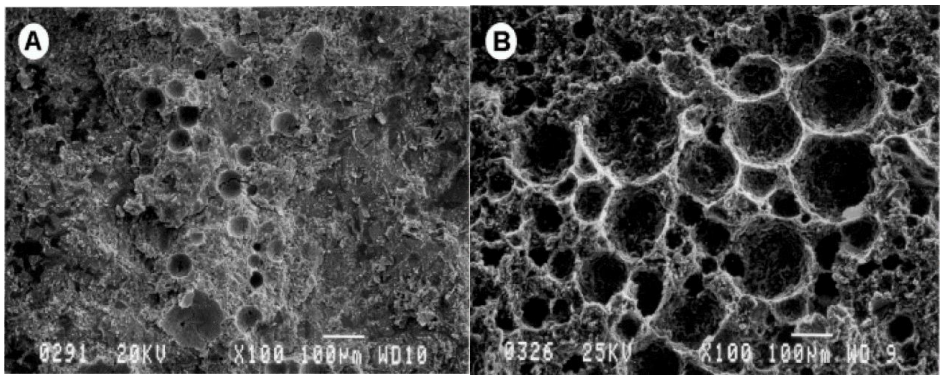

Figure 2-18 SEM micrographs of relatively high strength sample (A, 4622 psi) and relatively low strength sample (B, 3663 psi) (Cross et al., 2000)

Kozikowski et al. (2005) prepared concrete mixtures with non-vinsol AEAs that were retempered from 0.39 of w/c to 0.42, along with control samples at w/cm = 0.42 that were not retempered. A negligible effect was observed on compressive strength with 0.03 the in w/c, indicating the impact of the observed clustering. A plot of compressive strength and average clustering rating also demonstrated that when the clustering rating exceeded 1.0, the compressive strength exhibited a drop, as shown in Figure 2-19. However, Kosmatka et al. (2003) indicated that around an 8% compressive strength decrease should be expected with an increase of w/c of 0.03.

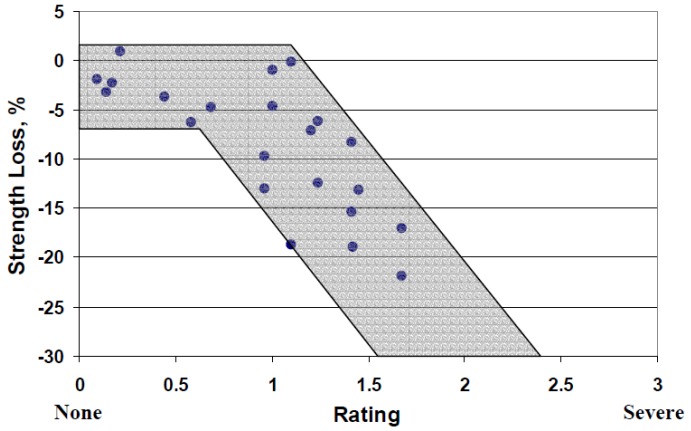

Figure 2-19 Relationship between clustering rating and Strength loss (Kozikowski et al 2005)

Ram et al. (2013) conducted research on air content system in slip form paving concrete for the Wisconsin DOT. The scanned images of extracted core specimens from the pavement are shown in Figure 2-20. According to the images, it was clear that air void clustering was generated around the aggregate which may have caused strength loss. However, the correlation between air void clustering and compressive strength was not established in this study.

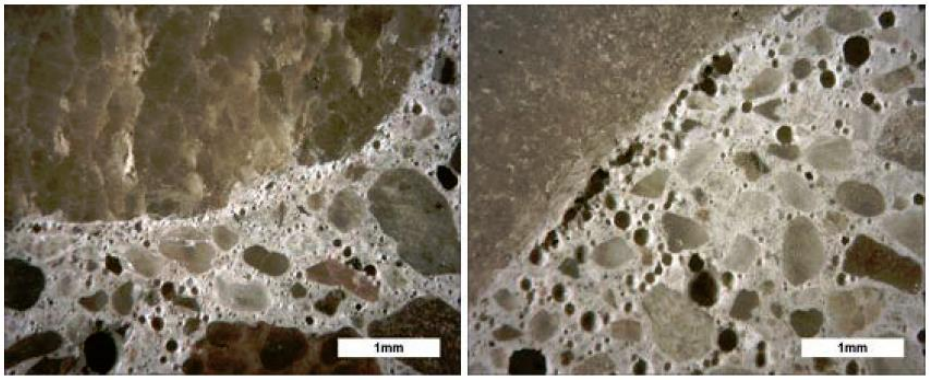

Figure 2-20 Scanned images of extracted core from pavement (Ram et al 2013)

Guo et al. (2017) compared an ultrasonic technique with the ASTM C457 test to evaluate air void properties at early and hardened ages. The results showed that even though two types of samples had similar air void contents, there was a significant difference in strength. Thus the

relationship between air content and compressive strengthwas not linear. According to the scanned pattern of concrete slabs in Figure 2-21, both types of concrete had similar air contents. More small air voids were clearly observed in the ITZ area in a Type 3 sample (Table 2-5) with a much higher loss of strength than a Type 2 sample. This indicated that air void distribution as clustering around coarse aggregates could reduce the bond between aggregates and cement paste.

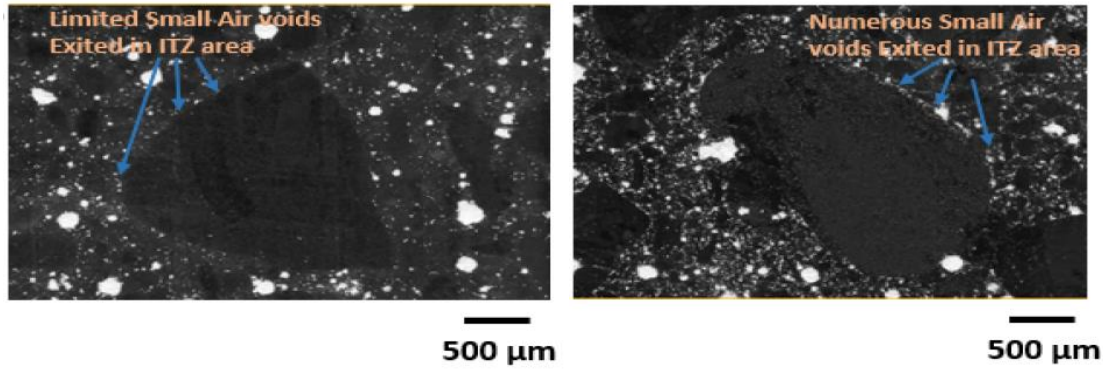

Figure 2-21 Scanned pattern of concrete slabs of sample type 2(left) and type3 (right) (Shuaicheng Guo et al., 2017)

Table 2-5 Compressive strength for 3 types of sample (Shuaicheng Guo et al., 2017)

Sample	Compressive Strength (MPa)		
	Day 3	Day 7	Day 28
Type 1	35.8	42.4	48.7
Type 2	29.0	37.7	45.1
Type 3	20.1	25.1	30.0

Monhamad et al. (2007) conducted an experimental program to identify the important factors affecting air entrained concrete and to check if strength was related to air void clustering. According to the comparison between relative low strength specimen with 3390 psi and normal strength specimen with 3750 psi, similar air bubble performance was shown in micrographs in

Figure 2-22. The air contents of relatively low strength and high strength sample were 6.6 and 7.7 percent respectively. Therefore, it seems that strength reduction was not attributed to air void clustering but might result from high air content.

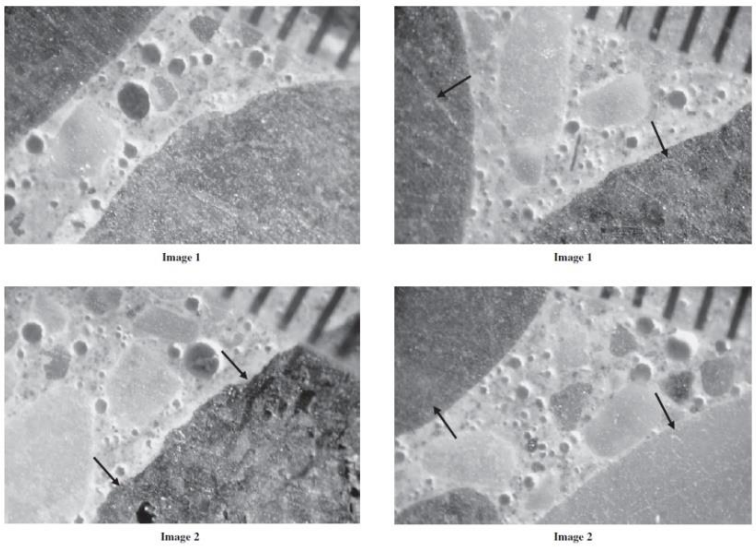

Figure 2-22 Stereomicroscope images of relatively low strength (left two) and relatively high strength samples (right two) (Monhamad et al (2007)

Naranjo, (2007) separately determined the potential change of strength due to clustering at each mix in Table 2-6. The result showed no significant strength loss was observed. Figure 2-23 of 28-day compressive strength vs air content also indicated that the strength loss was due to w/c increase and not air void clustering.

Riding et al. (2015) also did similar tests and concluded that the strength loss after retempering might be related to the air content and water-cement ratio. No correlation was found between air void clustering and compressive strength.

Table 2-6 Compressive strength loss due to Air void clustering (Naranjo, A., 2007)

Mix #	Stage	Air Content, %	Actual Compressive Strength, psi	Adjusted Compressive Strength, psi	Strength Change Potentially due to Clustering, %
1	1	2.1	7630	7630	
	2	5.8	5580	5820	-4.3
	3	6.1	5370	5210	3.0
2	1	2.0	7940	7940	
	2	4.1	6700	6860	-2.4
	3	4.5	6410	6200	3.3
3	1	1.7	7640	7640	
	2	5.9	5600	5580	0.4
	3	6.2	5280	4970	5.9
4	1	1.9	7710	7710	
	2	8.4	4430	4500	-1.6
	3	9.0	3810	3740	1.8
5	1	2.0	7880	7880	
	2	4.0	7030	6860	2.4
	3	3.7	6790	6560	3.4
6	1	2.1	8400	8400	
	2	6.9	5680	5770	-1.6
	3	6.8	5400	5380	0.4
7	1	2.1	8190	8190	
	2	8.5	4990	4830	3.2
	3	9.0	4380	4110	6.6

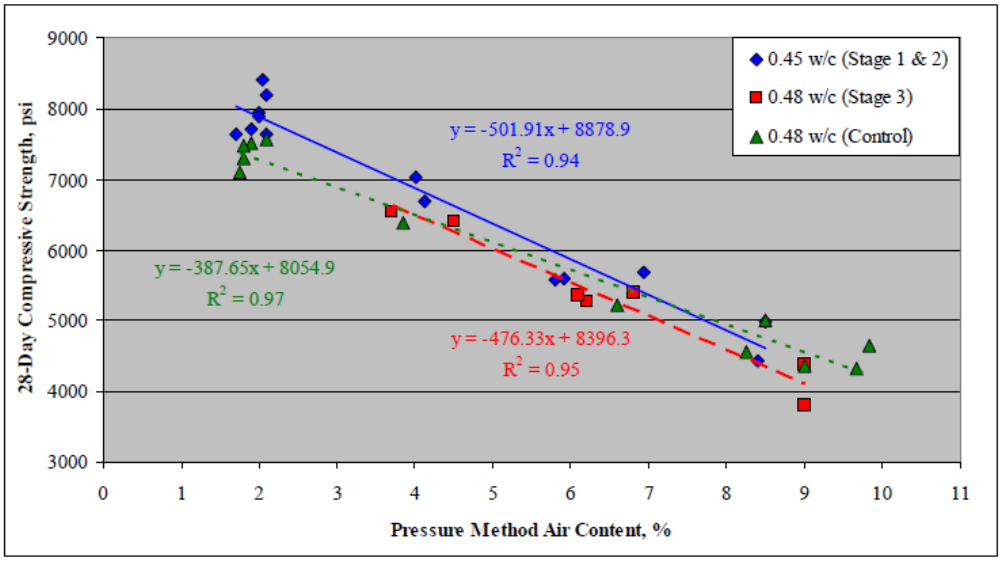

Figure 2-23 28-Days compressive strength vs Air content (Naranjo, A., 2007)

CHAPTER 3. EXPERIMENTAL WORK

In this study, six variables were considered in the experimental matrix. For each variable, there were two options. A full factorial design of 6 variables would require a total 64 (2^6) mixtures. Low alkali (LA) cement and Type IL (TIL) cement were adopted as cement. Fly ash with high carbon (A) content and low carbon (B) content were used. Limestone (L) and river gravel (G) were adopted as coarse aggregate. As for chemical admixture type, one had less effect on clustering (1) and the other had a much effect on clustering (2) based on chemical composition. With (Yes) or without (No) retempering for mixtures was regarded as different mixing procedures. 70℉ and 90℉ were adopted as temperature levels of mixing water. Besides the above 64 mixtures, additional mixtures with a concrete temperature of 90 ℉ were also made to investigate effect of high temperatures on clustering. A statistical method was used for analysis of the results.

3.1 Materials

3.1.1 Cement

Two types of cement were used in this study, including Type IL cement and low alkali cement. The chemical composition of the cements in this research study are presented in Table 3-1.

Table 3-1 Cement characteristics

Cement Type	Chemical Composition											
	SiO_2	Al_2O_3	Fe_2O_3	SO_3	CaO	MgO	K_2O	Na_2O	P_2O_5	TiO_2	SrO	Mn_2O_3
Low alkali cement	21.08	4.19	3.27	2.95	64.27	2.42	0.53	0.13	0.06	0.25	0.09	0.07
TIL cement	20.07	4.9	3.43	3.28	65.5	0.94	0.69	0.13	0.16	0.25	0.19	0.28

Note: Equivalent alkali content (%Na2O + 0.658 × %K2O) is 0.48% for LA and 0.58% for TIL.

3.1.2 Fly Ash

Two sources of Class C fly ash were adopted in this study. The quality of fly ash has effects on concrete, which depends on fineness, LOI content, chemical composition, moisture content, etc. The chemical characteristics are shown in Table 3-2. The big difference between Fly ash A and Fly B was LOI value, indicating different carbon content in fly ash. Fly ash B has a better quality with lower LOI.

Table 3-2 Chemical composition of fly ash

Fly ash	Chemical Composition											
	SiO_2	Al_2O_3	Fe_2O_3	SO_3	CaO	MgO	K_2O	Na_2O	P_2O_5	TiO_2	BaO	SrO	Mn_2O_3
Fly ash A	40.72	20.45	6.08	1.02	21.61	4.35	0.63	1.36	0.83	1.51	0.58	0.31	0.04
Fly ash B	38.49	21.92	6.04	1.04	22.43	4.17	0.6	1.53	1.1	1.57	0.58	0.32	0.05

Note: LOI of Fly ash A is 2.00 %; Moisture of Fly ash is 0.07%
LOI of Fly ash B is 0.21 %; Moisture of Fly ash is 0.03%

3.1.3 Aggregate

Natural river sand was selected as fine aggregate in all mixtures. Two types of coarse aggregate were adopted: limestone (L) and river gravel (G). Aggregates properties were

determined in accordance with ASTM C127 (2012) and ASTM C136 (2006). The aggregate properties are presented in Table 3-3, and the gradation curves are shown in Figure 3-1. Two types of coarse aggregates were included because of their reported effect on air void systems and air void clustering. Limestone had a crushed surface and an angular shape with a lower absorption capacity of 0.55%. The river gravel had a round shape and smooth surface with a higher absorption capacity of 1.67%.

Table 3-3 Aggregate properties

Materials	Specific Gravity (SSD)	Specific Gravity (OD)	Absorption Capacity (%)
Natural Sand	2.65	2.61	1.49
Coarse Limestone	2.70	2.69	0.55
River Gravel	2.68	2.63	1.67

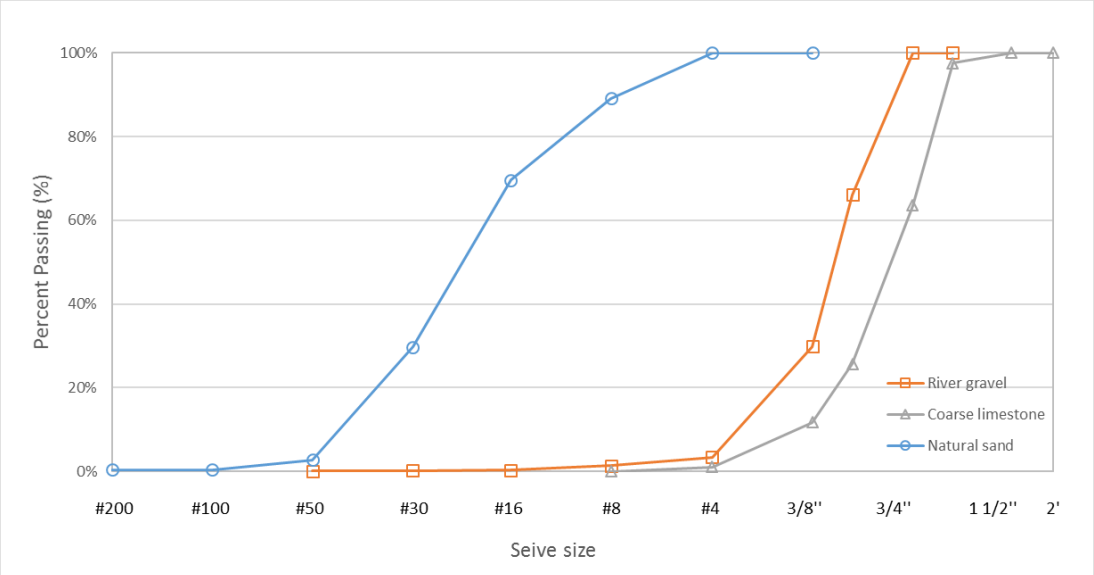

Figure 3-1 Gradation curve of fine and coarse aggregate

3.1.4 Chemical Admixture

Two types of chemical admixture were used in this study. The characteristics of each are shown in Table 3-4. As for the type of AEAs, vinsol-rosin based and vinsol-amine-fatty acid were adopted. As for water reducer, polycarboxolate based was used in both types of chemical admixture, but the gravity was different.

Table 3-4 Characteristics of chemical admixture

Chemical number	Name	Composition	Gravity
1	AEA	vinsol-rosin based	1.03
	WRs	polycarboxolate based	1.03
2	AEA	vinsol+amine+fatty acid	1.10
	WRs	polycarboxolate based	1.10

3.2 Mix proportion

Two groups of concrete with and without retempering were adopted in this study. All mixtures had an initial w/c of 0.42 and mixtures with retempering were later retempered to increase the w/c to 0.45. The target air content without retempering was 5%-7%. The mixture proportions are summarized in Table 3-5.

Table 3-5 concrete mixture proportions with or without retempering (lb/yd^3)

Concrete Type	Cement (LA or TIL)	SCM (A or B)	Mixing Water70°F and 90°F	Retempering Water	w/c	Aggregate	
						Fine (natural river sand)	Coarse (Limestone or Gravel)
Without retempering	439	110	230	-	0.42	1347	1785
With retempering	439	110	230	17	0.45	1347	1785

3.3 Sample Preparation

A drum mixer was used to perform mixing. The concrete mix procedure followed ASTM C192 (2013) and the volume of each mixture was designed to be $1ft^3$. For each mixture, two groups of samples were prepared with or without retempering.

For the group without retempering, before mixing, the temperature of water was controlled at 70°F or 90°F. The coarse aggregates and AEA were first placed in the mixer and mixed for the 30s. Sand and three-quarters of water are added to the mixer and mixed for another 30s. The cement and fly ash were added with the rest of the water. 3 minutes for mixing, 3 minutes for rest and another 2 minutes for mixing were conducted. After finishing, fresh properties of concrete were measured including temperature, slump, unit weight and air content. Nine cylinders were cast for compressive strength and imaging analysis including air void clustering evaluation and air-void analysis. Sample preparation was otherwise in accordance with ASTM C192. All cylinders are covered in the laboratory for 24 hours and then stripped and placed in the curing chamber at 72 ℉ and relative humidity of 99%.

For the group with retempering, after the mixing procedure, the concrete stayed in the drum mixer for 15 minutes. Retempering water was then added to the concrete with another 2 minutes mixing. The same tests and cylinder casting were performed as the group without retempering.

For the high temperature mixtures, all the materials were heated to 90°F in a hot-room before mixing.

3.4 Tests and Methods

All mixtures were tested for hardened properties containing compressive strength, air void clustering and rapid air analysis.

3.4.1 Fresh Concrete Properties

In this study, slump, unit weight and air content were measured for each mixture. The procedure for each above test was followed by ASTM C138, ASTM C143 and ASTM 231 respectively.

3.4.2 Compressive Strength

All the sample cylinders were cast into 4x8 inch molds and placed in room temperature for the first 24 hours. Specimens were then demolded and moved into curing room with standard environment conditions (72°F, 99% relative humidity). Two specimens were tested at each of 7 and 28 days. The compressive strength testing was in accordance with ASTM C39. The compression test machine used in this test, is shown in Fig.3-2.

Figure 3-2 Compressive test machine

3.4.3 Air void Clustering Evaluation

Air void clustering evaluation consisted of three processes, including sample cutting, sample polishing and sample rating. The reference pictures were utilized to compare with sample image and a clustering value was rated based on comparison.

3.4.3.1 Sample preparation

A 4x4x1 in sample was prepared for air void clustering testing as shown in Figure 3-3. After cutting, the samples were marked with an orthogonal grid by ink pen (Figure 3-4 a) and then polished until all of the marking was removed to ensure uniform polishing. The polishing equipment used is shown in Figure 3-4(b). Typically, about 35 coarse aggregate particles above 0.5-in were selected to be marked by black pen as shown in Figure 3-4 (c).

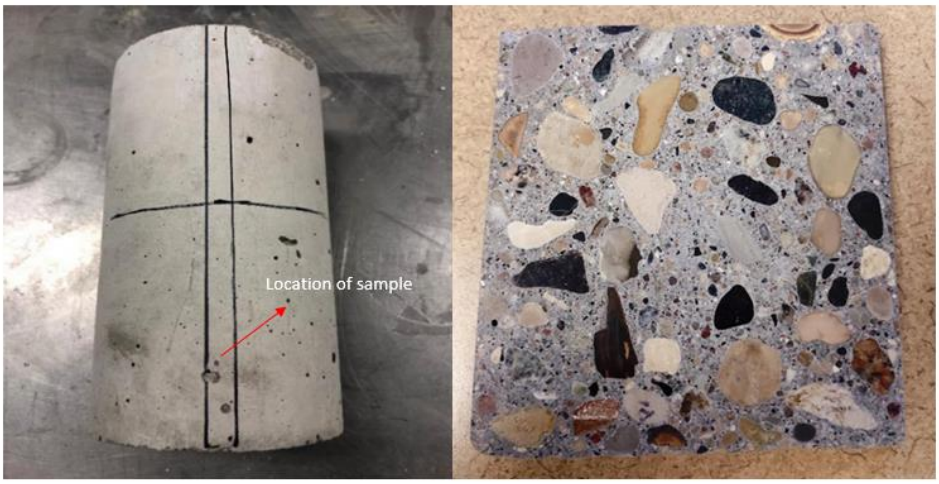

(a) Indicator line for cutting (b) Cut sample

Figure 3-3 Cutting sample preparation

(a) Sample drawn with orthogonal grid (b) Polishing disk and machine

(c) Polished sample with marked number

Figure 3-4 Sample preparation for clustering rating

3.4.3.2 Air Void Clustering Rating

The air void clustering rating method used in this study was developed by Kozikowski et al. (2005). After sample marked shown in Figure 3-4 (c), each aggregate particle was rated for clustering severity under a stereo microscope. The rating of clustering severity was based on the visual reference pictures. Each aggregate rating was recorded, and the sum of ratings divided by a number of selecting aggregates was used to report clustering severity of the sample. A sample calculation is shown in Table 3-6 below.

Table 3-6 Sample calculation for clustering rating of one specimen

Mix ID	Number of aggregates for each clustering rating level				Average clustering
	0	1	2	3	(0x13+1x19+2x2+3x1)/35=0.74
15	13	19	2	1	

3.4.4 Rapid Air Analysis

The steps of preparation for hardened air-void analysis is shown in Figure 3-5. A Rapid-Air 457 analyzer was used in this study. The provided software was used for analysis, and the test steps were based on ASTM C 457. Some critical settings of software for air void analysis was mention here. The grey-threshold was set up as 170, which was dependent on image comparison between raw image and analysis image. If the green area in the analysis image matched air voids in the raw image, the selected threshold value was suitable for testing (Hanson, 2012), shown in Figure 3-6. The traverse length was determined by maximum aggregate size. 2413 mm (95in) was used in this study because the aggregate size was 25 mm (1.0 in). Three lines per analysis frame were chosen based on guidance by Naranjo (2007).

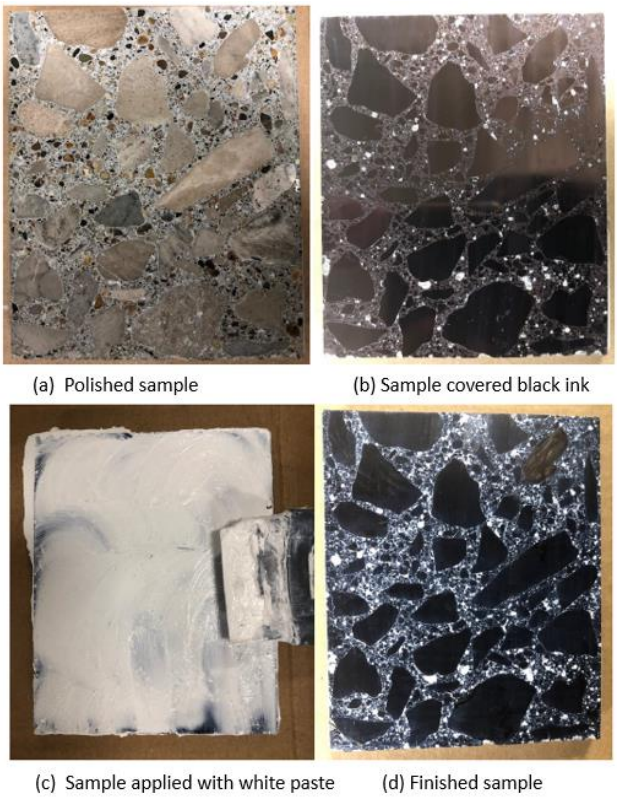

Figure 3-5 Sample preparation steps for rapid air void analysis

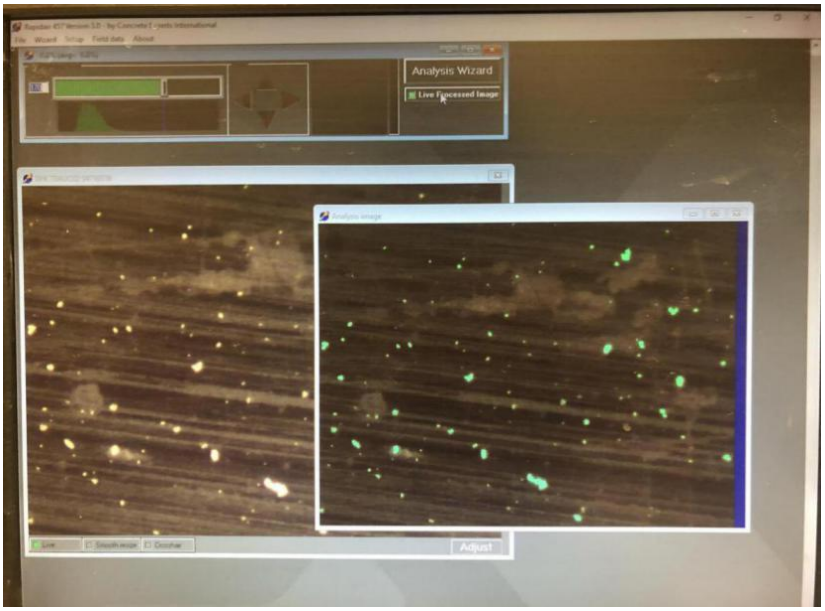

Figure 3-6 Screenshot of CXI software

3.4.5 Statistical Analysis

Six independent variables were included in the laboratory study to investigate their effects on concrete properties and air void clustering: cement type (CMT), fly ash type (FAT), aggregate type (AGT), admixture type (ADT), mixing water temperature level (MWT) and retempering process (RTP). The result was analyzed in JMP, a statistical software package. When multiple variables were in a linear regression model, multicollinearity could happen in that two high correlation independent variables caused an incorrect conclusion. If one variable had a significant effect on the result, the correlated variables that showed as insignificant appeared to be significant when they were taken as a group (Mohamad A. Nagi et al 2007). To decrease effect of multicollinearity among independent variables in the analysis, a stepwise linear regression method was utilized.

Stepwise linear regression controlled multiple variables by adding or subtracting to the model one by one with specific requirements and left the variables that best explained the results. In this study, six main effect independent variables and all possible interactions among the main variables were considered. A 95% significance level was used in this study, which meant that the variables with P-value smaller than 0.05 had a significant effect on response in the model. R^2 equal to 0.50 represented 50% of response could be explained by the variables. If the R^2 was high, the response could be adequately predicted by variables. If the R^2 was small, the response was influenced by variables to a lesser degree, and kept relatively stable (Mohamad A. Nagi et al. 2007).

CHAPTER 4. RESULTS AND DISCUSSION

Six variables were considered in this study: cement type (CMT), Fly ash type (FAT), coarse aggregate type (AGT), chemical admixture type (ADT), retempering (RTP) and mixing water temperature (MWT). The Mix ID was used to present combination of different variables in each mixture. The Mix ID was arranged as shown in Figure 4-1. For example TIL-A-1-L-70 meant that the mixture used TIL cement, fly ash A, limestone and 70°F mixing water. The effects of these variables on concrete performance were analyzed.

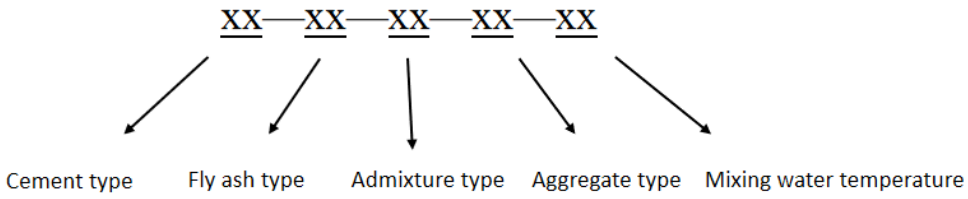

Figure 4-1 The Mix ID arrangement

4.1 Fresh Concrete Properties

4.1.1 Fresh Property Result and Observation

The Fresh properties of concrete with and without retempering are shown in Table 4-1.

Table 4-1 Fresh Concrete Properties

Mix Number	Mix ID	Slump(in)		Unit Weight (lb/yd^3)		Air Content (%)	
		No	Yes	No	Yes	No	Yes
1	TIL-A-1-L-70	1.6	2.1	146.80	147.40	6.2	4.3
2	TIL-A-1-L-90	2.2	3.0	145.32	146.92	6.3	5.0
3	TIL-A-1-G-70	2.1	2.4	147.20	148.40	5.0	3.9
4	TIL-A-1-G-90	1.8	2.6	147.20	148.20	6.0	3.8
5	TIL-A-2-L-70	1.0	3.0	144.20	142.80	6.7	7.2
6	TIL-A-2-L-90	1.0	2.5	146.60	145.60	6.0	6.1
7	TIL-A-2-G-70	2.0	5.0	146.40	145.40	5.7	5.6
8	TIL-A-2-G-90	2.0	4.3	145.00	144.20	5.8	6.3
9	TIL-B-1-L-70	1.3	3.6	146.20	141.60	6.3	8.0
10	TIL-B-1-L-90	1.4	3.2	146.00	141.60	6.1	7.9
11	TIL-B-1-G-70	3.4	7.0	143.80	142.80	6.9	7.2
12	TIL-B-1-G-90	2.0	2.5	146.00	145.60	5.6	5.6
13	TIL-B-2-L-70	1.8	3.4	147.40	146.40	5.2	5.3
14	TIL-B-2-L-90	1.5	3.3	147.00	145.60	5.5	6.0
15	TIL-B-2-G-70	1.5	2.7	147.00	147.00	5.0	4.9
16	TIL-B-2-G-90	2.3	4.8	143.80	142.00	7.0	7.3
17	LA-A-1-L-70	1.8	2.2	147.00	147.40	5.6	5.5
18	LA-A-1-L-90	2.8	4.2	143.60	144.40	6.6	6.6
19	LA-A-1-G-70	1.0	2.5	147.20	144.00	5.5	6.0
20	LA-A-1-G-90	0.6	2.0	146.80	146.20	5.4	6.6
21	LA-A-2-L-70	1.5	2.2	147.60	146.80	5.0	4.5
22	LA-A-2-L-90	2.6	3.2	145.20	142.80	6.3	6.9
23	LA-A-2-G-70	2.7	3.6	145.80	145.40	5.1	5.0
24	LA-A-2-G-90	2.1	3.8	147.00	145.60	5.0	5.3
25	LA-B-1-L-70	0.8	2.5	148.00	145.20	5.2	6.5
26	LA-B-1-L-90	2.5	3.5	144.80	142.80	6.7	7.4
27	LA-B-1-G-70	1.5	3.0	148.40	142.40	5.0	6.4
28	LA-B-1-G-90	1.7	2.6	147.00	146.20	5.1	5.3
29	LA-B-2-L-70	1.2	3.0	147.20	142.60	5.4	7.9
30	LA-B-2-L-90	2.7	3.4	146.80	145.60	5.6	6.5
31	LA-B-2-G-70	1.0	3.0	147.20	146.00	5.5	6.0
32	LA-B-2-G-90	2.2	4.1	144.80	142.60	6.7	7.6

Note: TIL= TIL 1 cement; LA=Low alkali cement; A=Low quality fly ash; B=High quality fly ash; 1=less effect on clustering; 2=more effect on clustering; L=limestone; G=gravel; 70=70°F mixing water; 90=90°F mixing water; No= without retempering, Yes=with retempering

The slump test results are presented in Figures 4-2 and 4-3. In all mixes, the slump was increased after retempering, as expected.

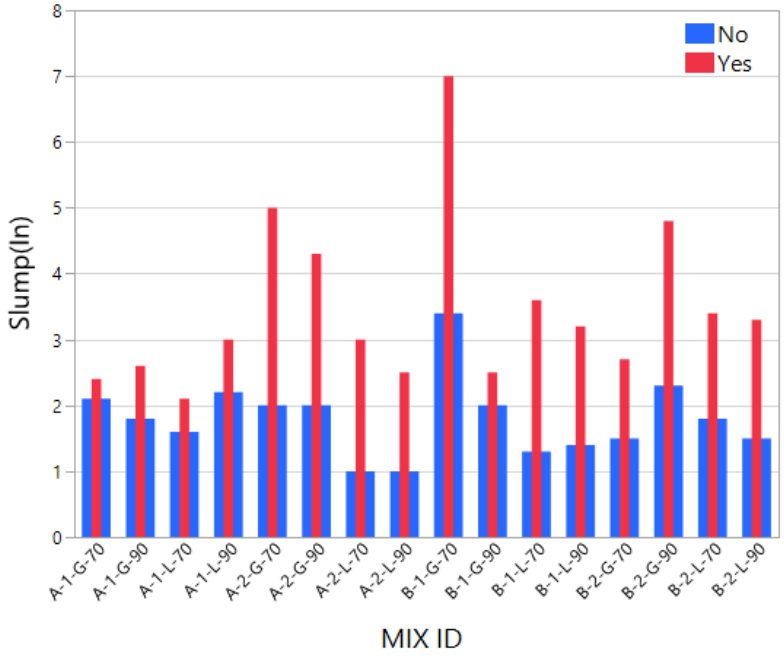

Figure 4-2 Slump –TIL cement

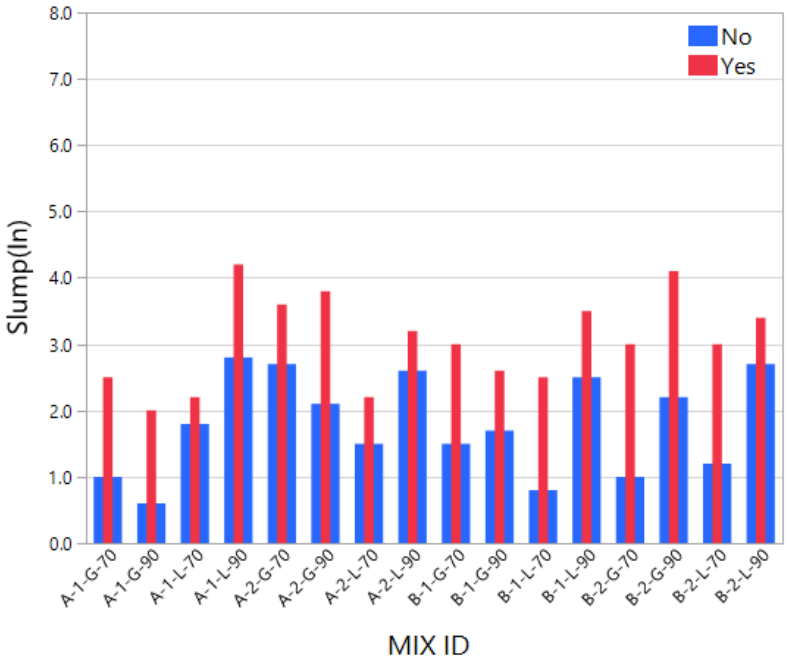

Figure 4-3 Slump –LA cement

The air content results are presented in Figures 4-4 and 4-5 For TIL cements, a large reduction of air content was observed in four retempering mixtures. All four of these mixtures included fly ash A, type 1 admixture. For most of the low-alkali cement mixtures, air content increased or kept stable with retempering. Mixtures with stable or litter smaller air content with retempering resulted from some uncontrolled reasons, for example, the retempering mixtures were tested in later stages than were initial mixtures.

The Unit weight results are presented in Figures 4-6 and 4-7. With retempering, unit weight decreased in most mixtures. The few mixtures with unit weight increase after retempering corresponded to those with air content change, as seen in previous figures.

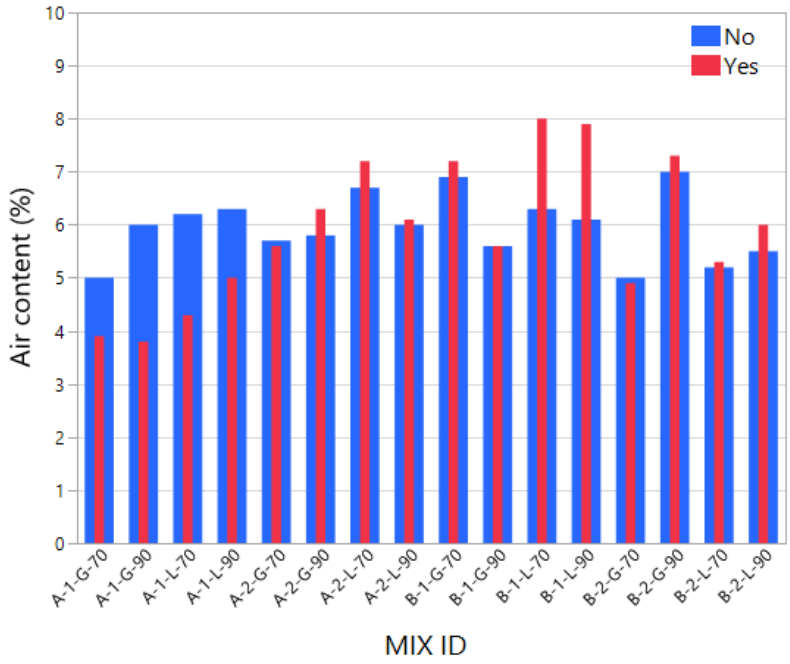

Figure 4-4 Air content-TIL cement

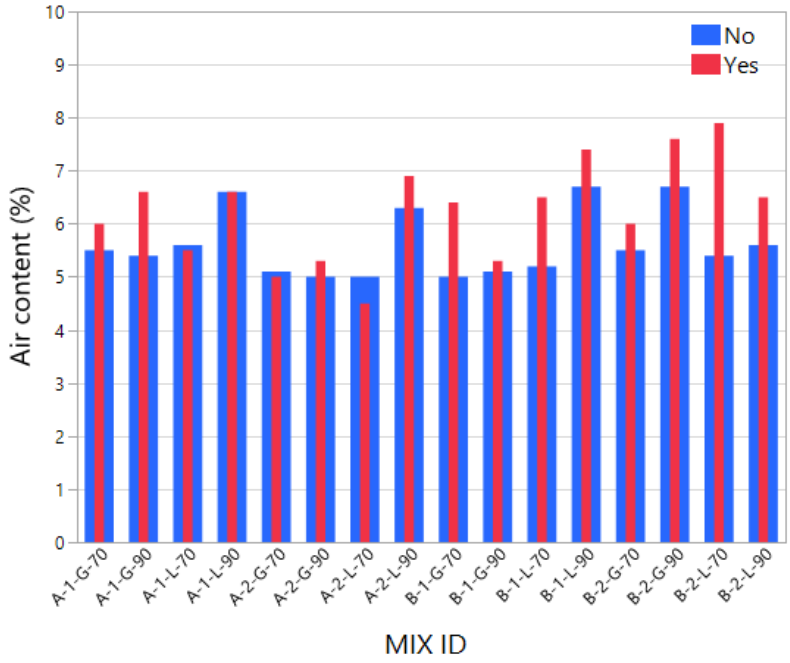

Figure 4-5 Air content-LA cement

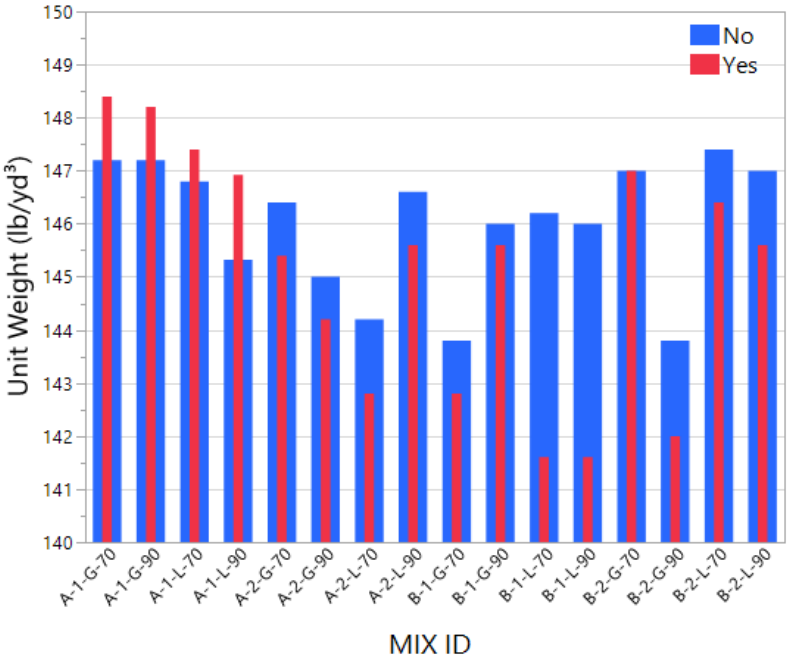

Figure 4-6 Unit weight-TIL cement

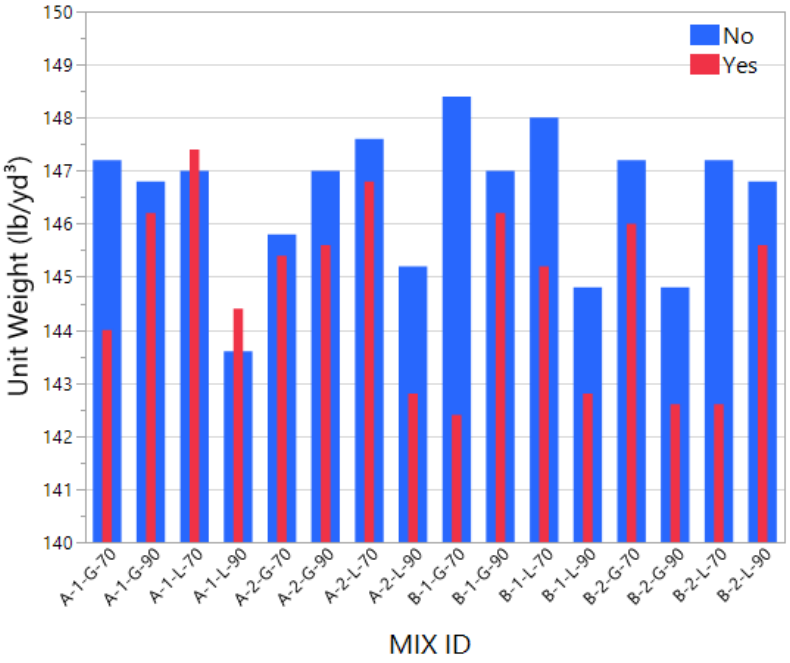

Figure 4-7 Unit weight-LA cement

4.1.2 Statistical Analysis for the Result of Fresh Properties

4.1.2.1 Slump

The statistical analysis of slump test data is shown in Table 4-2. The coefficient of determination (R^2) was 0.698 indicating 69.8% of slump test could be predicted by the listed independent variables. Significant individual effect on slump was the RTP as P-value of RTP<0.0001 below 0.05. Significant two-way interaction effects included CMT*AGT, CMT*MWT and AGT*MWT. Significant three-way interaction effect included FAT*ADT*AGT, FAT*ADT*MWT, ADT*AGT*MWT. The relative effects of a change in significant variables on slump could be judged by coefficients are listed in Table 4-2 in the last column. The negative coefficient indicated a reduction effect, and the positive coefficient indicated growth effect. The absolute value of the coefficient showed the magnitude of the impact on slump by variables. For example, the coefficient of RTP was -0.7281, and it indicated

0.7281 inch slump reduction if mixtures were without retempering compared to mixtures with retempering. On average, the slump of mixtures with retempering increased by 83%.The retempering increasing slump observed in Table 4-2 was consistent with previous observation of data. Although the other individual variables had no significant effect on slump, the interactions among cement type, aggregate type, fly ash type, admixture type and mixing water temperature did affect slump as shown in Table 4-3.

Previous research mentioned that an increase of alkali content in concrete reduced workability because of the acceleration of cement hydration by alkali cation (Li, Afshinnia, and Rangaraju 2016). However, in this study, cement type did not show significant effect on slump. That might be because of the small difference of alkali content between TIL cement mixtures and Low alkali cement mixtures.

Based on the above discussion, the major finding of the statistical analysis was that RTP was the most important individual factor affecting slump.

Table 4-2 Statistic analysis of slump test result

Rsquare (adj)=0.698			
Independent variables	P-value	Independent variables	Coefficient
RTP	<.0001	RTP[No]	-0.7281
CMT*AGT	0.0036	CMT[LA]*AGT[G]	-0.2375
CMT*MWT	0.0069	CMT[LA]*MWT[70]	-0.2188
AGT*MWT	0.0117	AGT[G]*MWT[70]	0.2031
FAT*ADT*AGT	0.0013	FAT[A]*ADT[1]*AGT[G]	-0.2656
FAT*ADT*MWT	0.0095	FAT[A]*ADT[1]*MWT[70]	-0.2094
ADT*AGT*MWT	0.0040	ADT[1]*AGT[G]*MWT[70]	0.2344

Note: CMT =cement type, FAT=Fly ash type, AGT= coarse aggregate type, ADT= chemical admixture type, RTP= retempering; MWT=mixing water temperature

Table 4-3 Mean Slump for significant variables

Independent Variable		Mean Slump	% Change in slump measurement (%)
RTP	No	1.8	83.3
	Yes	3.3	

4.1.2.2 Air content

Statistical analysis of air content is shown in Table 4-4. The coefficient of determination (R^2) indicated that 82.4% of air content result could be predicted by list independent variables. Significant individual factors effecting air content were FAT, AGT, RTP and MWT. According to the analysis, a few interactions among two, three, or four variables were observed, which indicated complex chemical or physical interactions occurring in the concrete mixture. All these interactions would influence the individual variable effect on air content. Table 4-5 described the mean air content for significant variables. The air content increased 8.8% with fly ash type used changing from A to B. This was due to higher loss of ignition of fly ash A. Fly ash with unburned carbon inside would have interactions with AEAs. Fewer available AEAs for air bubble stabilization would cause air content reduction after retempering (Whiting and Nagi 1998; Jolicoeur et al. 2009).

Changing the aggregate from gravel to limestone, resulted in the air content increasing by 7%, likely because the shape of limestone was more angular and rougher. The higher inter friction between aggregates would make it easier to produce air bubbles and prevent them from collapse. The retempering process increased air content by 5.2% because of additional water increasing particle dispersion. The concrete with 90°F mixing water temperature had 7% more air than that of mixtures with 70°F mixing water. In mixing stage, the coarse aggregate, the AEA and the water were first mixed with each other. Most air bubbles were produced at this time. The

higher mixing water temperature decreased surface tension and interface energy of water, thus, more air bubbles were generated with mixing. Meanwhile, AEAs molecules were absorbed to the air bubble surface and form a liquid film, thus, air bubbles became stable.

Based on statistical analysis of air content test results, fly ash B, limestone, retempering and higher mixing water temperature would increase air content of concrete in comparison with the other options.

Table 4-4 Statistical analysis of Air content test result

Rsquare (adj)=0.824			
Independent variables	P-value	Independent variables	Coefficient
FAT	<.0001	FAT[A]	-0.2781
AGT	0.0003	AGT[G]	-0.2063
RTP	0.0063	RTP[No]	-0.1469
MWT	0.0006	MWT[70]	-0.1938
CMT*RTP	0.0015	CMT[LA]*RTP[No]	-0.1750
CMT*MWT	0.0469	CMT[LA]*MWT[70]	-0.1031
FAT*ADT	0.0178	FAT[A]*ADT[1]	-0.1250
FAT*RTP	<.0001	FAT[A]*RTP[No]	0.2594
ADT*AGT	0.0115	ADT[1]*AGT[G]	-0.1344
ADT*MWT	0.0273	ADT[1]*MWT[70]	0.1156
CMT*FAT*ADT	<.0001	CMT[LA]*FAT[A]*ADT[1]	0.3844
CMT*AGT*MWT	0.0178	CMT[LA]*AGT[G]*MWT[70]	0.1250
FAT*ADT*AGT	0.0025	FAT[A]*ADT[1]*AGT[G]	0.1656
FAT*ADT*RTP	0.0178	FAT[A]*ADT[1]*RTP[No]	0.1250
FAT*ADT*MWT	0.0034	FAT[A]*ADT[1]*MWT[70]	-0.1594
FAT*AGT*RTP	0.0237	FAT[A]*AGT[G]*RTP[No]	-0.1188
ADT*AGT*MWT	0.0002	ADT[1]*AGT[G]*MWT[70]	0.2188
CMT*FAT*ADT*RTP	0.0004	CMT[LA]*FAT[A]*ADT[1]*RTP[No]	-0.2031
CMT*FAT*ADT*MWT	0.0006	CMT[LA]*FAT[A]*ADT[1]*MWT[70]	0.1938
CMT*FAT*AGT*MWT	0.0237	CMT[LA]*FAT[A]*AGT[G]*MWT[70]	0.1188
FAT*ADT*AGT*MWT	0.0004	FAT[A]*ADT[1]*AGT[G]*MWT[70]	0.2000

Table 4-5 Mean Air content for significant variables

Independent variables		Mean Air Content (%)	% Change in air content measurement
FAT	A	5.7	8.8
	B	6.2	
AGT	G	5.7	7.0
	L	6.1	
RTP	No	5.8	5.2
	Yes	6.1	
MWT	70	5.7	7.0
	90	6.1	

4.1.2.3 Unit weight

The statistical analysis of unit weight test result was shown in Table 4-6. The lower coefficient of determination (R^2) indicates that unit weight was relatively stable when considering only these variables because only 45.2% of unit weight result could be explained by variables. Fly ash type and retempering had a significant effect on unit weight as expected. Other variables in Table 4-6 showed little impact on unit weight. The mean unit weight for significant variables was described in Table 4-7.

Table 4-6 Unit weight analysis

Rsquare (adj)=0.452			
Independent variables	P-value	Independent variables	Coefficient
FAT	0.0352	FAT[A]	0.3600
RTP	0.0002	RTP[No]	0.6688
FAT*ADT	0.0107	FAT[A]*ADT[1]	0.4413
FAT*RTP	0.0113	FAT[A]*RTP[No]	-0.4375
CMT*FAT*ADT	0.0048	CMT[LA]*FAT[A]*ADT[1]	-0.4913
ADT*AGT*MWT	0.0007	ADT[1]*AGT[G]*MWT[70]	-0.6025

Table 4-7 Mean Unit weight for significant variables

Independent variables		Mean unit weight (lb/yd^3)	% Change in unit weight measurement
FAT	A	145.95	-0.50
	B	145.23	
RTP	No	146.26	-0.92
	Yes	144.92	

4.1.2.4 Relationship between air content and unit weight

In order to investigate the relationship between air content and unit weight, in addition to six existing variables, air content was added to the model as a continuous variable. The statistical analysis result is presented in Table 4-8. The high coefficient of determination (R2 =0.917) indicated a good model that the results could be mostly predicted by variables. In the previous analysis for unit weight, the coefficient of determination was only 0.452.When air content as a continuous variable was added to the model, the R2 changed from 0.452 to 0.917, which showed that air content had a significant effect on unit weight. More air content in concrete indicated low density. This was also confirmed by the P-value (<0.0001) of air content in Table 4-8, which was smaller than 0.05.

The relationship between air content and unit weight was plotted in Figure 4-8. Regardless of retempering, there was an apparent similar linear relationship between air content and unit weight. The trend line of mixtures without retempering was above that of mixtures with retempering which were due to higher w/c. The small angle between the two trend lines might be within experimental variation.

Table 4-8 Statistical analysis of unit weight with air content factor

Rsquare (adj)=0.917			
Independent variables	P-value	Independent variables	Coefficient
AGT	0.0045	AGT[G]	-0.2228
RTP	<.0001	RTP[No]	0.4282
CMT*FAT	0.0338	CMT[LA]*FAT[A]	-0.1463
FAT*ADT	0.0018	FAT[A]*ADT[1]	0.2365
CMT*AGT*MWT	0.0242	CMT[LA]*AGT[G]*MWT[70]	-0.1615
ADT*AGT*MWT	0.0023	ADT[1]*AGT[G]*MWT[70]	-0.2443
CMT*FAT*ADT*RTP	0.0199	CMT[LA]*FAT[A]*ADT[1]*RTP[No]	-0.1764
CMT*AGT*RTP*MWT	0.0382	CMT[LA]*AGT[G]*RTP[No]*MWT[70]	0.1427
CMT*ADT*AGT*RTP*MWT	0.0060	CMT[LA]*ADT[1]*AGT[G]*RTP[No]*MWT[70]	0.1961
Air Content (%)	<.0001	Air Content (%)	-1.6377

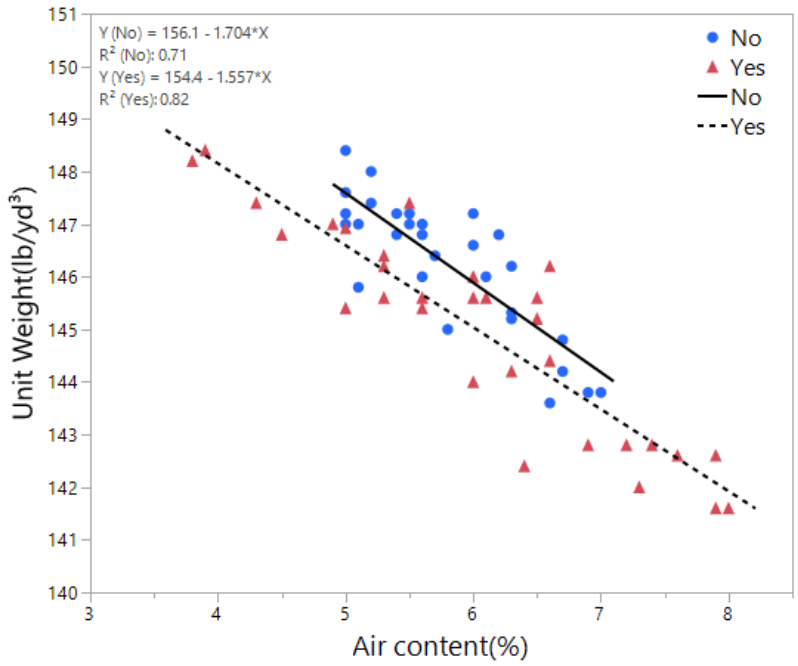

Figure 4-8 Relationship between air content and unit weight

4.2 Hardened concrete properties

4.2.1 Compressive Strength Results and Observations

The results of compressive strength are presented in Table 4-9, Figure 4-9, and Figure 4-10. In most mixtures with retempering, compressive strength decreased.

Table 4-9 7-days and 28 days Compressive strength result

Mix ID	Mix ID	7-days compressive strength(psi)		28-days compressive strength(psi)	
		No	Yes	No	Yes
1	TIL-A-1-L-70	5318	4900	6842	6242
2	TIL-A-1-L-90	5444	5524	6357	6600
3	TIL-A-1-G-70	4371	4547	5589	5303
4	TIL-A-1-G-90	3944	4182	5734	5881
5	TIL-A-2-L-70	4844	4443	5867	5770
6	TIL-A-2-L-90	4666	4471	6024	5071
7	TIL-A-2-G-70	4079	3034	5303	4560
8	TIL-A-2-G-90	4028	3665	4598	4233
9	TIL-B-1-L-70	5461	3972	6635	4913
10	TIL-B-1-L-90	4884	4127	5594	5106
11	TIL-B-1-G-70	4052	3636	4776	3890
12	TIL-B-1-G-90	4688	3985	5908	4980
13	TIL-B-2-L-70	5500	4712	6419	5922
14	TIL-B-2-L-90	5236	4523	5908	4980
15	TIL-B-2-G-70	4411	3942	5659	5501
16	TIL-B-2-G-90	3827	3442	4454	4211
17	LA-A-1-L-70	5172	4912	6905	6551
18	LA-A-1-L-90	4164	3781	5187	5340
19	LA-A-1-G-70	4525	3954	6013	5529
20	LA-A-1-G-90	4865	4342	6094	5817
21	LA-A-2-L-70	4959	4844	6692	6597
22	LA-A-2-L-90	3707	3586	4995	4917
23	LA-A-2-G-70	4446	4001	5747	5546
24	LA-A-2-G-90	4621	4094	6149	5604
25	LA-B-1-L-70	4978	4299	6551	5863
26	LA-B-1-L-90	4256	4040	5761	5437
27	LA-B-1-G-70	4896	4316	6201	5674
28	LA-B-1-G-90	4844	4359	6292	5598
29	LA-B-2-L-70	4962	3702	6390	4983
30	LA-B-2-L-90	3805	3357	4889	4442
31	LA-B-2-G-70	4787	4141	5796	5529
32	LA-B-2-G-90	3637	3419	4867	4622

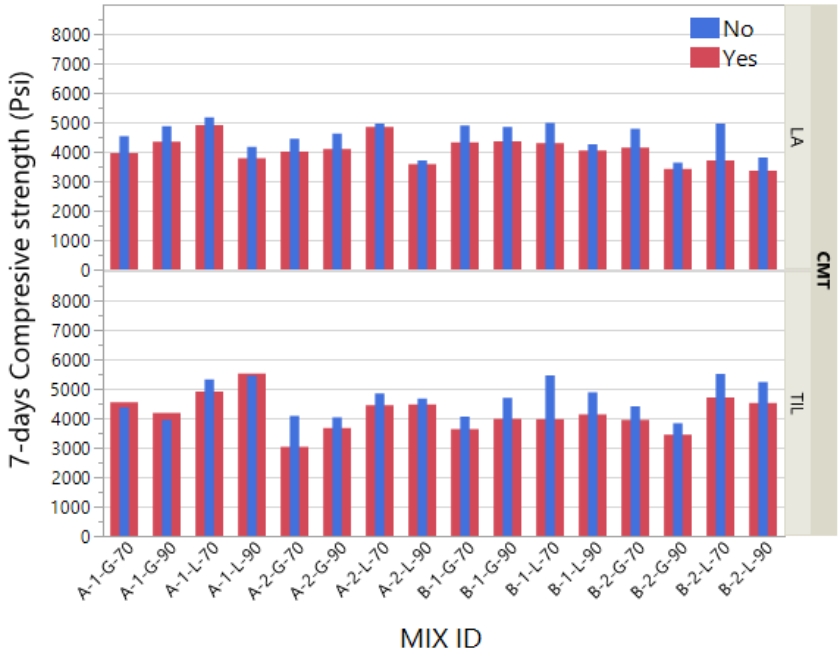

Figure 4-9 7-days compressive strength

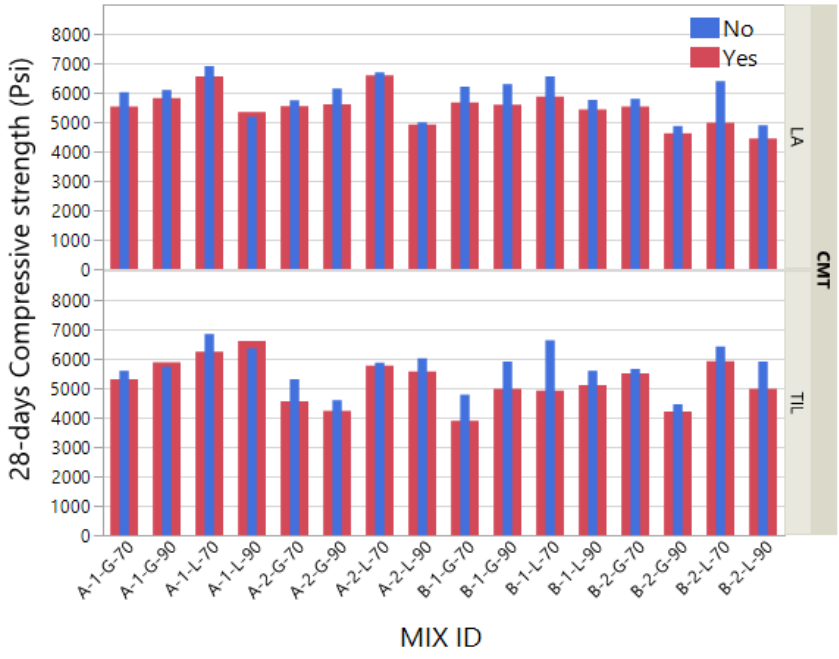

Figure 4-10 28-days compressive strength

4.2.2 Statistical Analysis of Compressive Strength Data

The statistical analysis of 7-day and 28-day compressive strength test results is presented in Tables 4-10 and 4-11. The coefficient of determinations (R^2 =0.853 and R^2 =0.867) were relatively high, indicating a good model explained by the listed independent variables. Comparing 7-days and 28-days compressive regression results, in Table 4-10, five variables showed a significant effect on 7-day compressive strength except FAT, but all six variables were included in Figure 4-11. This showed fly ash had less effect on the early compressive strength of concrete but contributed more strength to concrete in the long term because pozzolantic reactions between cement and fly ash were relative slow (reference). So, different effect of fly ash type A and B on compressive strength was identified in 28 days.

In Table 4-12 and 4-13, the mean compressive strength for significant variables are presented. Changing from admixture 1 to 2, the compressive strength in 7 days and 28 days decreased by 6.8% and 6.7% respectively. As previous discussed, admixture 1 absorbed by fly ash A decreased air content in concrete. Thus, mixture with admixture 2 had higher air content causing lower compressive strength. Compressive strength of concrete with limestone was higher than that of concrete with gravel, by 10.1% and 8.2% at 7 days and 28 days respectively because irregular shape and rough surface of limestone increased bonding strength between the paste and the aggregate creating a higher strength. As for retempering, compressive strength decreased by 10.3% and 7.7% at both 7 days and 28 days.

As for a temperature effect, although a higher temperature of mixing water should increase the hydration of concrete leading to high strength, the effect of temperature was significant on air content and thus indirectly influenced the compressive strength. Therefore higher mixing water temperature decreased compressive strength by 6.0% and 7.3% respectively

at 7 days and 28 days. In addition, the different mixing water temperature had a more noticeable difference in the compressive strength of concrete in long term.

Concrete with fly ash B showed lower compressive strength compared with fly ash A with 5.7% of strength loss.

Cement type contribution to the compressive strength is more complex. Concrete with low alkali cement showed relatively lower compressive strength of concrete in 7 days but higher compressive strength at 28 days comparing than that of concrete with TIL cement. However, the change of compressive was small and was in agreement with previous findings that no significant compressive strength change in 7-days and 28 days when alkali content in concrete was below 0.60% (Li, Afshinnia, and Rangaraju 2016).

Table 4-10 Statistical analysis of 7- day compressive strength

Rsquare (adj)=0.853			
Independent variables	P-value	Independent variables	Coefficient
CMT	0.0278	CMT[LA]	-63.8594
ADT	<.0001	ADT[1]	153.8594
AGT	<.0001	AGT[G]	-210.4531
RTP	<.0001	RTP[No]	236.3281
MWT	<.0001	MWT[70]	134.4219
CMT*AGT	<.0001	CMT[LA]*AGT[G]	233.0469
CMT*MWT	0.0002	CMT[LA]*MWT[70]	116.1094
FAT*RTP	0.0047	FAT[A]*RTP[No]	-84.0469
ADT*MWT	0.0101	ADT[1]*MWT[70]	-75.6719
AGT*MWT	0.0013	AGT[G]*MWT[70]	-97.0469
RTP*MWT	0.0458	RTP[No]*MWT[70]	57.6094
CMT*FAT*ADT	<.0001	CMT[LA]*FAT[A]*ADT[1]	-132.9531
CMT*AGT*MWT	0.0012	CMT[LA]*AGT[G]*MWT[70]	-98.1719
FAT*ADT*AGT	0.0360	FAT[A]*ADT[1]*AGT[G]	-60.6719
FAT*ADT*MWT	0.0265	FAT[A]*ADT[1]*MWT[70]	64.4531
CMT*FAT*AGT*MWT	0.0007	CMT[LA]*FAT[A]*AGT[G]*MWT[70]	-103.6094
FAT*ADT*AGT*MWT	0.0036	FAT[A]*ADT[1]*AGT[G]*MWT[70]	86.9219

Table 4-11 Statistical analysis of 28- day compressive strength

Rsquare (adj)=0.867			
Independent variables	P-value	Independent variables	Coefficient
CMT	0.0012	CMT[LA]	113.2500
FAT	<.0001	FAT[A]	162.5938
ADT	<.0001	ADT[1]	194.0313
AGT	<.0001	AGT[G]	-228.0000
RTP	<.0001	RTP[No]	226.3125
MWT	<.0001	MWT[70]	212.6250
CMT*AGT	<.0001	CMT[LA]*AGT[G]	214.8125
CMT*MWT	0.0009	CMT[LA]*MWT[70]	117.2500
FAT*RTP	0.0036	FAT[A]*RTP[No]	-100.2188
ADT*MWT	<.0001	ADT[1]*MWT[70]	-156.6563
AGT*MWT	<.0001	AGT[G]*MWT[70]	-163.4375
CMT*FAT*ADT	<.0001	CMT[LA]*FAT[A]*ADT[1]	-196.0000
CMT*AGT*MWT	0.0026	CMT[LA]*AGT[G]*MWT[70]	-104.4375
FAT*ADT*MWT	0.0064	FAT[A]*ADT[1]*MWT[70]	93.3125
ADT*AGT*MWT	0.0035	ADT[1]*AGT[G]*MWT[70]	-100.5938
CMT*FAT*AGT*MWT	0.0005	CMT[LA]*FAT[A]*AGT[G]*MWT[70]	-122.9063
CMT*ADT*AGT*MWT	0.0118	CMT[LA]*ADT[1]*AGT[G]*MWT[70]	85.4063

Table 4-12 Mean 7-days compressive strength for significant variables

Independent variables		Mean 7 days compressive strength (psi)	% Change in strength
CMT	LA	4305	3.0
	TIL	4433	
ADT	1	4523	-6.8
	2	4215	
AGT	G	4159	10.1
	L	4580	
RTP	No	4606	-10.3
	Yes	4133	
MWT	70	4504	-6.0
	90	4235	

Table 4-13 Mean 28-days compressive strength for significant variables

Independent variables		Mean 28 days compressive strength (psi)	% Change in strength
CMT	LA	5706	-4.0
	TIL	5479	
FAT	A	5755	-5.7
	B	5429	
ADT	1	5786	-6.7
	2	5398	
AGT	G	5364	8.2
	L	5805	
RTP	No	5819	-7.7
	Yes	5366	
MWT	70	5805	-7.3
	90	5379	

4.2.3 Air Void System Data and Observations

Rapid air analysis was conducted in accordance with ASTM C 457, and the results are presented in Table 4-14 and 4-15. Figure 4-11 shows that fresh air content was consistent with harden air content. Although, there were some differences between fresh air content and hardened air content but it was within a normal 2% (Whiting and Nagi 1998; Naranjo, A. 2007).

Table 4-14 Hardened concrete characteristics in all chords

MIX ID	No retempering			Retempering		
	Hardened Air (%)	Spacing Factor (mm)	Specific Surface (mm^-1)	Hardened Air (%)	Spacing Factor (mm)	Specific Surface (mm^-1)
TIL-A-1-L-70	6.3	0.122	37.91	3.2	0.283	22.10
TIL-A-1-L-90	4.7	0.265	19.83	5.4	0.163	30.26
TIL-A-1-G-70	4.2	0.176	31.62	3.0	0.298	21.58
TIL-A-1-G-90	4.1	0.240	23.04	4.4	0.243	22.29
TIL-A-2-L-70	5.5	0.172	28.42	5.9	0.202	23.45
TIL-A-2-L-90	6.6	0.124	36.47	5.7	0.155	31.19
TIL-A-2-G-70	5.2	0.175	28.57	4.3	0.185	29.82
TIL-A-2-G-90	3.9	0.221	25.98	5.0	0.201	25.30
TIL-B-1-L-70	6.0	0.239	19.61	6.5	0.141	32.22
TIL-B-1-L-90	4.6	0.252	21.03	5.7	0.157	30.48
TIL-B-1-G-70	4.7	0.207	25.48	6.7	0.095	47.04
TIL-B-1-G-90	6.7	0.108	41.41	6.1	0.099	46.99
TIL-B-2-L-70	4.0	0.269	20.95	5.5	0.131	37.34
TIL-B-2-L-90	4.6	0.180	29.43	5.7	0.130	36.89
TIL-B-2-G-70	5.1	0.204	24.81	5.2	0.153	32.76
TIL-B-2-G-90	6.4	0.114	40.12	6.8	0.153	29.05
LA-A-1-L-70	5.6	0.176	27.68	4.2	0.218	25.35
LA-A-1-L-90	5.5	0.193	25.44	7.1	0.185	23.48
LA-A-1-G-70	4.3	0.366	14.94	4.3	0.241	22.68
LA-A-1-G-90	3.8	0.186	31.16	5.2	0.208	24.21
LA-A-2-L-70	4.6	0.229	23.22	5.0	0.177	28.95
LA-A-2-L-90	4.2	0.151	36.60	7.7	0.138	29.29
LA-A-2-G-70	4.4	0.150	36.14	3.5	0.171	35.26
LA-A-2-G-90	4.2	0.229	24.09	4.0	0.145	38.98
LA-B-1-L-70	6.2	0.145	31.84	6.9	0.097	45.69
LA-B-1-L-90	5.6	0.136	35.63	6.8	0.109	40.62
LA-B-1-G-70	4.9	0.181	28.56	7.3	0.149	28.45
LA-B-1-G-90	3.9	0.206	27.71	5.4	0.150	33.08
LA-B-2-L-70	3.4	0.172	35.27	6.1	0.116	40.18
LA-B-2-L-90	3.8	0.164	35.14	6.5	0.098	46.09
LA-B-2-G-70	4.8	0.260	21.17	6.7	0.164	27.31
LA-B-2-G-90	7.7	0.123	32.83	8.8	0.121	29.19

Table 4-15 Harden concrete characteristics in chords over 30 micron

MIX ID	No retempering			Retempering		
	Hardened Air (%)	Spacing Factor (mm)	Specific Surface (mm^{-1})	Hardened Air (%)	Spacing Factor (mm)	Specific Surface (mm^{-1})
TIL-A-1-L-70	5.8	0.217	22.00	3.1	0.458	13.87
TIL-A-1-L-90	4.6	0.372	14.32	5.2	0.228	21.99
TIL-A-1-G-70	4.0	0.277	20.50	2.9	0.507	12.87
TIL-A-1-G-90	3.9	0.372	15.29	4.2	0.438	12.59
TIL-A-2-L-70	5.3	0.245	20.29	5.7	0.282	16.99
TIL-A-2-L-90	6.1	0.193	24.17	5.4	0.261	18.93
TIL-A-2-G-70	5.0	0.273	18.73	4.1	0.295	19.05
TIL-A-2-G-90	3.8	0.289	20.12	4.9	0.249	20.67
TIL-B-1-L-70	5.9	0.317	14.95	6.3	0.178	25.89
TIL-B-1-L-90	4.5	0.372	14.40	5.5	0.225	21.71
TIL-B-1-G-70	4.5	0.339	15.81	6.1	0.181	25.84
TIL-B-1-G-90	6.2	0.196	23.69	5.6	0.187	26.05
TIL-B-2-L-70	3.9	0.344	16.55	5.2	0.179	27.98
TIL-B-2-L-90	4.5	0.233	23.08	5.5	0.170	28.76
TIL-B-2-G-70	5.0	0.254	20.16	5.0	0.197	25.89
TIL-B-2-G-90	6.1	0.151	30.94	6.6	0.203	22.28
LA-A-1-L-70	5.3	0.272	18.28	4.1	0.317	17.72
LA-A-1-L-90	5.3	0.254	19.56	7.0	0.231	18.99
LA-A-1-G-70	4.3	0.462	11.90	4.2	0.311	17.77
LA-A-1-G-90	3.6	0.353	16.82	5.0	0.282	18.10
LA-A-2-L-70	4.5	0.310	17.36	4.7	0.266	19.72
LA-A-2-L-90	4.0	0.228	34.79	7.4	0.190	22.06
LA-A-2-G-70	4.1	0.244	22.95	3.2	0.304	20.51
LA-A-2-G-90	4.1	0.295	18.93	3.8	0.204	28.44
LA-B-1-L-70	5.9	0.228	20.80	6.3	0.167	27.57
LA-B-1-L-90	5.4	0.193	25.65	6.3	0.206	22.40
LA-B-1-G-70	4.7	0.262	20.04	7.0	0.224	19.59
LA-B-1-G-90	3.8	0.294	19.73	5.1	0.217	23.29
LA-B-2-L-70	3.2	0.294	21.18	5.7	0.190	25.40
LA-B-2-L-90	3.7	0.239	24.63	6.0	0.149	31.38
LA-B-2-G-70	4.1	0.354	15.77	6.4	0.279	16.37
LA-B-2-G-90	7.3	0.189	22.32	8.4	0.182	20.24

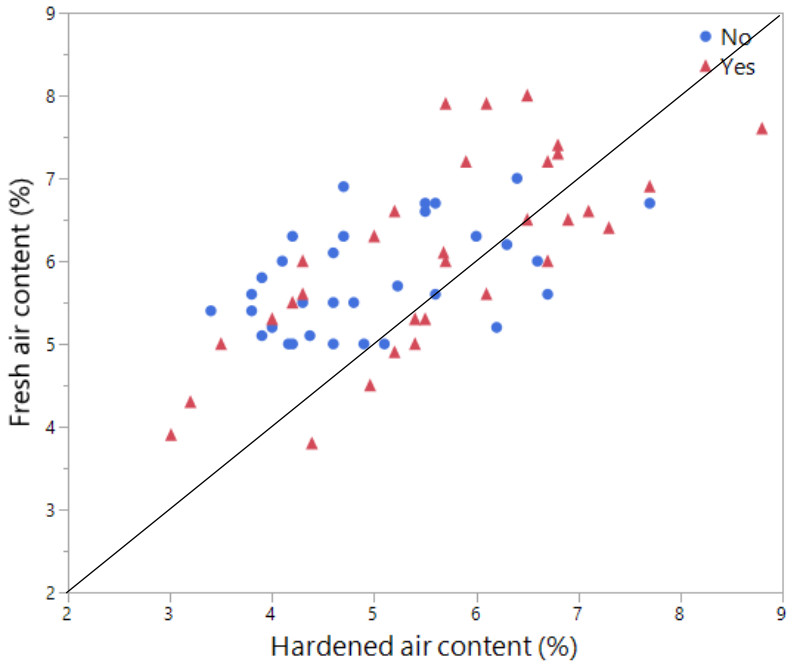

Figure 4-11 Fresh air content vs hardened air content

Figure 4-12 presents the change of spacing factor of mixtures with retempering. Decreasing spacing factor was observed in 22 of 32 groups. Figure 4-13 showed the change of specific surface of mixtures with retempering. This show increasing of specific surface was observed in 18 of 32 groups. This observation was consistent with Figure 4-14 that with increasing of spacing factor value, specific surface value decreased. Specific surface indicated number and size of air bubbles for a given volume of air. If two mixtures had a same air content, the mixture with small specific surface had less number of air voids but larger air bubbles. Random distribution with less number of air voids would have larger distance between air bubbles resulting in higher spacing factor. As previous discussion, retempering increased air content and more air content increased more air voids relatively. Thus, retempering possibly increased specific surface and decreased spacing factor.

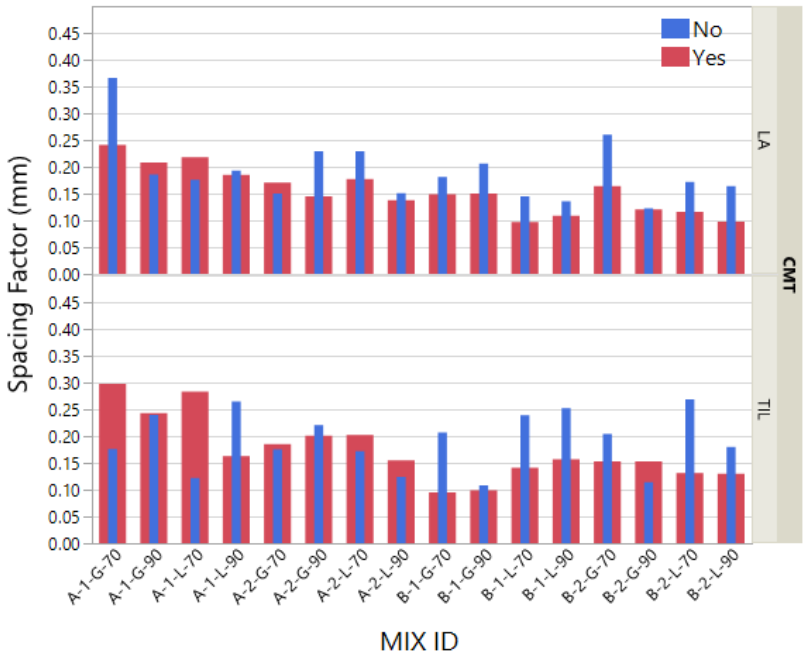

Figure 4-12 Change in spacing factor with retempering

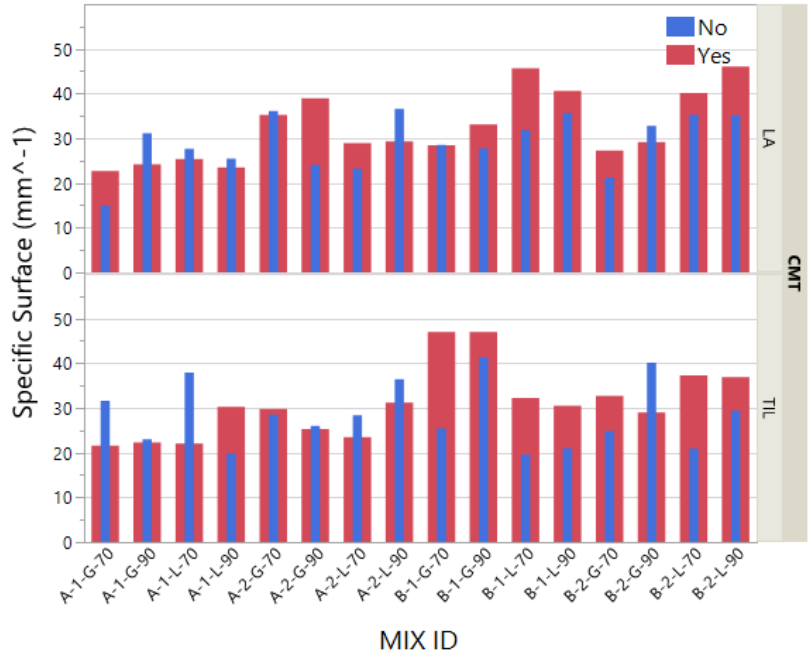

Figure 4-13 Change in specific surface with retempering

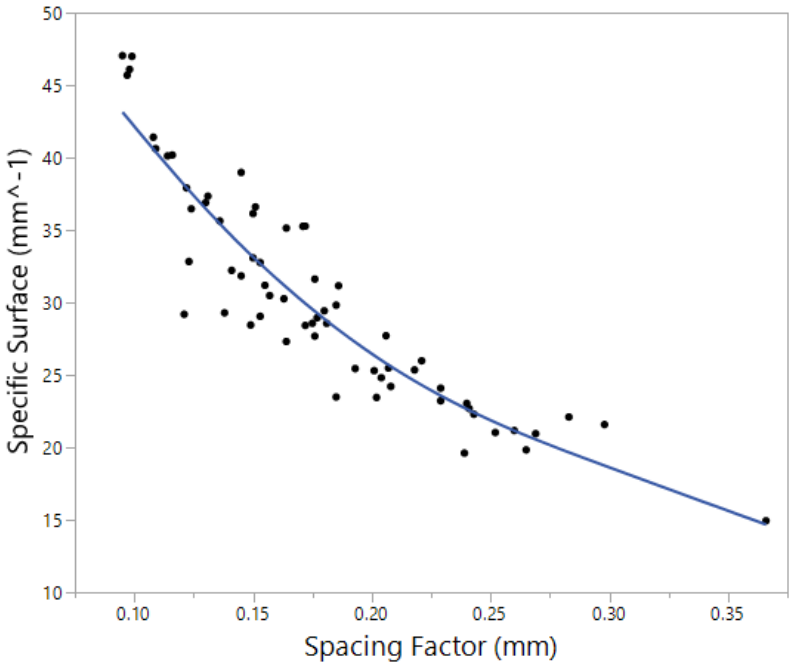

Figure 4-14 relationship between spacing factor and specific surface

4.2.4 Statistical Analysis of Hardened Air Results

The statistical analysis of spacing factor analysis is shown in Table 4-16. The Rsquare (0.432) was low, indicating that spacing factor was relatively stable with these variables. Fly ash type, retempering and mixing water temperature had a significant effect on spacing factor. Fewer interactions among variables in Table 4-16 also showed a stable spacing factor. The mean spacing for significant variables is described in Table 4-17. Changing from fly ash A to B, spacing factor decreased by 21.3%. This is consistent with the analysis of the air content.

Spacing factor decreased by 14% with retempering. This was consistent with observation in Figure 4-12. Retempering increased w/c resulting in more air. Meanwhile, the additional agitation by retempering process could make a better air voids distribution. The higher mixing water temperature caused slightly decreased spacing factor.

Table 4-16 Statistical analysis of spacing factor

Rsquare (adj)=0.432			
Independent variables	P-value	Independent variables	Coefficient
FAT	0.0001	FAT[A]	0.0213
RTP	0.0127	RTP[No]	0.0134
MWT	0.0358	MWT[70]	0.0112
FAT*ADT	0.0172	FAT[A]*ADT[1]	0.0128
FAT*RTP	0.007	FAT[A]*RTP[No]	-0.0146
CMT*FAT*AGT	0.0383	CMT[LA]*FAT[A]*AGT[G]	-0.0110

Table 4-17 Mean spacing factor for significant variables

Independent variables		Mean spacing factor (mm)	% Change in spacing factor
FAT	A	0.1996	-21.3
	B	0.157	
RTP	No	0.1917	-14.0
	Yes	0.1649	
MWT	70	0.1895	-1.8
	90	0.1671	

The statistical analysis of specific surface is shown in Table 4-18. The spacing factor was also stable, indicated by relatively low Rsquare (R^2=0.450). Fly ash type and retempering significant affecting spacing factor also had apparent influence on specific surface. The mean specific surface for significant variables was described in Table 4-19. The change of specific surface by fly ash type and retempering was consistent with spacing factor change. Although mixing water temperature did not show significant effect on specific surface in Table 4-18 but it could be reasonable because the change of spacing factor was very small, only 1.8%.

Table 4-18 Statistical analysis of specific surface

Rsquare (adj)=0.450			
Independent variables	P-value	Independent variables	Coefficient
FAT	0.0003	FAT[A]	-2.6417
RTP	0.0326	RTP[No]	-1.4917
CMT*AGT	0.0122	CMT[LA]*AGT[G]	-1.7655
FAT*ADT	0.0326	FAT[A]*ADT[1]	-1.4917
FAT*RTP	0.0045	FAT[A]*RTP[No]	2.0205
CMT*FAT*AGT	0.0003	CMT[LA]*FAT[A]*AGT[G]	2.6680

Table 4-19 Mean specific surface for significant variables

Independent variables		Mean specific surface (mm^{-1})	% Change in specific surface
FAT	A	27.6656	19.1
	B	32.9491	
RTP	No	28.8156	10.4
	Yes	31.7991	

4.3 Air void clustering

4.3.1 Air Void Clustering Results and Observations

The result of air void clustering are presented in Figures 4-15 and 4-16. In most mixtures, air void clustering increased with retempering. As discussed before, higher air content is likely to increase the chance of clustering around the coarse aggregate. In A-1-L-90-TIL group, air void clustering decreased because of lower air content with retempering. However, the other groups with air content reduction all showed an increase of air void clustering with the retempering. Air void clustering was observed in both mixtures with and without retempering, therefore, retempering might not be the cause of air void clustering, but it will aggravate clustering severity. Further, the average of clustering of mixtures without retempering in TIL cement groups was higher in that of LA cement groups. But the enhancement of clustering of mixtures with retempering in LA cement groups was higher than that of TIL cement groups.

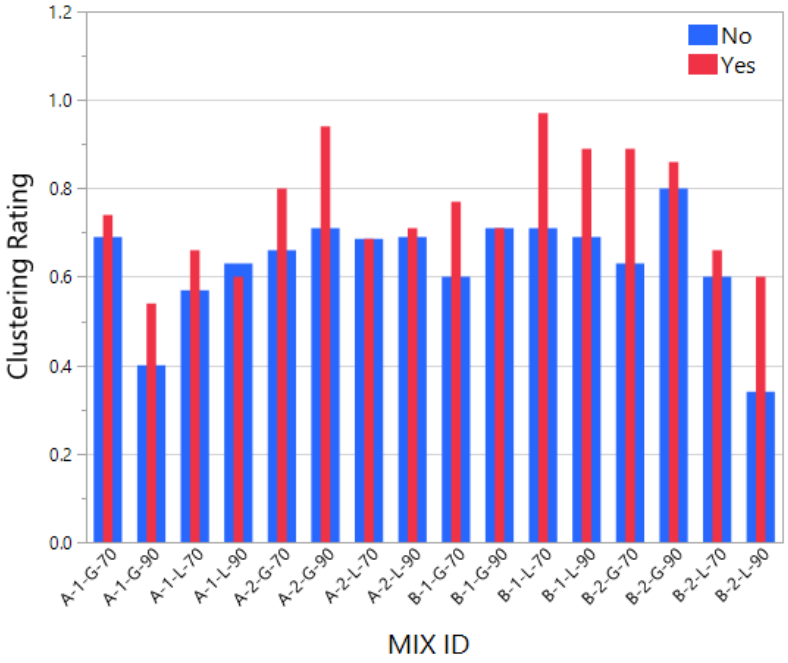

Figure 4-15 Clustering result-TIL cement

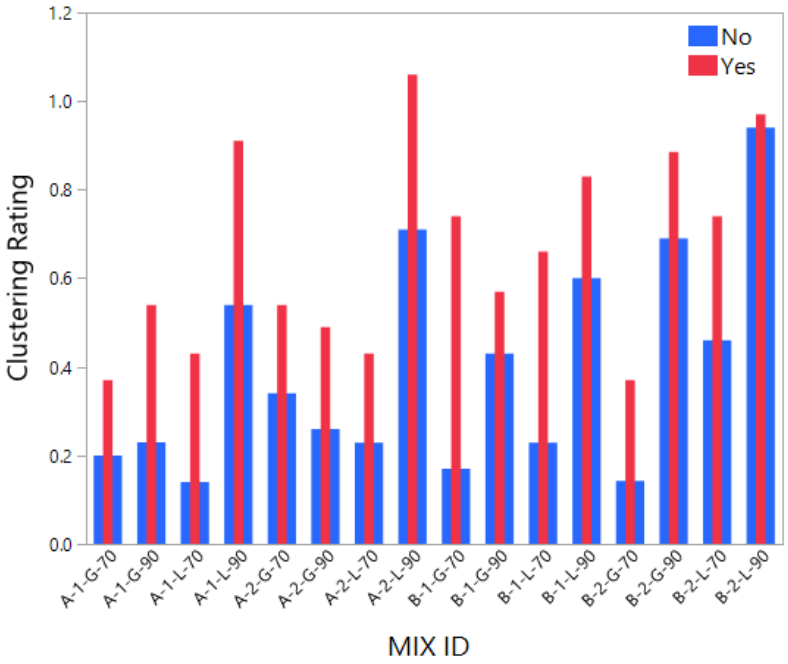

Figure 4-16 Clustering result-LA cement

4.3.2 Statistical Analysis of Air Void Clustering

The statistical analysis of air void clustering is presented in Table 4-20. The coefficient of determination (R^2 =0.895) represented 89.5% of air void clustering could be predicted by listed independent variables. Significant individual effects on air void clustering included all six variables. According to the coefficients in Table 4-20, Low alkali cement, fly ash A, admixture 1, river gravel, without retempering, and 70° F mixing water all contributed to clustering reduction. The mean air void clustering for significant variables is shown in Table 4-21. Retempering had the largest effect in that air void clustering increased by 37.4% with retempering. Changing from LA cement to TIL cement, air void clustering increased by 31.6% as same seen in Figure 4-14 and 4-15, which might be related to limestone included.

The air void clustering with 90° F mixing water temperature increased by 22.7% comparing that of 70 ° F mixing water temperature. As discussed before, the higher temperature increased air content and air bubbles, thus, more air bubbles had a higher chance accumulating around coarse aggregate. Fly ash B had 15.2% higher clustering than fly ash A. This might be directly influenced by air content reduction when using fly ash A in concrete. Admixture type and coarse aggregate type had a similar effect on air void clustering. Limestone and admixture 2 increased air void clustering by 11.6% and 11.1% respectively. Limestone was produced by machine, and the rough and irregular surface of limestone possible attracted air to the aggregate surface. The river gravel had a smoother surface and larger absorption ability than limestone, which might reduce air bubbles adhesion to the aggregate surface.

Table 4-20 Statistical analysis of air void clustering

Rsquare (adj)=0.895			
Independent variables	P-value	Independent variables	Coefficient
CMT	<.0001	CMT[LA]	-0.0828
FAT	<.0001	FAT[A]	-0.0426
ADT	0.0015	ADT[1]	-0.0320
AGT	0.0010	AGT[G]	-0.0336
RTP	<.0001	RTP[No]	-0.0959
MWT	<.0001	MWT[70]	-0.0619
CMT*FAT	0.0353	CMT[LA]*FAT[A]	-0.0202
CMT*ADT	0.0357	CMT[LA]*ADT[1]	-0.0201
CMT*AGT	<.0001	CMT[LA]*AGT[G]	-0.0573
CMT*RTP	0.0005	CMT[LA]*RTP[No]	-0.0362
CMT*MWT	<.0001	CMT[LA]*MWT[70]	-0.0776
FAT*ADT	0.0192	FAT[A]*ADT[1]	-0.0227
ADT*MWT	0.0097	ADT[1]*MWT[70]	0.0253
AGT*MWT	0.0059	AGT[G]*MWT[70]	0.0272
CMT*FAT*ADT	0.0020	CMT[LA]*FAT[A]*ADT[1]	0.0312
CMT*ADT*AGT	0.0001	CMT[LA]*ADT[1]*AGT[G]	0.0408
CMT*AGT*MWT	0.0005	CMT[LA]*AGT[G]*MWT[70]	0.0360
FAT*AGT*MWT	<.0001	FAT[A]*AGT[G]*MWT[70]	0.0431
FAT*RTP*MWT	0.0097	FAT[A]*RTP[No]*MWT[70]	0.0253
ADT*AGT*MWT	0.0482	ADT[1]*AGT[G]*MWT[70]	0.0188
CMT*FAT*ADT*AGT	0.0148	CMT[LA]*FAT[A]*ADT[1]*AGT[G]	-0.0237
CMT*FAT*ADT*MWT	0.0014	CMT[LA]*FAT[A]*ADT[1]*MWT[70]	-0.0325
CMT*FAT*ADT*AGT*MWT	0.0068	CMT[LA]*FAT[A]*ADT[1]*AGT[G]*MWT[70]	-0.0267

Table 4-21 Mean clustering for significant variables

Independent variables		Mean Clustering	% Change in clustering rating
CMT	LA	0.526	31.6
	TIL	0.692	
FAT	A	0.566	15.2
	B	0.652	
ADT	1	0.577	11.1
	2	0.641	
AGT	G	0.576	11.6
	L	0.643	
RTP	No	0.513	37.4
	Yes	0.705	
MWT	70	0.547	22.7
	90	0.671	

4.3.3 Relationship between Air Void Clustering and Air Content

In order to investigate the relationship between air void clustering and air content, besides six variables, air content was added to the statistical model as a continuous variable. The result of statistical analysis of clustering was shown in Table 4-22. The coefficient of determination was 0.864, indicating a good model for prediction. The determination of the coefficient of air content was 0.0011 representing a significant effect on air void clustering. The relationship between air content and clustering was plotted in Figure 4-17. According to Table 4-22, the coefficient of air content was positive, representing an enhancement for air void clustering with increasing of air content.

In Figure 4-17 (a), the blue points represented non-retempered mixtures. With the increase of air content from 5% to 6%, the clustering range was from 0.1 to 0.85. At the same air content, some clustering ratings were large, and some were small. With air content increasing from 5% to 6%, increasing and decreasing of clustering were both observed. These characteristics showed the random distribution of clustering rating with air content increasing from 5% to 6% because the effect of the other variables on clustering was more evident than an effect of air content. However, air content ranging from 6% to 7%, the clustering was from 0.55 to 0.8. Although the points were also influenced by variables, all of them with air content from 6% to 7% had a higher clustering than that of air content from 5% to 6%. So, the air void clustering increased with the increase of air content. In this way, extending unit interval could make the relationship between air content and air void clustering more clearly. This observation was consistent with the statistical analysis.

In Figure 4-17 (b), the red points represented retempered mixtures and the range of air content was stretched from 3.5% to 8%. Form 3.5% to 6%, the air void clustering kept stabled. From 6% to 8%, the air void clustering had an increasing trend. So in mixtures with retempering,

air void clustering had an apparent increase with air content over 6%. Thus, if the concrete with retempering had air content below 6%, it was better for concrete because of low and stable clustering.

Table 4-22 Statistical analysis of air void clustering

Rsquare (adj)=0.864			
Independent variables	P-value	Independent variables	Coefficient
CMT	<.0001	CMT[LA]	-0.0828
FAT	0.0331	FAT[A]	-0.0255
ADT	0.0043	ADT[1]	-0.0316
RTP	<.0001	RTP[No]	-0.0868
MWT	<.0001	MWT[70]	-0.0499
CMT*FAT	0.0406	CMT[LA]*FAT[A]	-0.0221
CMT*ADT	0.0364	CMT[LA]*ADT[1]	-0.0226
CMT*AGT	<.0001	CMT[LA]*AGT[G]	-0.0571
CMT*RTP	0.0248	CMT[LA]*RTP[No]	-0.0253
CMT*MWT	<.0001	CMT[LA]*MWT[70]	-0.0712
AGT*MWT	0.0162	AGT[G]*MWT[70]	0.0262
CMT*ADT*AGT	0.0008	CMT[LA]*ADT[1]*AGT[G]	0.0381
CMT*AGT*MWT	0.0116	CMT[LA]*AGT[G]*MWT[70]	0.0282
FAT*AGT*MWT	0.0006	FAT[A]*AGT[G]*MWT[70]	0.0395
CMT*FAT*ADT*MWT	0.0002	CMT[LA]*FAT[A]*ADT[1]*MWT[70]	-0.0445
Air content (%)	0.0011	Air content (%)	0.0619

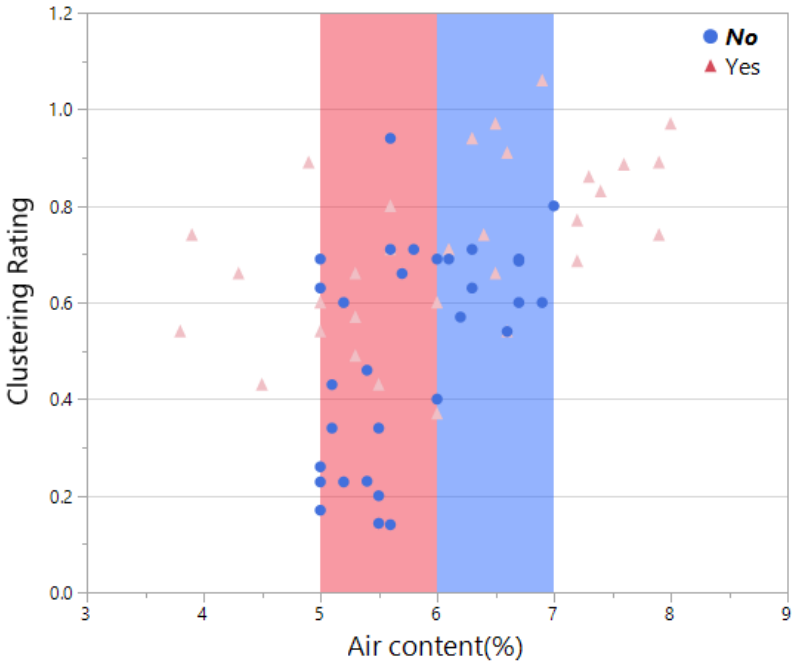

(a)

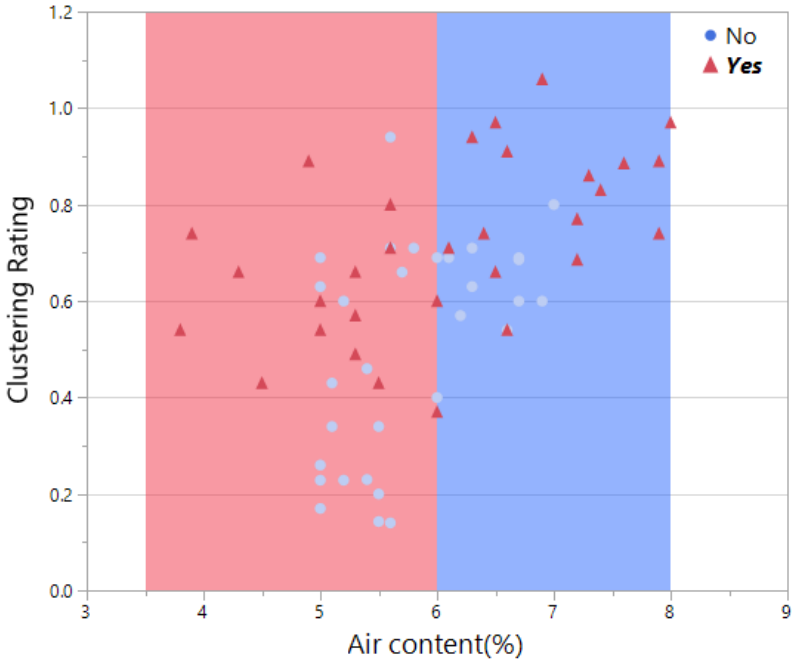

(b)

Figure 4-17 Relationship between air content and clustering

Using the statistical method could establish a model to describe the relationship between air content and clustering, but it could not present the local real change in Figures 4-17. In order to simplify the data, reduce the variables' effect on clustering, and make it clear to see the trend in mixtures with or without retempering, the mean value of clustering at each 0.5% air content range was used to represent the clustering at this range. The result obtained by this method is presented in Table 4-23. Figure 4-18 plotted the mean clustering change with an increase of air content range, which was consistent with Figure 4-17. Comparing two curves, the retempering curve was above no retempering curve indicating an increase in air void clustering with the retempering. Without retempering, mean clustering increased at the range of air content from 5% to 6.5% and kept stable at the range of air content from 6.0% to 7.0%. With retempering, mean clustering increased at the range of air content from 6.0% to 7.0% and kept stable at the range of air content from 3.5% to 6.5% and from 6.5% to 8.0%.

In addition, the air void clustering remaining stable was observed when the air content increased to a certain level or with retempering. It seemed that there was a critical air content for effect of air content limitation and retempering limitation on air void clustering.

Table 4-23 Mean clustering at different air content range

Air content range	Mean clustering (Before retempering)	Mean Clustering (After retempering)
3.5-4.0	-	0.64
4.0-4.5	-	0.66
4.5-5.0	-	0.66
5.0-5.5	0.39	0.57
5.5-6.0	0.48	0.65
6.0-6.5	0.63	0.62
6.5-7.0	0.65	0.83
7.0-7.5	-	0.79
7.5-8.0	-	0.87

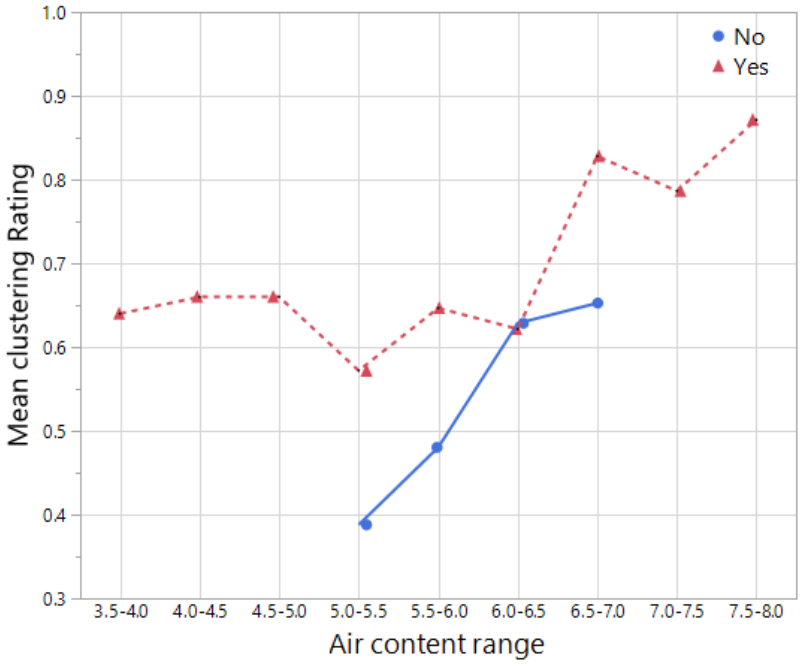

Figure 4-18 The relationship between mean clustering and air content range

The reason for air content limitation and retempering limitation may be clarified using simulations in Figure 4-19. From a to b, air content increases 1% from 5% to 6% with the retempering process, the air void clustering changes from 0 to 2. From c to d, air content still increases 1% from 6% to 7%. However, the air void clustering stays at 2. This is due to two reasons. First, two air bubbles layers observed indicates a severity of 2, yet the air content increases, more air bubbles might increase the number of bubbles but they are still in two layers. Another reason may be the coarseness of the rating system with only four levels.

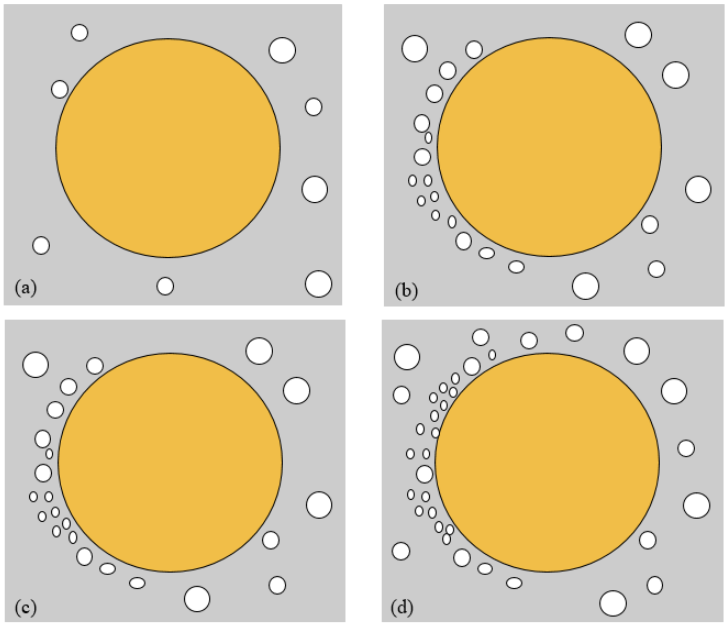

Figure 4-19 Simulation of limited effect of air content on air void clustering; (a) without retempering, air content=5%, clustering =0; (b) with retempering, air content=6%, clustering =2; (c) without retempering, air content=6%, clustering =2; (d) with retempering, air content=7%, clustering=2

The simulation of limitation effect of retempering on air void clustering is shown in Figure 4-20. Comparing a and b, they have the same air content, but b has been retempered. Different air void distributions are observed, but the severity of air void clustering is the same.

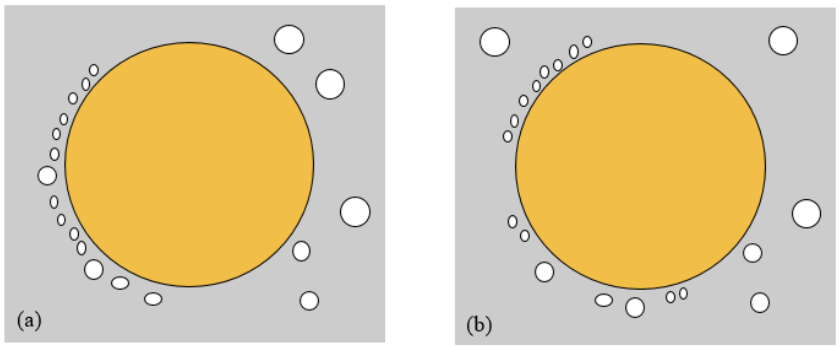

Figure 4-20 Simulation of limited effect of retempering on air void clustering; (a) without retempering, air content=5%, clustering =1; (b) with retempering, air content=6%, clustering =1;

4.3.4 Clustering Sensitivity Index

Based on the previous discussion, an increase of water could entrain more air and then lead to higher air void clustering by the mixing action (William L.Dolch), but the data indicate that air content and the retempering process had a limited effect on air void clustering. Meanwhile, there was an observation that if the air content and air void clustering of concrete were lower, the increase of air void clustering was higher at the same air content with the retempering process. Thus, an assumption was made that there is a balance between retempering process and air content for air void clustering. At lower air content before retempering, the process of adding water dominated the air void clustering around aggregate in retempering concrete. At higher air content in concrete before retempering, the process of adding water had less effect on air void clustering, and the air content dominated the air void clustering. Therefore, a term has been proposed as clustering sensitivity index (CSI), which is a ratio of clustering rating to air content, shown in Eq. 1. The CSI of 32 mixes are presented in Table 4-24. The result of simplified data is presented in Table 4-25 and plotted in Figure 4-21.

It was clear to see that clustering change increased with a decrease of clustering sensitivity Index. Also, the R^2 =0.929 was relatively high, indicating a good linear trend. Thus, the lower CSI represented that concrete was sensitive to air void clustering with the retempering process.

$$Clustering\ Sensitivity\ Index = \frac{air\ void\ clustering\ rating * 100}{air\ content} \quad \text{Eq.1}$$

Table 4-24 CSI values in 32 mixtures

MIX ID	CSI	Clustering change	MIX ID	CSI	Clustering change
TIL-A-1-L-70	9.19	0.09	LA-A-1-L-70	2.50	0.29
TIL-A-1-L-90	10.00	-0.03	LA-A-1-L-90	8.18	0.37
TIL-A-1-G-70	13.80	0.05	LA-A-1-G-70	3.64	0.17
TIL-A-1-G-90	6.67	0.14	LA-A-1-G-90	4.26	0.31
TIL-A-2-L-70	10.23	0.00	LA-A-2-L-70	4.57	0.20
TIL-A-2-L-90	11.50	0.02	LA-A-2-L-90	11.27	0.35
TIL-A-2-G-70	11.58	0.14	LA-A-2-G-70	6.67	0.20
TIL-A-2-G-90	12.24	0.23	LA-A-2-G-90	5.20	0.23
TIL-B-1-L-70	11.27	0.26	LA-B-1-L-70	4.40	0.43
TIL-B-1-L-90	11.31	0.20	LA-B-1-L-90	8.96	0.23
TIL-B-1-G-70	8.70	0.17	LA-B-1-G-70	3.40	0.57
TIL-B-1-G-90	12.68	0.00	LA-B-1-G-90	8.43	0.14
TIL-B-2-L-70	11.54	0.06	LA-B-2-L-70	8.52	0.28
TIL-B-2-L-90	6.18	0.26	LA-B-2-L-90	16.79	0.03
TIL-B-2-G-70	12.60	0.26	LA-B-2-G-70	2.60	0.23
TIL-B-2-G-90	11.43	0.06	LA-B-2-G-90	10.30	0.20

Table 4-25 Mean clustering change corresponding to CSI range

CSI Range	Mean clustering change
2-4	0.314
4-6	0.293
6-8	0.200
8-12	0.213
12-14	0.125
14-16	0.135
16-18	0.030

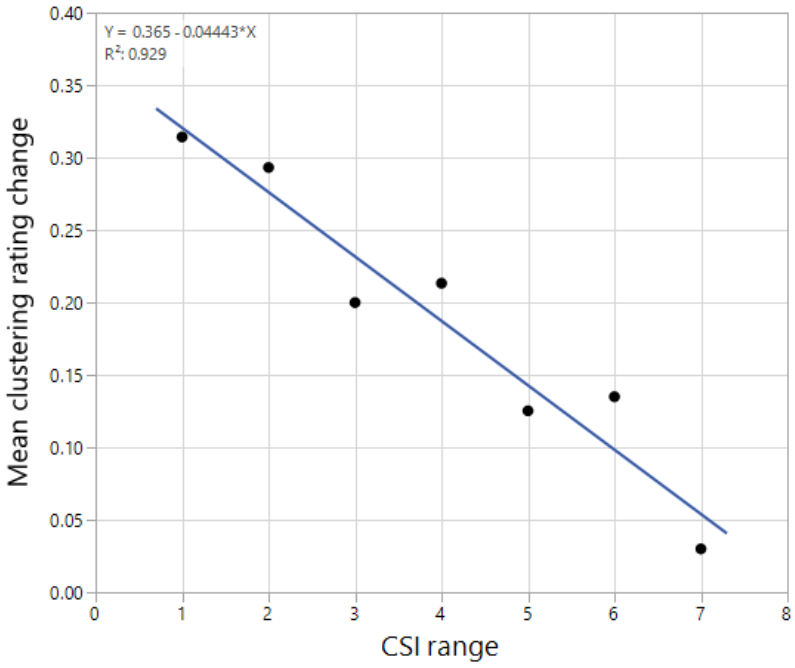

Figure 4-21 Relationship between CSI and clustering change

4.3.5 Effect of Air Void Clustering on Compressive Strength

In order to investigate the relationship between air void clustering and compressive strength, besides six variables, air void clustering was added to the statistical model as a continuous variable. The statistical analysis of the compressive strength is shown in Table 4-26 and Table 4-27. The air void clustering as a continuous variable showed a significant effect on compressive strength. As for 28-days compressive strength, RTP did not show significant effect on compressive strength indicating insignificant effect of 0.03 w/c change on 28-days compressive strength.

Table 4-26 Statistical analysis of the relationship between air void clustering and 7 days compressive strength

Rsquare (adj)=0.717			
Independent variables	P-value	Independent variables	Coefficient
CMT	<.0001	CMT[LA]	-189.3738
ADT	0.0097	ADT[1]	105.2720
AGT	<.0001	AGT[G]	-261.41.06
RTP	0.0454	RTP[No]	90.9047
CMT*AGT	0.0007	CMT[LA]*AGT[G]	146.1314
Clustering	<.0001	Clustering	-1516.873

Table 4-27 Statistical analysis of the relationship between air void clustering and 28 days compressive strength

Rsquare (adj)=0.659			
Independent variables	P-value	Independent variables	Coefficient
ADT	0.0131	ADT[1]	133.3434
AGT	<.0001	AGT[G]	-291.6482
ADT*MWT	0.0405	ADT[1]*MWT[70]	-108.6557
AGT*MWT	0.0352	AGT[G]*MWT[70]	-111.9691
Clustering	<.0001	Clustering	-1894.645

The relationship between air void clustering and predicted compressive strength was plotted in Figure 4-22. A downward trend was observed between compressive strength and air void clustering in both mixtures with and without retempering. The trend in mixtures with retempering were more apparent. Due to amount of scatter, it could only be an initial estimation

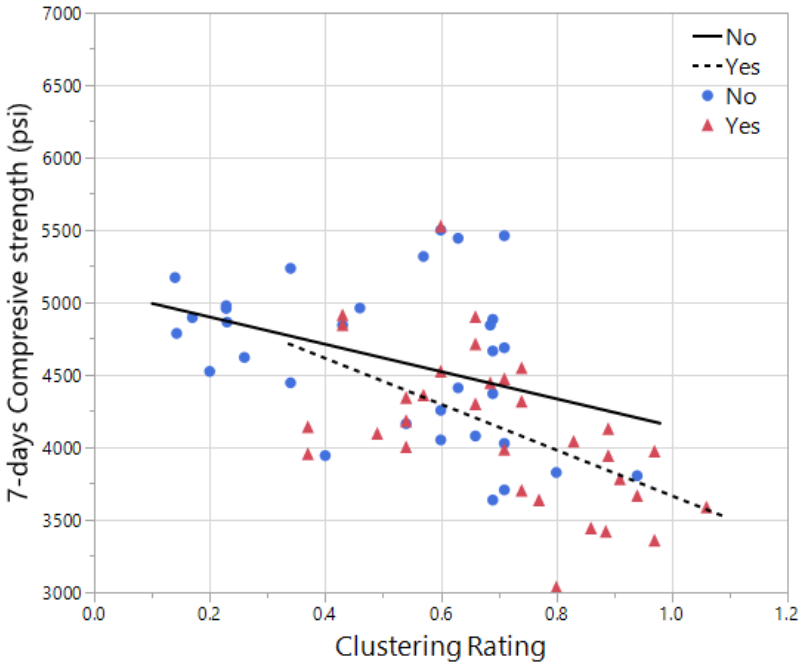

(a) Relationship between clustering and 7 days compressive strength

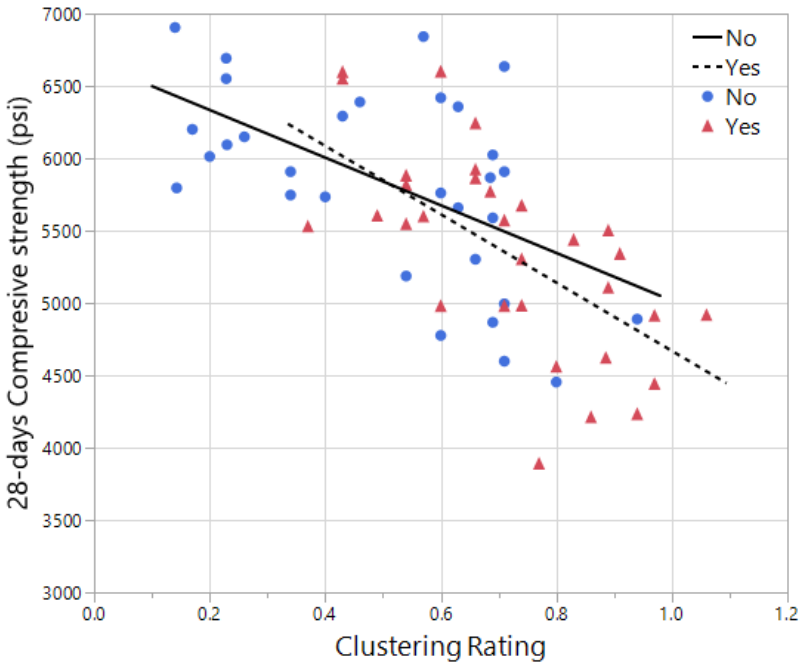

(b) Relationship between clustering and 28 days compressive strength

Figure 4-22 Relationship between compressive strength and clustering

In order to see the change of compressive strength clearly in mixtures with or without retempering, the mean compressive strength at each 0.2 clustering change was used to represent the clustering at this range. Figure 4-23 plotted the change of mean compressive strength with an increase of air clustering range. A decrease in compressive strength was observed with increasing clustering range. The lines of with or without retempering was closer in 28 days. When the clustering was small than 0.6, the compressive strength change kept stable or even increased. However, a sharp decrease of compressive strength was observed when the clustering was above 0.6. Since it was difficult to exclude the influence of other variables on compressive strength, this relationship could only be used as a quantitative analysis. But an initial indication could be drawn that air void clustering had a negative effect on compressive strength.

According to the above discussion, air void clustering seemed to reduce the compressive strength, but air content and w/c ratio could also decrease the compressive strength with retempering. As the previous study mentioned that an increase of 0.03 w/c ratio had an insignificant effect on compressive strength loss. (Kozikowski). Meanwhile, based on statistical result before, RTP showed on significant effect on 28-days compressive strength. So, strength loss with retempering was only due to air void content and air void clustering. To differentiate these two factors, comparative analysis of compressive strength 28 days are presented in Table 4-28. There is a rule of thumb that 1% extra air content leads to 2-6% compressive strength loss. 4% compressive strength reduction per air content was adopted in this study. In Table 4-28, most mixtures showed negative values for strength loss potentially by air void clustering. These results confirm that air void clustering could reduce compressive strength after retempering.

The average strength loss change was only around 9.07% with the retempering process, which is consistent with the clustering ratings in this study which were than 1.

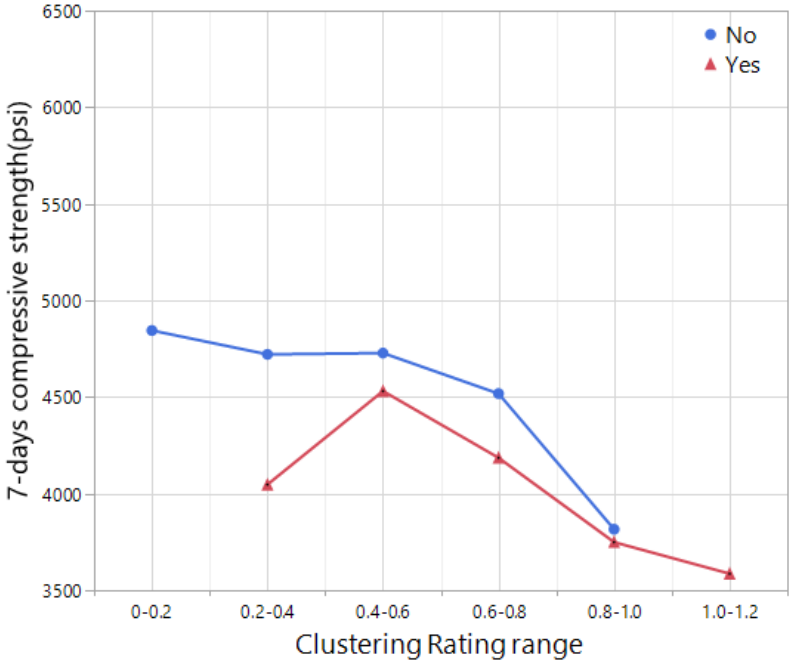

(a) 7-days compressive strength change at different clustering range

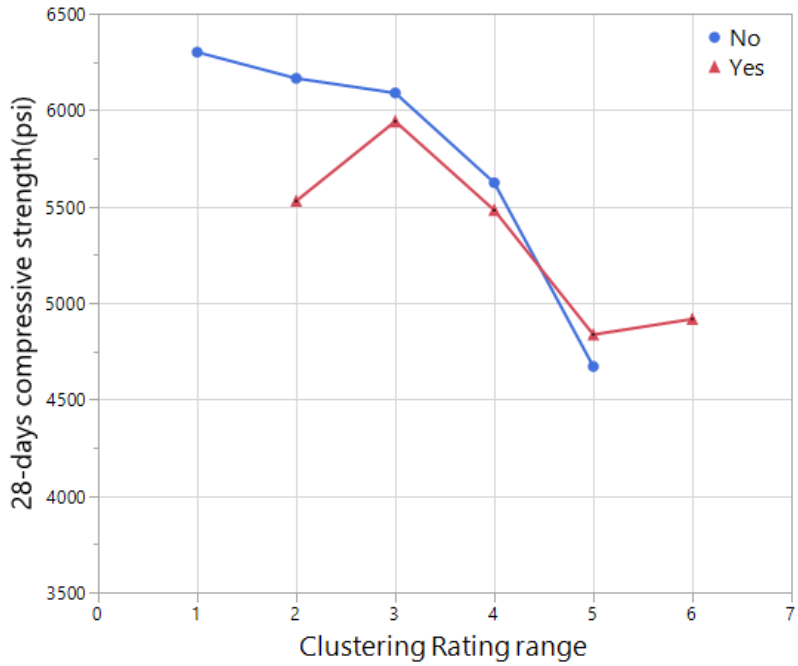

(b) 28-days compressive strength change at different clustering range

Figure 4-23 The relationship between compressive strength and clustering range

Table 4-28 Compressive strength loss due to air void clustering

MIX ID	Actual compress strength, without retempering, psi	Actual compress strength, with retempering, psi	Air change (%)	Adjusted compressive strength, with retempering, psi	Strength change potentially due to clustering, %
A-1-L-70	6842	6242	-1.90	7361.99	-17.94
A-1-L-90	6357	6600	-1.30	6687.56	-1.33
A-1-G-70	5589	5303	-1.10	5834.92	-10.03
A-1-G-90	5734	5881	-2.20	6238.59	-6.08
A-2-L-70	5867	5770	0.5	5749.66	0.35
A-2-L-90	6024	5071	0.10	5999.90	-18.32
A-2-G-70	5303	4560	-0.10	5324.21	-16.76
A-2-G-90	4598	4233	0.50	4506.04	-6.45
B-1-L-70	6635	4913	1.70	6183.82	-25.87
B-1-L-90	5594	5106	1.80	5191.23	-1.67
B-1-G-70	4776	3890	0.30	4718.69	-21.30
B-1-G-90	5908	4980	0.00	5908.00	-18.63
B-2-L-70	6419	5922	0.10	6393.32	-7.96
B-2-L-90	5908	4980	0.50	5789.84	-16.26
B-2-G-70	5659	5501	-0.10	5681.64	-3.28
B-2-G-90	4454	4211	0.30	4400.55	-4.50
A-1-L-70	6905	6551	-0.10	6932.62	-5.83
A-1-L-90	5187	5340	0.00	5187.00	2.87
A-1-G-70	6013	5529	0.50	5892.74	-6.58
A-1-G-90	6094	5817	1.20	5801.49	0.27
A-2-L-70	6692	6597	0.50	6825.84	-3.47
A-2-L-90	4995	4917	0.60	4875.12	0.85
A-2-G-70	5747	5546	-0.10	5769.99	-4.04
A-2-G-90	6149	5604	0.30	6075.21	-8.41
B-1-L-70	6551	5863	1.30	6210.35	-5.92
B-1-L-90	5761	5437	0.70	5599.69	-2.99
B-1-G-70	6201	5674	1.40	5853.74	-3.17
B-1-G-90	6292	5598	0.20	6241.66	-11.50
B-2-L-70	6390	4983	2.50	5751.00	-15.41
B-2-L-90	4889	4442	0.90	4713.00	-6.10
B-2-G-70	5796	5529	0.50	5680.08	-2.73
B-2-G-90	4867	4622	0.90	4691.79	-1.51

4.3.6 Effect of High Concrete Temperature on Air Void Clustering and Compressive Strength

In order to investigate the temperature effect on air void clustering in details, additional two mixtures were done with 90°F concrete temperature. The fresh properties of concrete are presented in Table 4-29. The compressive strength and clustering are shown in Table 4-30. The compressive strength loss due to air void clustering is presented in Table 4-31.

Table 4-29 Fresh properties

Mix ID	Slump(in)		Unit Weight (lb/yd^3)		Air Content (%)	
	No	Yes	No	Yes	No	Yes
TIL-MWT70°F	1.0	3.0	144.2	143.4	6.7	7.2
TIL-MWT90°F	1.0	2.5	146.6	145.6	6.0	6.1
TIL-CT90°F	1.4	3.0	145.2	141.0	5.3	7.3
LA-MWT70°F	1.5	2.2	147.6	146.8	5.0	5.3
LA-MWT90°F	2.6	3.2	145.2	142.8	6.3	6.9
LA-CT90°F	1.2	2.2	146.8	144.4	4.2	5.2

Table 4-30 Clustering and compressive strength

Mix ID	Clustering		7 days Compressive strength, psi		28 days Compressive strength, psi	
	No	Yes	No	Yes	No	Yes
TIL-MWT70°F	0.69	0.69	4844	4443	5867	5770
TIL-MWT90°F	0.69	0.71	4666	4471	6024	5571
TIL-CT90°F	0.63	0.80	3465	3040	5202	4349
LA-MWT70°F	0.23	0.43	4959	4844	6692	6597
LA-MWT90°F	0.71	1.06	3707	3586	4995	4917
LA-CT90°F	0.29	0.57	4615	4077	6123	4978

Table 4-31 Compressive strength loss due to air void clustering

Mix ID	Air change	Clustering change	28 days Compressive strength with retempering, psi	Adjusted 28 days compressive strength with retempering, psi	Strength loss due to potential air void clustering,%
TIL-MWT70°F	0.5	0.00	5770	5750	0.35
TIL-MWT90°F	0.1	0.02	5571	6000	-7.70
TIL-CT90°F	2.0	0.17	4349	4786	-10.04
LA-MWT70°F	0.3	0.20	6597	6612	-0.22
LA-MWT90°F	0.6	0.35	4917	4875	0.85
LA-CT90°F	1.0	0.28	4978	5878	-18.08

Figure 4-24 shows air content change in different temperature conditions. It is clear to see that the highest air content change in CT90°F mixtures, which indicated that increasing temperature increases the air content after retempering. Figure 4-25 shows air void clustering change in different temperature conditions. The air void clustering in CT 90°F was higher than that of MWT70°F, so the high temperature would also aggravate much more air void clustering after retempering. As discussion before, more air bubbles were generated with mixing process at high temperature.

According to Table 4-31, the strength loss due to potential air void clustering was more evident in CT90°F mixture. Comparing two cement mixtures, compressive strength with low alkali cement was more sensitive to air void clustering

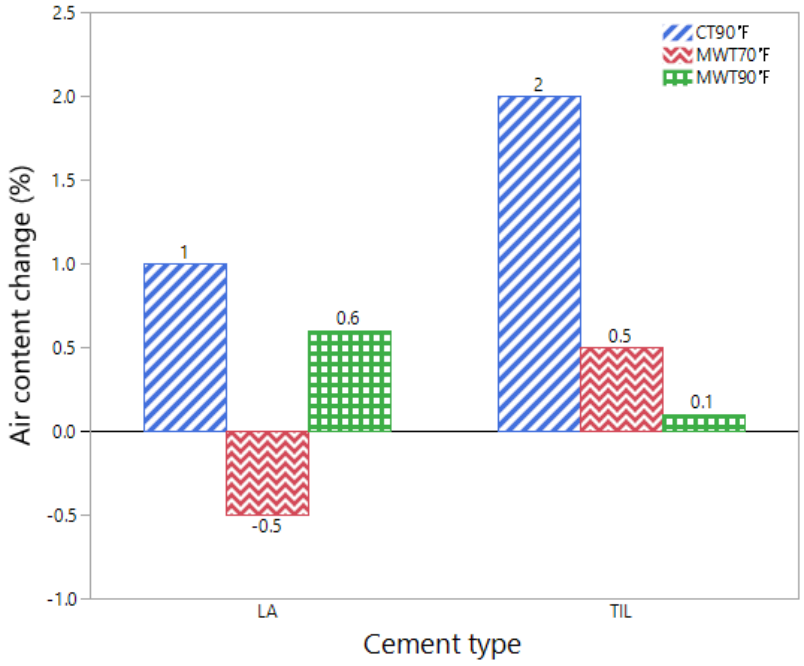

Figure 4-24 Comparing air content change in different temperature conditions

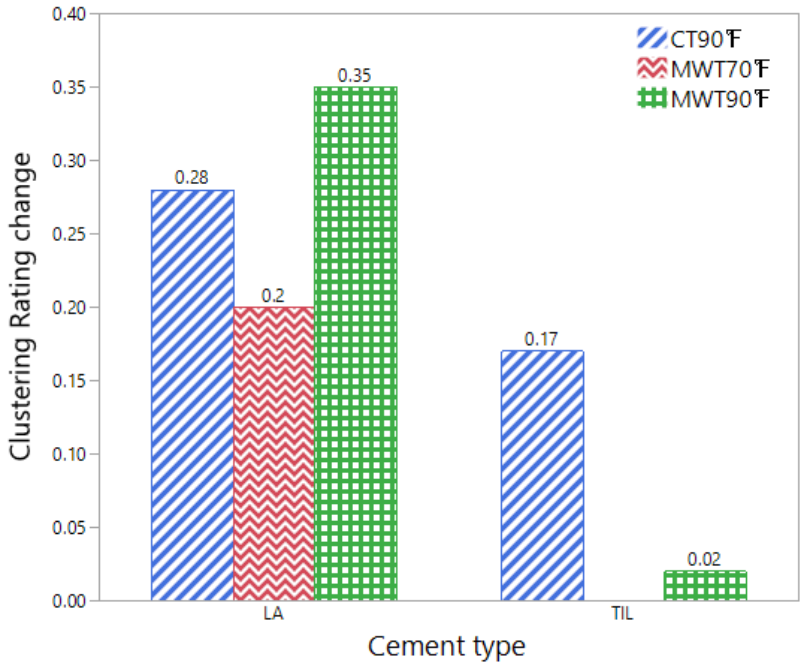

Figure 4-25 comparing clustering change in different temperature conditions

4.3.7 The Relationship between Air Void Clustering and Air Void System

In order to investigate the relationship between air void clustering and air void system, a 3-D model was established as shown in Figure 4-26. The three coordinates were clustering, spacing factor and specific surface. Each ball represents a mixture point. The size of the ball represents the severity of clustering. The larger the bubble size is, the more clustering potential is. The color of balls indicates the magnitude of spacing factor. The redder the bubble color changes from blue, the larger the spacing factor is.

According to Figure 4-26, most large balls had a blue color, and the distribution of balls is from the left bottom corner to the right top corner. This shows that clustering possibly happened more easily in an air void system with low spacing factor and high specific surface.

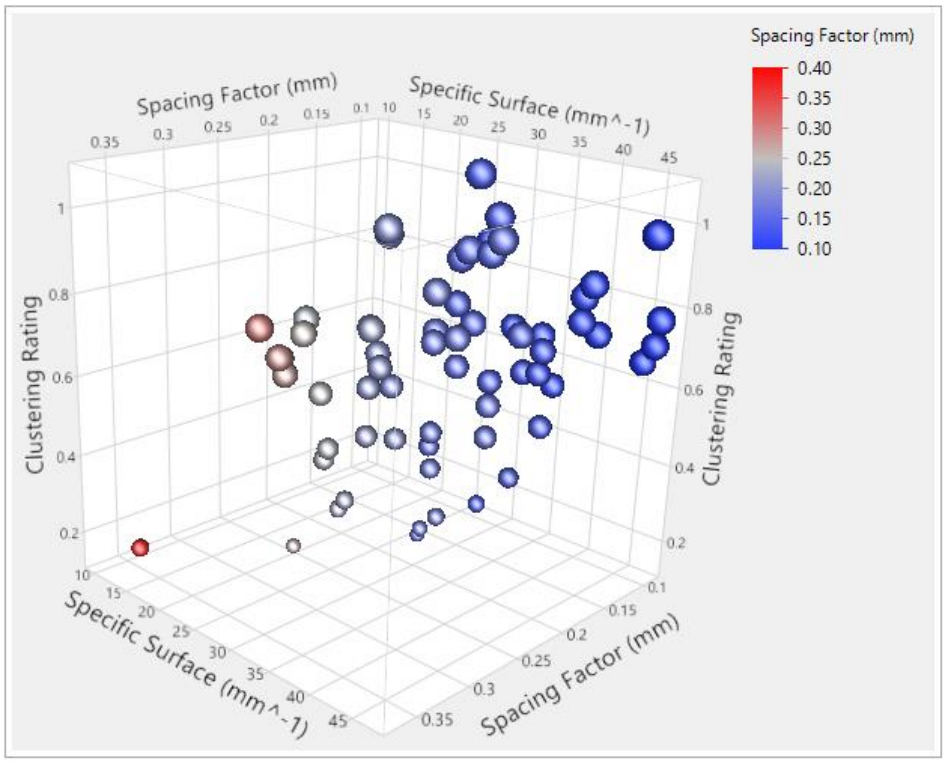

Figure 4-26 3D model for relationship among clustering, spacing factor and specific surface.

Table 4-32 shows the difference of air content with and without the retempering process in air void chords below 30 microns. A positive difference shows that air content composed of fine air voids increases with retempering and the negative difference shows that air content decreases with fine air voids. For example, in TIL-A-1-L-70 mixtures, the difference of air content (chords ≦ 30 microns) is -0.33. That means air content with small air voids reduced 0.33% when the mixture with retempering.

According to Table 4-32, in all 32 groups, most groups have a positive difference and only 9 groups have negative values of difference. Among these 9 groups, some also have an air content reduction with retempering, which might contribute to the negative values. Therefore, it seems that the retempering produced more small air voids with chords smaller than 30 microns and might increase fineness of the air void system.

In the discussion at the middle of this chapter, air void clustering increased with retempering. So, when small air bubbles increased with retempering, the clustering rating also increased. Based on the above analysis, it confirmed previous research finding that clustering increased a finer air void system (Naranjo, A. 2007).

Table 4-32 Air content, chords below 30 microns

Mix number	Mix ID	Air content (%) , chords below 30 micron		
		No retempering	Retempering	Difference
1	TIL-A-1-L-70	0.45	0.12	-0.33
2	TIL-A-1-L-90	0.13	0.21	0.08
3	TIL-A-1-G-70	0.21	0.10	-0.11
4	TIL-A-1-G-90	0.14	0.16	0.02
5	TIL-A-2-L-70	0.22	0.18	-0.04
6	TIL-A-2-L-90	0.41	0.30	-0.11
7	TIL-A-2-G-70	0.22	0.20	-0.02
8	TIL-A-2-G-90	0.11	0.12	0.01
9	TIL-B-1-L-70	0.14	0.20	0.06
10	TIL-B-1-L-90	0.12	0.24	0.12
11	TIL-B-1-G-70	0.18	0.64	0.46
12	TIL-B-1-G-90	0.53	0.57	0.04
13	TIL-B-2-L-70	0.09	0.27	0.18
14	TIL-B-2-L-90	0.14	0.24	0.10
15	TIL-B-2-G-70	0.11	0.19	0.08
16	TIL-B-2-G-90	0.31	0.24	-0.07
17	LA-A-1-L-70	0.24	0.15	-0.09
18	LA-A-1-L-90	0.15	0.15	0.00
19	LA-A-1-G-70	0.05	0.10	0.05
20	LA-A-1-G-90	0.22	0.15	-0.07
21	LA-A-2-L-70	0.12	0.22	0.10
22	LA-A-2-L-90	0.22	0.26	0.04
23	LA-A-2-G-70	0.27	0.22	-0.05
24	LA-A-2-G-90	0.12	0.21	0.09
25	LA-B-1-L-70	0.33	0.60	0.27
26	LA-B-1-L-90	0.28	0.50	0.22
27	LA-B-1-G-70	0.19	0.29	0.10
28	LA-B-1-G-90	0.15	0.24	0.09
29	LA-B-2-L-70	0.22	0.40	0.18
30	LA-B-2-L-90	0.19	0.48	0.29
31	LA-B-2-G-70	0.10	0.31	0.21
32	LA-B-2-G-90	0.35	0.36	0.01

4.4 Neural Network Analysis of Predicting the Relationships among Air Content, Air Void Clustering and Compressive Strength

Based on the above analysis, a statistical analysis method could help to obtain a result about compressive strength, however, in this study, many interrelated variables were investigated making it challenging to isolate the relationships among responses. Another modeling method was considered called Neural Network (ANN) modeling. This is a tool to get assess complex data (Torre et al. 2015). It has been widely used in civil engineering structure and concrete strength prediction (M. Bilgehan and P. Turgut. 2010). In this study, the NN process was compducted through the JMP software.

A neural network contains three layers: input layer, hidden layer, and output layer. The hidden layer could have multiple layers. A neural network structure diagram is shown in Figure 4-27.

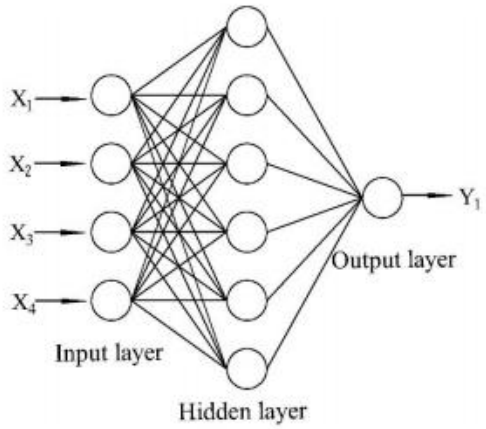

Figure 4-27 Neural network structure (Haojia Chai et al, 2018)

4.4.1 Neural Network Simulation Process

In order to get the relationship among air content, clustering and 28 compressive strength with six variables, air content, clustering, and six variables were set as X, which was in the input layer, and 28 compressive strength was set as Y in the output layer, shown in Figure 4-28.

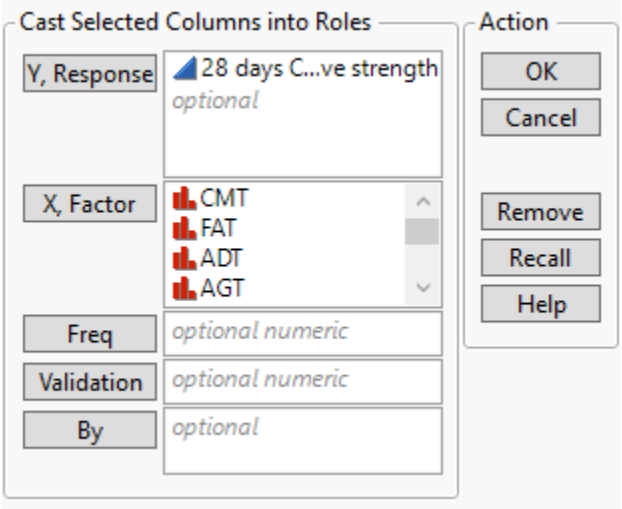

Figure 4-28 Select of X and Y for modeling

In Figure 4-29, KFold validation method was chosen because of the small size of the data set of this study. KFold means that the data are divided into K parts with one part used as a validation set, and the other parts are a training set. In this study, K=4 was selected so that 16 data points were used as validation and 48 were used as training. For each training run, the data were selected randomly. One hidden layer was used in this study because of the limited amount of data (Chai et al. 2018). Commonly, TanH activation function was selected. How many neuron numbers should be determined via trial and error method (Chai et al. 2018). In fitting options, transform covariates was selected, transforming all continuous variables into near-normal ones, which could help to mitigate the adverse effects of outliers or highly skewed distributions.

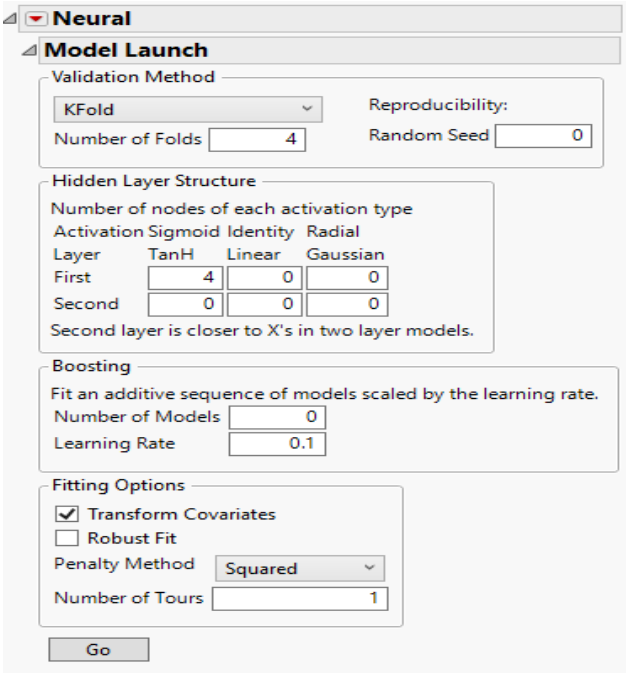

Figure 4-29 Neural parameters setting

When all the parameters were determined, the model was established. One of the example results is shown in Figure 4-30. The training utilized initial data with the learning ability of a machine to simulate a model. Validation results used some initial data to test the training model, whether it was good. The coefficient of determination (R^2) and root mean square error (RMSE) was used to evaluate simulation results. In the training phase, R^2 indicated how much the variable could explain the response. In the validation phase, R^2 was used to evaluate the performance of the model whether it was good. So the higher R^2 and lower RMSE in the validation phase were better. In addition, if the R^2 in the training phase was much larger than that of the validation test. The model was regarded as overfitting, which should be avoided. According to Figure 4.30, the Training R2 is 0.938 indicating that the NN model behaved well. The Validation R2 is 0.980, which meant that predicted data by the NN was almost the same as

the real ones. Further, RMSE in the validation phase was only 104.83. All these values have proven that the NN model was reliable to estimate the compressive strength of concrete.\

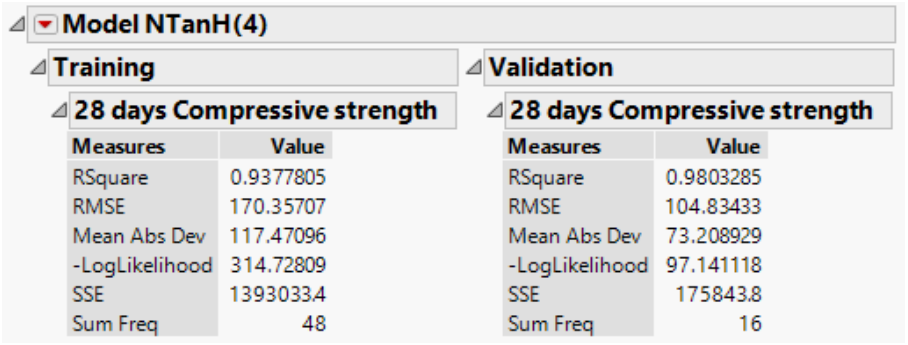

Model NTanH(4)

Training		Validation	
28 days Compressive strength		28 days Compressive strength	
Measures	Value	Measures	Value
RSquare	0.9377805	RSquare	0.9803285
RMSE	170.35707	RMSE	104.83433
Mean Abs Dev	117.47096	Mean Abs Dev	73.208929
-LogLikelihood	314.72809	-LogLikelihood	97.141118
SSE	1393033.4	SSE	175843.8
Sum Freq	48	Sum Freq	16

Figure 4-30 Neural modeling result

4.4.2 Determination of Neuron Number

In order to determine the optimum hidden layer neuron number, the trial and error method was used (Chai et al. 2018). The neuron number in the hidden layer was set to 4 to10, and the learning rate was at 0.01. For each neuron, the optimum learning error and epoch was selected by comparison with the results obtained through neural network training. The result of all network training is presented in Table 4-33. The relationship among neuron numbers of the hidden layer, validation error, and epoch of the neural network is shown in Figure 4-31. When the neuron number was 10, the RMSE was smallest at 0.37, and the epoch was 20. Therfore, the node number of the hidden layer was determined as 10.

Table 4-33 The performance of the network for different hidden neuron numbers (hidden neuron 4-7)

Hidden neuron number	Learning rate	Epoch number	Training		Validation	
			RMSE	Rsquare	RMSE	Rsquare
4	0.01	12	270.97	0.8514	139.11	0.9593
4	0.01	14	214.72	0.9067	160.98	0.9454
4	0.01	16	131.56	0.9649	151.62	0.9516
4	0.01	18	167.34	0.9433	222.82	0.8955
4	0.01	20	203.28	0.9164	187.49	0.9260
4	0.01	22	150.13	0.9544	125.69	0.9667
4	0.01	24	215.75	0.9058	111.29	0.9739
4	0.01	26	162.28	0.9467	236.85	0.8819
4	0.01	28	240.39	0.8831	120.15	0.9696
4	0.01	30	245.36	0.8782	142.46	0.9573
5	0.01	12	209.33	0.9113	158.04	0.9474
5	0.01	14	156.35	0.9505	120.97	0.9692
5	0.01	16	214.50	0.9079	135.15	0.9602
5	0.01	18	186.16	0.9257	292.38	0.8469
5	0.01	20	121.35	0.9684	207.99	0.9226
5	0.01	22	134.22	0.9635	282.72	0.8318
5	0.01	24	229.16	0.8937	53.07	0.9941
5	0.01	26	260.31	0.8629	46.67	0.9954
5	0.01	28	200.66	0.9185	178.12	0.9332
5	0.01	30	179.17	0.9312	182.23	0.9406
6	0.01	12	170.00	0.9415	82.92	0.9855
6	0.01	14	117.39	0.9705	261.77	0.8773
6	0.01	16	186.02	0.9307	79.00	0.9864
6	0.01	18	170.47	0.9377	127.05	0.9711
6	0.01	20	195.67	0.9225	21.28	0.999
6	0.01	22	183.65	0.9318	47.11	0.9953
6	0.01	24	137.03	0.962	156.73	0.9483
6	0.01	26	116.18	0.9711	193.61	0.9329
6	0.01	28	163.57	0.9426	129.32	0.9701
6	0.01	30	211.12	0.9098	8.72	0.9998
7	0.01	12	142.56	0.9594	279.66	0.8283
7	0.01	14	131.84	0.9646	155.42	0.9502
7	0.01	16	114.48	0.9733	67.15	0.9907
7	0.01	18	218.73	0.9045	34.79	0.9973
7	0.01	20	209.93	0.9103	68.95	0.9902
7	0.01	22	109.85	0.9754	94.52	0.9816
7	0.01	24	161.54	0.9469	130.20	0.9650
7	0.01	26	172.52	0.9406	109.64	0.9736
7	0.01	28	146.89	0.9561	85.08	0.9851
7	0.01	30	119.43	0.9715	91.18	0.9817

Table 4-33 The performance of the network for different hidden neuron numbers (hidden neuron 8-10)

8	0.01	12	220.47	0.9016	97.66	0.9799
8	0.01	14	97.31	0.9808	98.51	0.9796
8	0.01	16	83.48	0.9851	422.88	0.6799
8	0.01	18	15.389	0.9995	305.68	0.8327
8	0.01	20	183.84	0.9316	23.21	0.9989
8	0.01	22	166.28	0.9441	51.13	0.9945
8	0.01	24	144.44	0.9578	109.59	0.9747
8	0.01	26	133.64	0.9639	164.51	0.9430
8	0.01	28	112.52	0.9742	118.88	0.9708
8	0.01	30	75.62	0.9877	46.98	0.996
9	0.01	12	12.78	0.9693	156.82	0.9467
9	0.01	14	83.25	0.9859	159.72	0.9474
9	0.01	16	110.05	0.9741	122.39	0.9730
9	0.01	18	175.2	0.9375	5.05	0.9999
9	0.01	20	209.04	0.911	22.186	0.9989
9	0.01	22	241.91	0.8832	68.09	0.9898
9	0.01	24	271.22	0.8531	24.92	0.9986
9	0.01	26	188.88	0.9273	24.50	0.9988
9	0.01	28	88.02	0.9845	124.51	0.966
9	0.01	30	103.14	0.9783	103.72	0.9778
10	0.01	12	129.03	0.9643	125.05	0.9720
10	0.01	14	161.51	0.9472	84.91	0.9848
10	0.01	16	116.26	0.9726	61.99	0.9919
10	0.01	18	206.79	0.9135	37.89	0.9969
10	0.01	20	195.69	0.9220	0.727	0.9999
10	0.01	22	233.65	0.8895	53.92	0.9939
10	0.01	24	170.72	0.941	88.15	0.9836
10	0.01	26	223.59	0.8999	1.27	0.9999
10	0.01	28	0.9854	0.9999	261.23	0.8779
10	0.01	30	217.19	0.9045	6.20	0.9990

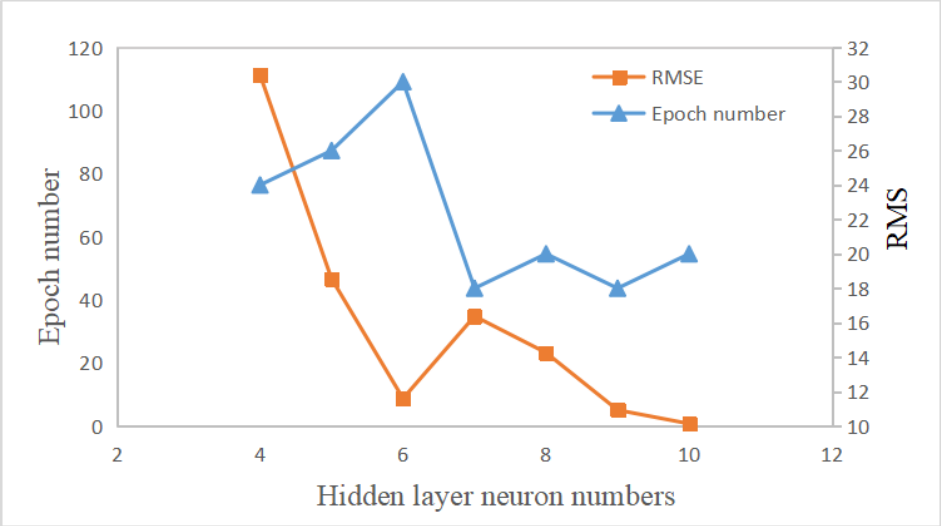

Figure 4-31 Epoch number and RMSE versus different hidden layer neuron number

The optimum learning rate was determined as 0.01 as presented in Table 4-34 and Figure 4-32. The lowest RMSE and high Rsquare was shown when the learning rate was 0.01.

Table 4-34 The performance of network simulation for different learning rate

Hidden neuron number	Learning rate	Epoch number	Training		Validation	
			RMSE	R^2	RMSE	R^2
10	0.01	20	195.69	0.9220	0.72	0.9999
10	0.02	20	84.29	0.9855	57.89	0.9931
10	0.03	20	206.5	0.9149	88.37	0.9829
10	0.04	20	116.46	0.9729	147.96	0.9519
10	0.05	20	91.86	0.9831	66.67	0.9904
10	0.06	20	235.76	0.8868	24.43	0.9988
10	0.07	20	109.37	0.9762	152.22	0.9491
10	0.08	20	234.96	0.8876	36.51	0.9973
10	0.09	20	207.44	0.9124	70.65	0.9897
10	0.10	20	71.05	0.9899	68.26	0.9899

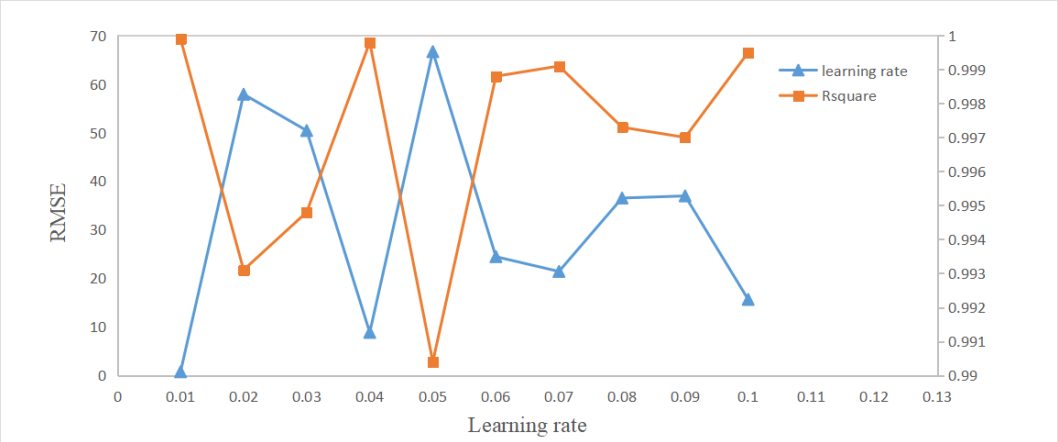

Figure 4-32 RMSE and Rsquare values versus different learning rate

4.4.3 NN Model Performance Analysis

Figure 4-33 shows the correlation between actual compressive strength values and predicted values obtained through the NN analysis method. The prediction in Figure 4-33 was based on the data in the training set. The equation of linear regression was y=0.9643x+146.9 while thedetermination of coefficient R^2 was 0.929. Figure 4-34 shows the validation result. It shows that actual data almost fell on the linear regression line.

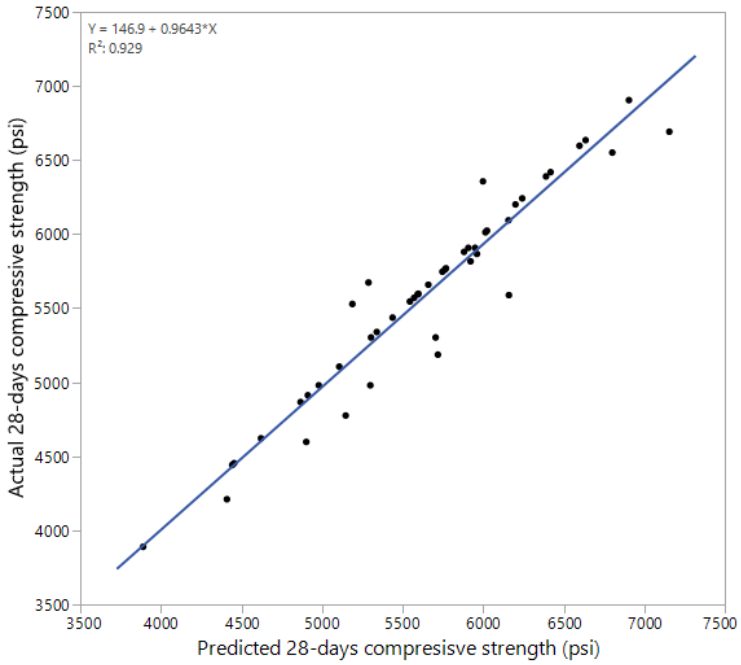

Figure 4-33 Comparison between training result through neural network and actual 28-days compressive strength data

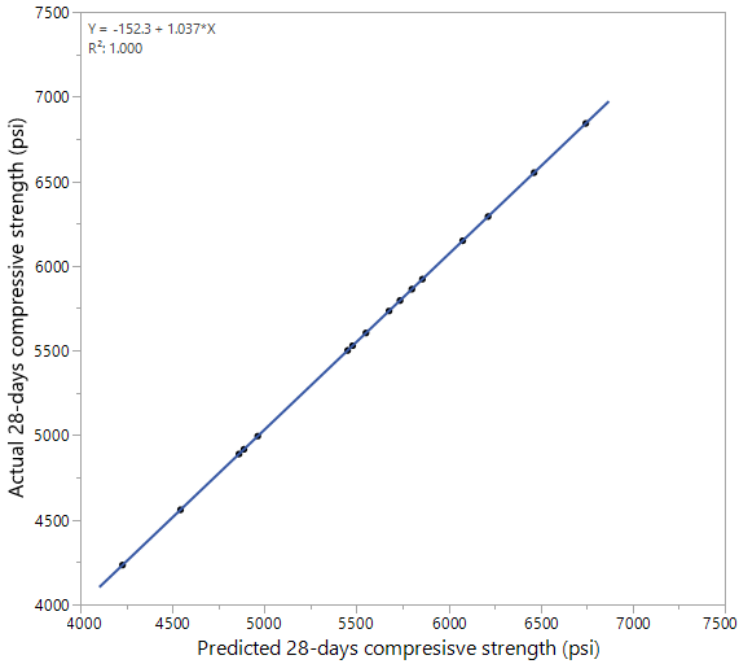

Figure 4-34 The validation results

4.4.4 Qualitative Analysis of the Relationship among Air Content, Air Void Clustering and Compressive Strength

Figure 4-35 shows the surface model in three-dimensional space. The surface runs from the upper left corner to lower right corner along the diagonal line. This shows a reduction of compressive strength could be resulted from increasing air content and air void clustering. The wave pattern of surface indicates that there is no linear relationship between air content, air void clustering, and 28 days compressive strength. However, the trend of the surface helps illustrate the negative effect of air void clustering and air content on compressive strength, and could help to make a qualitative analysis.

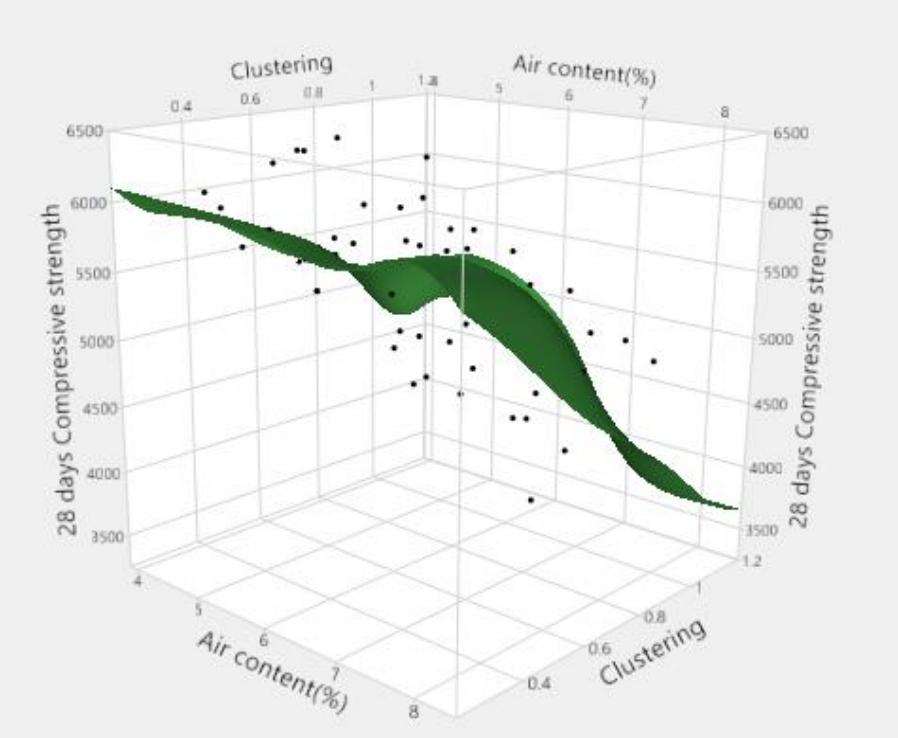

Figure 4-35 Relationship between, air content, clustering and 28 compressive strength

4.5 Analysis of Visual Rating Method of Air Void Clustering

In this study, the air void clustering rating method developed by Kozikowski et al. (2005) was conducted. Experimental photos were obtained that are similar to the reference pictures, as shown in Figure 4-36. Although the effect of air void clustering on compressive strength could be obtained, the result was inaccurate, which brought difficulties to quantitative analysis. For example, the compressive strength loss potentially due to clustering was confirmed. However, it was hard to draw the conclusion that the higher clustering caused the lower strength.

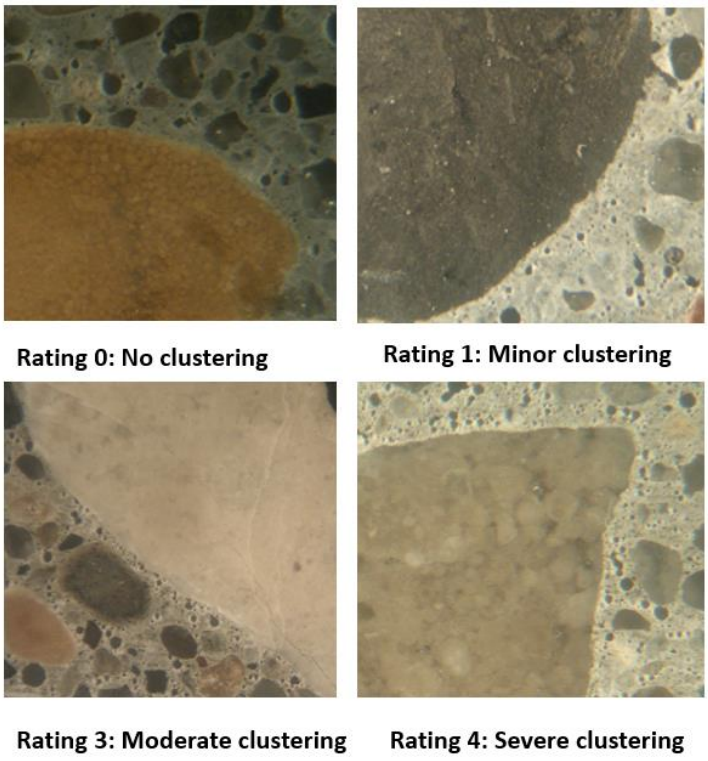

Figure 4-36 Clustering categories

Figure 4-37 illustrates potential errors when assessing bubble size based on cut and polished sections. This potential error has to be allowed for in any modelling.

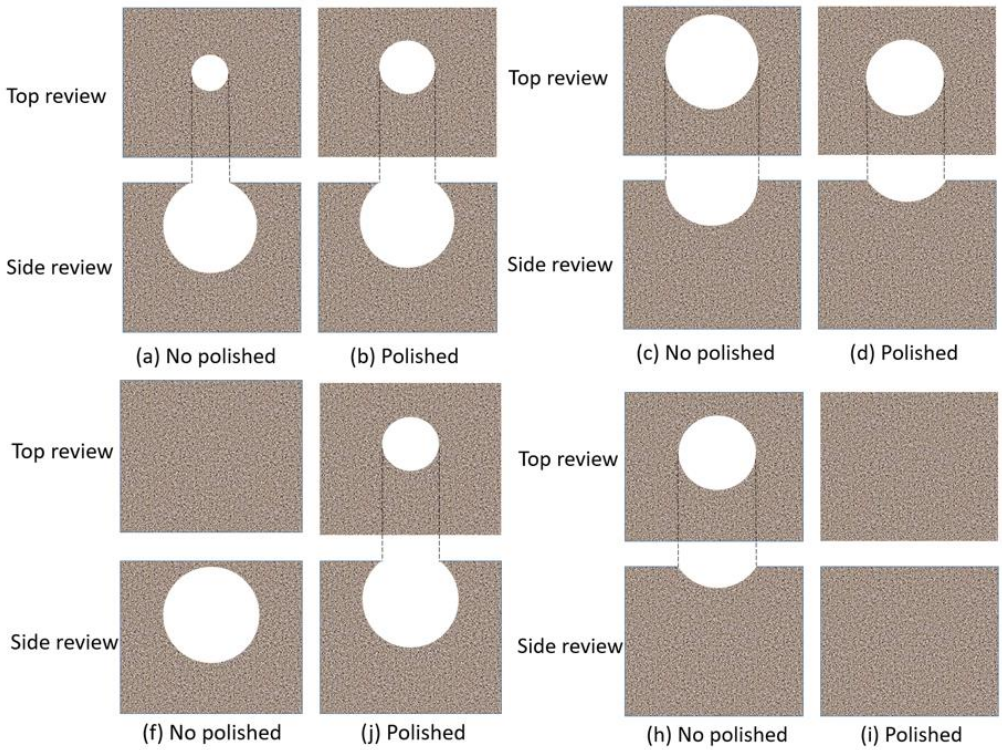

Figure 4-37 Air void change in the sample surface after polish

The clustering data with and without polishing is presented in Table 4-35. The comparison between polished and non-polished is shown in Figure 4-38. Increase and decrease of clustering after polish were both observed, which proved the above four kinds of observed air void size change on the sample surface. In this study, the clustering data after the polish was used.

Table 4-35 Clustering data with and without polish process

MIX ID	Polished		No polished	
	No	Yes	No	Yes
TIL-A-1-L-70	0.57	0.66	0.51	0.57
TIL-A-1-L-90	0.63	0.60	0.63	0.60
TIL-A-1-G-70	0.69	0.74	0.49	0.49
TIL-A-1-G-90	0.40	0.54	0.40	0.49
TIL-A-2-L-70	0.69	0.69	0.69	0.69
TIL-A-2-L-90	0.69	0.71	0.77	0.80
TIL-A-2-G-70	0.66	0.80	0.66	0.80
TIL-A-2-G-90	0.71	0.94	0.49	0.77
TIL-B-1-L-70	0.71	0.97	0.77	0.97
TIL-B-1-L-90	0.69	0.89	0.77	0.83
TIL-B-1-G-70	0.60	0.77	0.60	0.74
TIL-B-1-G-90	0.71	0.71	0.71	0.71
TIL-B-2-L-70	0.60	0.66	0.31	0.51
TIL-B-2-L-90	0.34	0.60	0.51	0.63
TIL-B-2-G-70	0.63	0.89	0.51	0.89
TIL-B-2-G-90	0.80	0.86	0.74	0.77
LA-A-1-L-70	0.14	0.43	0.14	0.06
LA-A-1-L-90	0.54	0.91	0.63	0.86
LA-A-1-G-70	0.20	0.37	0.20	0.37
LA-A-1-G-90	0.23	0.54	0.34	0.40
LA-A-2-L-70	0.23	0.43	0.23	0.43
LA-A-2-L-90	0.71	1.06	0.57	1.06
LA-A-2-G-70	0.34	0.54	0.34	0.54
LA-A-2-G-90	0.26	0.49	0.26	0.49
LA-B-1-L-70	0.23	0.66	0.23	0.57
LA-B-1-L-90	0.60	0.83	0.34	0.66
LA-B-1-G-70	0.17	0.74	0.20	0.74
LA-B-1-G-90	0.43	0.57	0.46	0.54
LA-B-2-L-70	0.46	0.74	0.46	0.74
LA-B-2-L-90	0.94	0.97	1.11	1.26
LA-B-2-G-70	0.14	0.37	0.14	0.34
LA-B-2-G-90	0.69	0.89	0.69	0.89

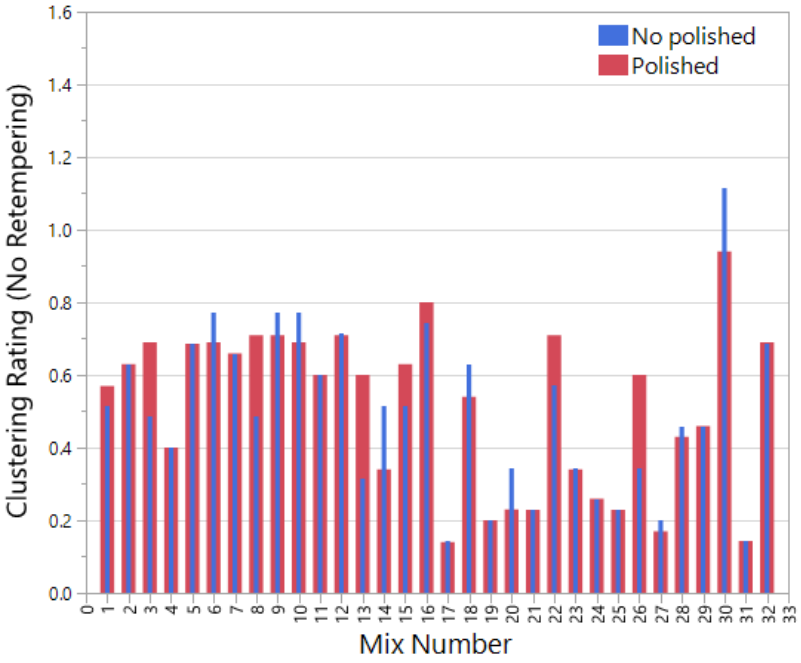

(a) Clustering variation without retempering

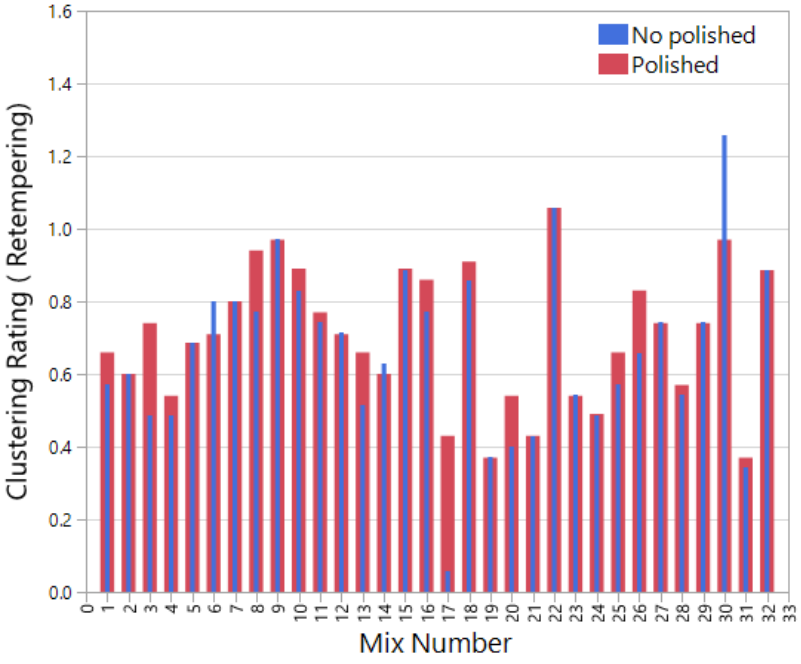

(b) Clustering variation with retempering

Figure 4-38 Clustering comparison of polished and no polished

Another error comes from a limitation of the rating method. As previously discussion, the same clustering rating could be obtained with different air void distribution around aggregates. In addition, the reference pictures only give a part of the aggregate surface. It was unclear whether the effect of air void clustering around the whole aggregate surface was different from that of the local surface. Meanwhile, air void number, size, and shape all affected compressive strength, but they were not defined in air void clustering. For example, two aggregates were rated as the same clustering severity, but the number, size, and shape of air voids that made up the air void clustering might be different. Whether this difference had a significant effect on the relationship between air void clustering and compressive strength was still unclear. Further, the manual analysis was also not subjective.

Although visual clustering rating method was a good way to figure out the effect of air void clustering on concrete, it still needs to be improved its errors and limitations.

CHAPTER 5. CONCLUSION AND RECOMMENDATION

5.1 Conclusions

Based on the results and discussions of the research in this study, the following conclusions have been made:

- Retempering can increase air content and air void clustering of concrete, and has effects on air void system. With retempering, spacing factor decreased and specific surface increased. Because clustering was observed in mixtures with or without retempering, the retempering may not be the cause of clustering formation, but it can aggravate its occurrence.
- Based on the statistical analysis, fly ash type and coarse aggregate type has a significant effect on both air content and air void clustering. When changing from fly ash A to B, and from river gravel to limestone, both air content and clustering increases. However, cement type and admixture type only had effects on air void clustering. Changing from low alkali cement to TIL cement, and from chemical admixture 1 to 2, air void clustering increased.
- High temperature not only increased the air content of concrete, but also enhanced air void clustering, and the loss of compressive strength.
- A Clustering Sensitive Index (CSI) was proposed to describe the sensitivity of concrete to air void clustering. A smaller Index indicates higher sensitivity of concrete to air void clustering and the effect of retempering on clustering increased.
- Air void clustering had a negative effect on compressive strength with an average change of strength loss was only 9.07% for the samples tested here.
- Retempering appeared to create finer air voids.

- Stepwise regression and neural network modelling were used to model the effects of multiple variables on concrete properties.

5.2 Further Work Recommendations

Although this study has gained insight into air void clustering. Some further work is still recommended. Air void clustering needs to be investigated in the field condition. The Clustering Sensitivity Index first proposed in this study should be investigated further to confirm its validity Further, the limitations of visual rating method need to be improved to represent the real situation of air void clustering around the aggregate.

ACKNOWLEDGMENTS

This study is based on part of upon work sponsored by the National Cooperative Highway Research Program, which is administered by the Transportation Research Board of the National Academies of Sciences, Engineering, and Medicine.

REFERENCES

ASTM Standard C150 / C150M-12. (2012). Standard specification for portland cement. West Conshohocken, PA: ASTM International. DOI: 10.1520/C0150_C0150M-12, www.astm.org.

ASTM Standard C127-12. (2012). Standard test method for density, relative density (specific gravity), and absorption of coarse aggregate. West Conshohocken, PA: ASTM International. DOI: 10.1520/C0127-12, www.astm.org.

ASTM Standard C136-06. (2006). Standard test method for sieve analysis of fine and coarse aggregates. West Conshohocken, PA: ASTM International. DOI: 10.1520/C0136-06, www.astm.org

ASTM Standard C192 / C192M-13. (2013). Standard practice for making and curing concrete test specimens in the laboratory. West Conshohocken, PA: ASTM International. DOI: 10.1520/C0192_C0192M, www.astm.org.

ASTM Standard C138 / C138M-12. (2012). Standard test method for density (unit weight), yield, and air content (gravimetric) of concrete. West Conshohocken, PA: ASTM International. DOI: 10.1520/C0138_C0138M-12, www.astm.org.

ASTM Standard C143 / C143M-12. (2012). Standard test method for slump of hydraulic-cement concrete. West Conshohocken, PA: ASTM International. DOI: 10.1520/C0143_C0143M-12, www.astm.org.

ASTM Standard C231 / C231M-10. (2010). Standard test method for air content of fresh mixed concrete by the pressure method. West Conshohocken, PA: ASTM International. DOI: 10.1520/C0231_C0231M-10, www.astm.org.

ASTM Standard C39 / C39M-12. (2012). Standard test method for compressive strength of cylindrical concrete specimens. West Conshohocken, PA: ASTM International. DOI: 10.1520/C0039_C0039M-12, www.astm.org.

ASTM Standard C457 / C457M-12. (2012). Standard test method for microscopical determination of parameters of the air-void system in hardened concrete. West Conshohocken, PA: ASTM International. DOI: 10.1520/C0457_C0457M-12,www.astm.org.

ASTM Standard C1231 / C1231M-14. (2014). Standard practice for use of unbonded caps in determination of compressive strength of hardened concrete cylinders. West Conshohocken, PA: ASTM International. DOI: 10.1520/C1231_C1231M-14, www.astm.org.

Billinger, Randall, Heather Mcleod, David Lankard, and Nick Scaglione. 2016. “Effects of Air Void Clustering on Concrete Compressive Strength. Paper by Jan Vosahlik, Kyle A. Riding, Asad Esmaeily, Randall Billinger, and Heather McLeod Discussion by David Lankard and Nick Scaglione.” (December): 819–22.

Chai, Haojie, Xianming Chen, Yingchun Cai, and Jingyao Zhao. 2018. “Artificial Neural Network Modeling for Predicting Wood Moisture Content in High Frequency Vacuum Drying Process.” Forests 10 (1): 16. https://doi.org/10.3390/f10010016.

Cross, William, Edward Dike, Kellar Jon, and Dan Johnston. 2000. “Investigation of Low Compressive Strengths of Concrete in Paving, Precast and Structural Concrete,” 90.

Du, Lianxiang, and Kevin J. Folliard. 2005. “Mechanisms of Air Entrainment in Concrete.” Cement and Concrete Research 35 (8): 1463–71. https://doi.org/10.1016/j.cemconres.2004.07.026.

Erdoğdu, Şakir. 2005. “Effect of Retempering with Superplasticizer Admixtures on Slump Loss and Compressive Strength of Concrete Subjected to Prolonged Mixing.” Cement and Concrete Research 35 (5): 907–12. https://doi.org/10.1016/j.cemconres.2004.08.020.

Guo, Shuaicheng, Qingli Dai, Xiao Sun, Ye Sun, and Zhen Liu. 2017. “Ultrasonic Techniques for Air Void Size Distribution and Property Evaluation in Both Early-Age and Hardened Concrete Samples.” Applied Sciences 7 (3): 290. https://doi.org/10.3390/app7030290.

Gutmann, Paul F. 1987. “Bubble Characteristics as They Pertain to Compressive Strength and Freeze-Thaw Durability.” MRS Proceedings 114 (85): 271. https://doi.org/10.1557/PROC-114-271.

Hanson, Todd D. 2012. “Evaluation of the Rapid Air 457 Air Void Analyzer, March 2012.” http://publications.iowa.gov/13573/1/MLR-2011-01_RapidAir_457.(2).docx.

Jolicoeur, Carmel, Thi Cong To, Éric Benoît, Russell Hill, Monique Pagé, Z. Zhang, Monique Pagé, et al. 2009. “Fly Ash-Carbon Effects on Concrete Air Entrainment : Fundamental Studies on Their Origin and Chemical Mitigation.” World of Coal Ash (WOCA) Conference, 1–23.

Jackson, F.H. 1944. Concrete containing air-entraining agents. Journal of the American Concrete Institute, Vol.40, pp.509–515

Kozikowski, Ronald L, and Jerzy Z Zemajtis. 2006. “Identifying Incompatible Combinations of Concrete Materials : - Volume II – Test Protocol” II (August).

Li, Zhengqi, Kaveh Afshinnia, and Prasada Rao Rangaraju. 2016. “Effect of Alkali Content of Cement on Properties of High Performance Cementitious Mortar.” Construction and Building Materials. https://doi.org/10.1016/j.conbuildmat.2015.10.110.

Mindess,S., Young, J.F. and Darwin, D.(2003). Concrete,2nd edn. Prentice.Hall, Upper Saddle River, New Jersey, USA.

Mehta, PK, and KC Hover. 2010. “Some Recent Problems with Air-Entrained Concrete.” Cement, Concrete and Aggregates 11 (1): 67. https://doi.org/10.1520/cca10104j.

Marx, J., Dugan and Myere Construction, Personal communication. Co., Inc., Cincinnati, OH,

February 1987

Mohamad A. Nagi, Paul A. Okamoto, Ronald L. Kozikowski, Kenneth Hover.2007. Evaluating Air-Entraining Admixtures for Highway Concrete. CONSTRUCTION TECHNOLOGY LABORATORIES, INC.Skokie, IL and CORNELL UNIVERSITY, Ithaca, NY

M.Bilgehan and P.Turgut.2010. The use of neural networks in concrete compressive strength estimation. Computers and Concrete, Vol. 7, No. 3 (2010) 271-283

Naranjo, A. (2007). Clustering of air voids around aggregates in air entrained concrete (Master's thesis). The University of Texas at Austin, Austin, TX.

Peter C. Taylor, Vagn C. Johansen, Luis A. Graf, Ronald L. Kozikowski, Jerzy Z. Zemajtis, Chiara F. Ferraris (2006). Identifying Incompatible Combinations of Concrete Materials: Volume I—Final Report. DOT F 1700.7 (8-72)

Pigeon, M., and Pleau, R. 1995. Durability of Concrete in Cold Climates. E & FN Spon, Ltd., London, England.

Riding, KA, A Esmaeily, and J Vosahlik. 2015. “Air Void Clustering.” Report No. K-TRAN: KSU-13-6, no. June: 115.

Ram, P., T. Van Dam, L. Sutter, G. Anzalone, and K. Smith. 2013. Field Study of Air Content Stability in the Slipform Paving Process. WisDOT ID no. 0092-11-06. Wisconsi Department of Transportation. Madison,WI.January.

Torre, A., F. Garcia, I. Moromi, P. Espinoza, and L. Acuña. 2015. “Prediction of Compression Strength of High Performance Concrete Using Artificial Neural Networks.” Journal of Physics: Conference Series 582 (1). https://doi.org/10.1088/1742-6596/582/1/012010.

Walker, H. N., Lane, D. S., & Stutzman, P. E. (2006). Petrographic methods of examinin hardened concrete: A petrographic manual (Report No. FHWA-HRT-04-150). McLean, VA: Federal Highway Administration

Will Hansen, Younjae Kang (2010). Durability Study of the US-23 Aggregate Test Road and Recent JPCP Projects with Premature Joint Deterioration. Michigan Department of Transportation Construction and Technology Division

Whiting, D. Stark, D., Control of air content in concrete, NCHRP report 258 (May,1983). Washington: Transportation Research Board, National Research Council.

APPENDIX A: FRESH CONCRETE RESULTS

Mix Number	Mix ID	Slump(in)		Unit Weight (lb/yd^3)		Air Content (%)	
		No	Yes	No	Yes	No	Yes
1	TIL-A-1-L-70	1.6	2.1	146.80	147.40	6.2	4.3
2	TIL-A-1-L-90	2.2	3.0	145.32	146.92	6.3	5.0
3	TIL-A-1-G-70	2.1	2.4	147.20	148.40	5.0	3.9
4	TIL-A-1-G-90	1.8	2.6	147.20	148.20	6.0	3.8
5	TIL-A-2-L-70	1.0	3.0	144.20	142.80	6.7	7.2
6	TIL-A-2-L-90	1.0	2.5	146.60	145.60	6.0	6.1
7	TIL-A-2-G-70	2.0	5.0	146.40	145.40	5.7	5.6
8	TIL-A-2-G-90	2.0	4.3	145.00	144.20	5.8	6.3
9	TIL-B-1-L-70	1.3	3.6	146.20	141.60	6.3	8.0
10	TIL-B-1-L-90	1.4	3.2	146.00	141.60	6.1	7.9
11	TIL-B-1-G-70	3.4	7.0	143.80	142.80	6.9	7.2
12	TIL-B-1-G-90	2.0	2.5	146.00	145.60	5.6	5.6
13	TIL-B-2-L-70	1.8	3.4	147.40	146.40	5.2	5.3
14	TIL-B-2-L-90	1.5	3.3	147.00	145.60	5.5	6.0
15	TIL-B-2-G-70	1.5	2.7	147.00	147.00	5.0	4.9
16	TIL-B-2-G-90	2.3	4.8	143.80	142.00	7.0	7.3
17	LA-A-1-L-70	1.8	2.2	147.00	147.40	5.6	5.5
18	LA-A-1-L-90	2.8	4.2	143.60	144.40	6.6	6.6
19	LA-A-1-G-70	1.0	2.5	147.20	144.00	5.5	6.0
20	LA-A-1-G-90	0.6	2.0	146.80	146.20	5.4	6.6
21	LA-A-2-L-70	1.5	2.2	147.60	146.80	5.0	4.5
22	LA-A-2-L-90	2.6	3.2	145.20	142.80	6.3	6.9
23	LA-A-2-G-70	2.7	3.6	145.80	145.40	5.1	5.0
24	LA-A-2-G-90	2.1	3.8	147.00	145.60	5.0	5.3
25	LA-B-1-L-70	0.8	2.5	148.00	145.20	5.2	6.5
26	LA-B-1-L-90	2.5	3.5	144.80	142.80	6.7	7.4
27	LA-B-1-G-70	1.5	3.0	148.40	142.40	5.0	6.4
28	LA-B-1-G-90	1.7	2.6	147.00	146.20	5.1	5.3
29	LA-B-2-L-70	1.2	3.0	147.20	142.60	5.4	7.9
30	LA-B-2-L-90	2.7	3.4	146.80	145.60	5.6	6.5
31	LA-B-2-G-70	1.0	3.0	147.20	146.00	5.5	6.0
32	LA-B-2-G-90	2.2	4.1	144.80	142.60	6.7	7.6

Note: TIL= TIL 1 cement; LA=Low alkali cement; A=Low quality fly ash; B=High quality fly ash; 1=less effect on clustering; 2=more effect on clustering; L=limestone; G=gravel; 70=70°F mixing water; 90=90°F mixing water; No= without retempering, Yes=with retempering

APPENDIX B: COMPRESSIVE STRENGTH RESULTS

Mix Number	Mix ID	7-days compressive strength(psi)		28-days compressive strength(psi)	
		No	Yes	No	Yes
1	TIL-A-1-L-70	5318	4900	6842	6242
2	TIL-A-1-L-90	5444	5524	6357	6600
3	TIL-A-1-G-70	4371	4547	5589	5303
4	TIL-A-1-G-90	3944	4182	5734	5881
5	TIL-A-2-L-70	4844	4443	5867	5770
6	TIL-A-2-L-90	4666	4471	6024	5071
7	TIL-A-2-G-70	4079	3034	5303	4560
8	TIL-A-2-G-90	4028	3665	4598	4233
9	TIL-B-1-L-70	5461	3972	6635	4913
10	TIL-B-1-L-90	4884	4127	5594	5106
11	TIL-B-1-G-70	4052	3636	4776	3890
12	TIL-B-1-G-90	4688	3985	5908	4980
13	TIL-B-2-L-70	5500	4712	6419	5922
14	TIL-B-2-L-90	5236	4523	5908	4980
15	TIL-B-2-G-70	4411	3942	5659	5501
16	TIL-B-2-G-90	3827	3442	4454	4211
17	LA-A-1-L-70	5172	4912	6905	6551
18	LA-A-1-L-90	4164	3781	5187	5340
19	LA-A-1-G-70	4525	3954	6013	5529
20	LA-A-1-G-90	4865	4342	6094	5817
21	LA-A-2-L-70	4959	4844	6692	6597
22	LA-A-2-L-90	3707	3586	4995	4917
23	LA-A-2-G-70	4446	4001	5747	5546
24	LA-A-2-G-90	4621	4094	6149	5604
25	LA-B-1-L-70	4978	4299	6551	5863
26	LA-B-1-L-90	4256	4040	5761	5437
27	LA-B-1-G-70	4896	4316	6201	5674
28	LA-B-1-G-90	4844	4359	6292	5598
29	LA-B-2-L-70	4962	3702	6390	4983
30	LA-B-2-L-90	3805	3357	4889	4442
31	LA-B-2-G-70	4787	4141	5796	5529
32	LA-B-2-G-90	3637	3419	4867	4622

APPENDIX C: RAPID AIR RESULTS OF CONCRETE

Mix Number	Mix ID	Hardened Data, All Chords			Hardened Data, Chords Over 30 Micron		
		No retemepring			Rerempering		
		Air content (%)	Spacing Factor (mm)	Specific Surface (mm^{-1})	Air content (%)	Spacing Factor (mm)	Specific Surface (mm^{-1})
1	TIL-A-1-L-70	6.26%	0.122	37.91	3.20%	0.283	22.10
2	TIL-A-1-L-90	4.71%	0.265	19.83	5.43%	0.163	30.26
3	TIL-A-1-G-70	4.16%	0.176	31.62	3.01%	0.298	21.58
4	TIL-A-1-G-90	4.08%	0.240	23.04	4.39%	0.243	22.29
5	TIL-A-2-L-70	5.54%	0.172	28.42	5.92%	0.202	23.45
6	TIL-A-2-L-90	6.55%	0.124	36.47	5.68%	0.155	31.19
7	TIL-A-2-G-70	5.23%	0.175	28.57	4.25%	0.185	29.82
8	TIL-A-2-G-90	3.88%	0.221	25.98	5.03%	0.201	25.30
9	TIL-B-1-L-70	6.02%	0.239	19.61	6.50%	0.141	32.22
10	TIL-B-1-L-90	4.63%	0.252	21.03	5.74%	0.157	30.48
11	TIL-B-1-G-70	4.68%	0.207	25.48	6.72%	0.095	47.04
12	TIL-B-1-G-90	6.70%	0.108	41.41	6.13%	0.099	46.99
13	TIL-B-2-L-70	4.02%	0.269	20.95	5.51%	0.131	37.34
14	TIL-B-2-L-90	4.63%	0.180	29.43	5.72%	0.130	36.89
15	TIL-B-2-G-70	5.11%	0.204	24.81	5.19%	0.153	32.76
16	TIL-B-2-G-90	6.42%	0.114	40.12	6.81%	0.153	29.05
17	LA-A-1-L-70	5.55%	0.176	27.68	4.20%	0.218	25.35
18	LA-A-1-L-90	5.46%	0.193	25.44	7.14%	0.185	23.48
19	LA-A-1-G-70	4.30%	0.366	14.94	4.32%	0.241	22.68
20	LA-A-1-G-90	3.81%	0.186	31.16	5.16%	0.208	24.21
21	LA-A-2-L-70	4.57%	0.229	23.22	4.96%	0.177	28.95
22	LA-A-2-L-90	4.21%	0.151	36.60	7.67%	0.138	29.29
23	LA-A-2-G-70	4.37%	0.150	36.14	3.45%	0.171	35.26
24	LA-A-2-G-90	4.23%	0.229	24.09	3.98%	0.145	38.98
25	LA-B-1-L-70	6.21%	0.145	31.84	6.90%	0.097	45.69
26	LA-B-1-L-90	5.63%	0.136	35.63	6.78%	0.109	40.62
27	LA-B-1-G-70	4.89%	0.181	28.56	7.29%	0.149	28.45
28	LA-B-1-G-90	3.92%	0.206	27.71	5.37%	0.150	33.08
29	LA-B-2-L-70	3.44%	0.172	35.27	6.07%	0.116	40.18
30	LA-B-2-L-90	3.84%	0.164	35.14	6.52%	0.098	46.09
31	LA-B-2-G-70	4.23%	0.260	21.17	6.71%	0.164	27.31
32	LA-B-2-G-90	7.69%	0.123	32.83	8.77%	0.121	29.19

APPENDIX D: AIR VOID CLUSTERING RATING RESULTS

Mix Number	Mix ID	Clustering	
		No retempering	Retempering
1	TIL-A-1-L-70	0.57	0.66
2	TIL-A-1-L-90	0.63	0.60
3	TIL-A-1-G-70	0.69	0.74
4	TIL-A-1-G-90	0.40	0.54
5	TIL-A-2-L-70	0.69	0.69
6	TIL-A-2-L-90	0.69	0.71
7	TIL-A-2-G-70	0.66	0.80
8	TIL-A-2-G-90	0.71	0.94
9	TIL-B-1-L-70	0.71	0.97
10	TIL-B-1-L-90	0.69	0.89
11	TIL-B-1-G-70	0.60	0.77
12	TIL-B-1-G-90	0.71	0.71
13	TIL-B-2-L-70	0.60	0.66
14	TIL-B-2-L-90	0.34	0.60
15	TIL-B-2-G-70	0.63	0.89
16	TIL-B-2-G-90	0.80	0.86
17	LA-A-1-L-70	0.14	0.43
18	LA-A-1-L-90	0.54	0.91
19	LA-A-1-G-70	0.20	0.37
20	LA-A-1-G-90	0.23	0.54
21	LA-A-2-L-70	0.23	0.43
22	LA-A-2-L-90	0.71	1.06
23	LA-A-2-G-70	0.34	0.54
24	LA-A-2-G-90	0.26	0.49
25	LA-B-1-L-70	0.23	0.66
26	LA-B-1-L-90	0.60	0.83
27	LA-B-1-G-70	0.17	0.74
28	LA-B-1-G-90	0.43	0.57
29	LA-B-2-L-70	0.46	0.74
30	LA-B-2-L-90	0.94	0.97
31	LA-B-2-G-70	0.14	0.37
32	LA-B-2-G-90	0.69	0.89

APPENDIX E: FRESH AND HARDENED HIGH TEMPERATURE CONCRETE RESULTS

Fresh Properties Results of High Temperature Concrete

Mix ID	Slump(in)		Unit Weight (lb/yd^3)		Air Content (%)	
	No retempering	Retemepring	No retempering	Retemepring	No retempering	Retemepring
TIL-CT90°F	1.4	3.0	145.2	141.0	5.3	7.3
LA-CT90°F	1.2	2.2	146.8	144.4	4.2	5.2

Note: TIL= TIL cement; LA=Low alkali cement; CT90°F = 90°F of concrete.

Compressive Strength and Clustering Results of High Temperature Concrete

Mix ID	7 days Compressive strength (Psi)		28 days Compressive strength (Psi)		Clustering	
	No retempering	Retempering	No retempering	Retempering	No retempering	Retempering
TIL-CT90°F	3465	3040	5202	4349	0.63	0.80
LA-CT90°F	4615	4077	6123	4978	0.29	0.57